Validation of Dispersion using the

Particle Tracking Model

In the Sacramento-San Joaquin Delta

by

Ryan James Wilbur

Thesis

Submitted in partial satisfaction of the requirements for the degree of

MASTER OF SCIENCE

in

Civil and Environmental Engineering

in the

OFFICE OF GRADUATE STUDIES

of the

UNIVERSITY OF CALIFORNIA

DAVIS

2000

Table of Contents

List of Figures

List of Tables

1. Introduction

The Particle Tracking Model (PTM) was developed by the California Department of Water Resource's (DWR) Delta Modeling Section. The purpose of the model is to simulate the transport and fate of individual, neutrally buoyant "particles" through the Sacramento – San Joaquin Delta.

The PTM model is a component of the Delta Modeling Section's Delta Simulation Model II (DSM2). DSM2 simulates the hydrodynamic, water quality, and particle movement throughout the Sacramento – San Joaquin Delta in three models: Hydro, Qual and PTM, respectively. Figure 1.1 shows the location of major cities on a schematic for the Delta region. Figure 1.2 shows the significant inflows and outflows in the Delta. The Delta is the confluence of the Sacramento River, San Joaquin River, East Side Tributaries and the open water of San Francisco Bay. The Western boundary condition used by DSM2 is the stage at Martinez. The tidal motion influences the entire Delta. Flow reverses direction due to the tidal motion throughout most of the Delta. Upstream on the major rivers the tide influences the stage only.

The PTM model uses the hydrodynamics determined by Hydro to extrapolate the averaged velocity in a channel to a psuedo three-dimensional velocity cross section. Assumed velocity profiles are used for this extrapolation. The velocity profiles assume the zero slip condition at the bottom and sides of the channel; while the fastest areas are the center of the transverse profile and the top of the water column. The selection of velocity profiles is equivalent to setting the longitudinal dispersion coefficient. In addition, movement due to mixing (in the transverse and vertical) is superimposed on the advective motion. Data collected by the USGS are used to guide the selection of the velocity profiles. These new profiles are then compared to a tracer study to determine if the accuracy of the PTM is improved.

The PTM was originally developed by Gilbert Bogle, a consultant working for Water Engineering and Modeling, in 1992. Several modifications have been made by DWR and Dr. Bogle to improve this model to account for particular phenomena such as tidal effects and channel branches. The model was rewritten by Nicky Sandhu of DWR in Java and C++ to take advantage of object-oriented programming. Input-output was also updated to be consistent with the DSM2 model. Calibration of the advective characteristics was performed by Tara Smith of DWR. A limited investigation of dispersive characteristics of the Delta was performed by Dr. Bogle, but a full calibration was not completed. This is the goal of this study: to calibrate the dispersive characteristics of the Particle Tracking Model.

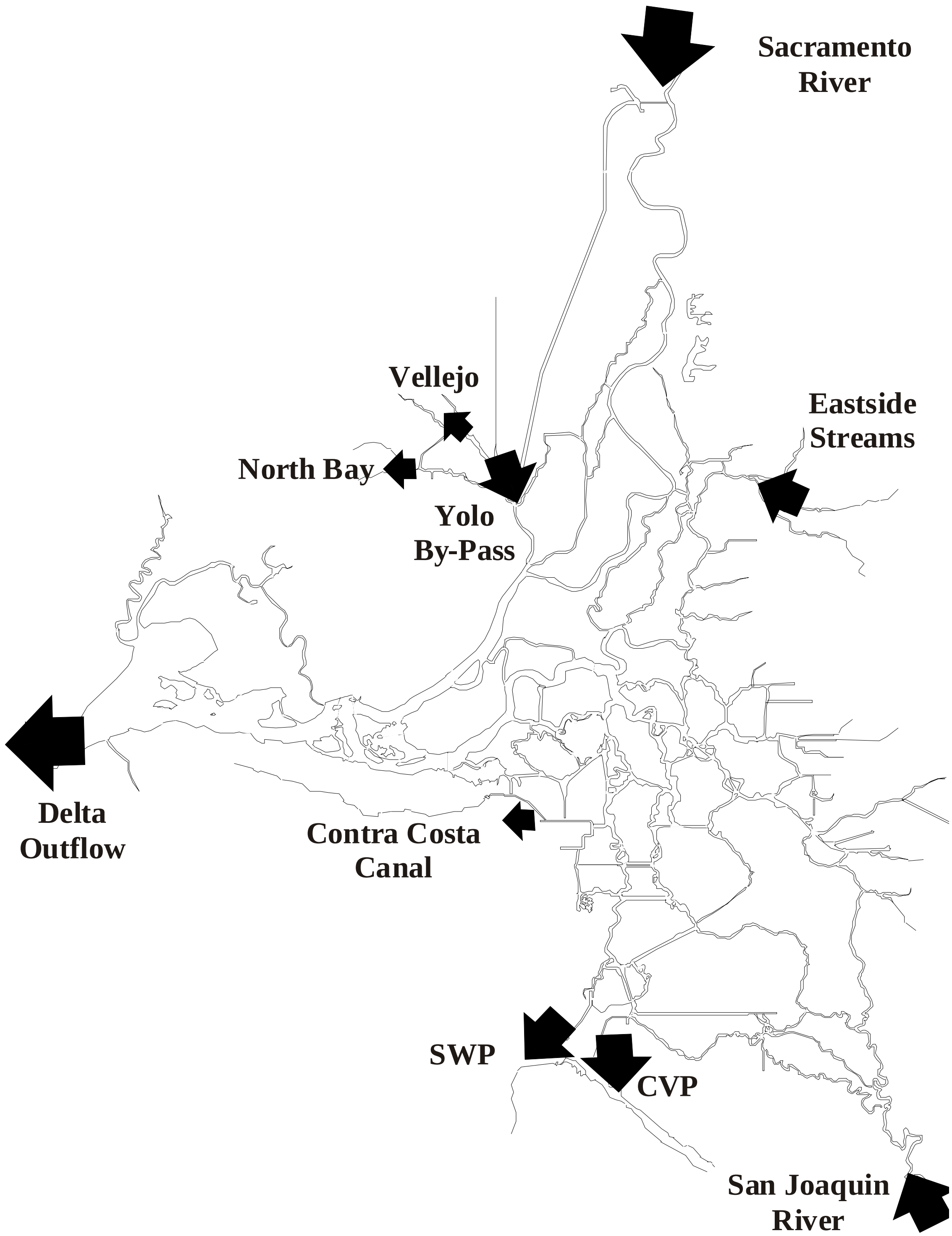

Figure 1.1: Major Waterways of the Sacramento – San Joaquin Delta

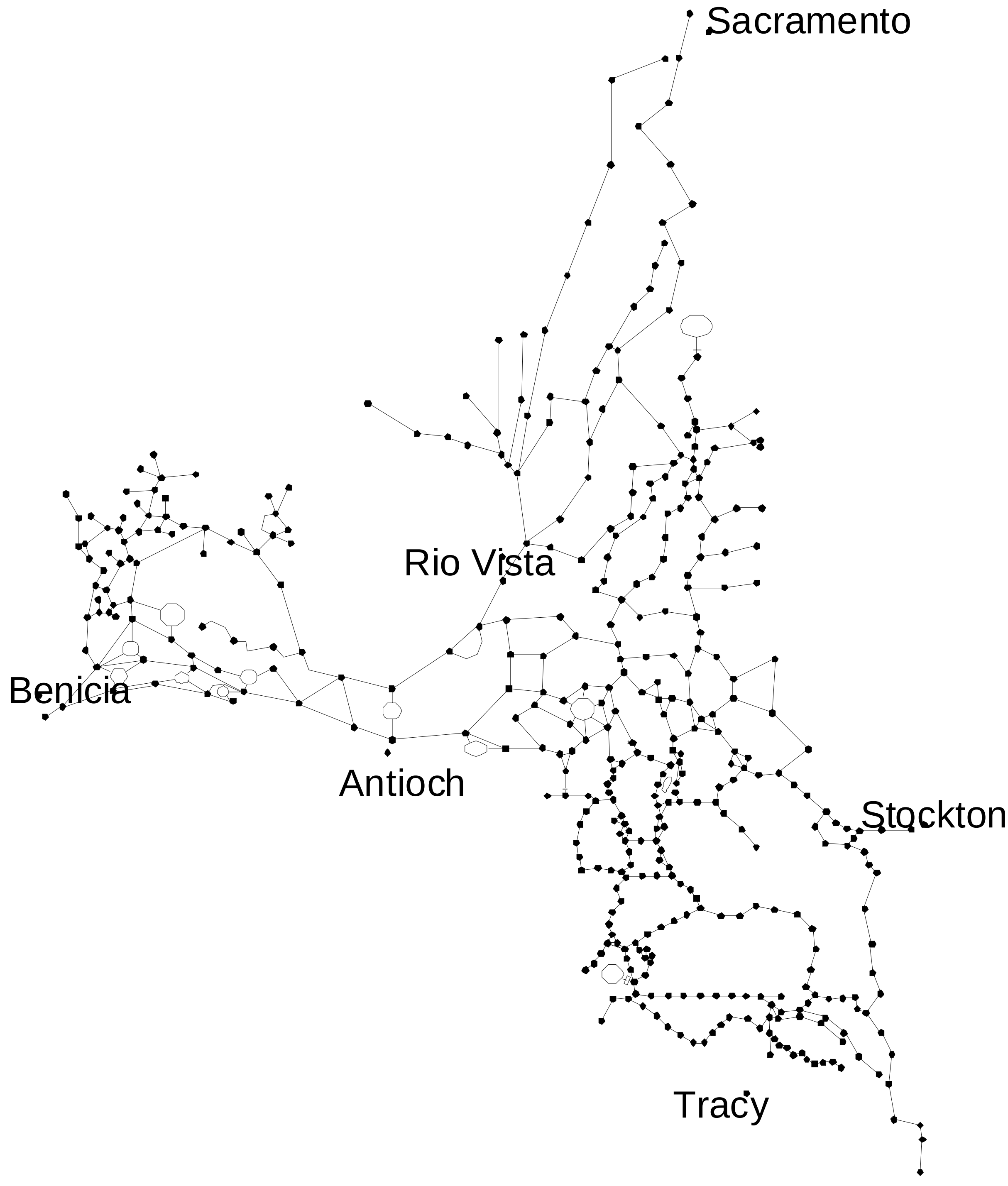

Figure 1.2: Schematic of the Sacramento – San Joaquin Delta

2. Literature Review

The principle mechanisms associated with mass transfer in all aquatic environments are advection, diffusion, and dispersion. Advection, sometimes referred to as convection, is the process in which the river's velocity transports the dissolved or suspended mass downstream. Modeling advection is primarily concerned with simulating the hydrodynamics correctly.

Diffusion and dispersion are often grouped together and treated as one process that is superimposed on advective movement. They are, however, fundamentally different processes. Diffusion is the process in which the motion of individual fluid particles is proportional to the concentration gradient between the two locations. This is usually referred to as molecular diffusion. Turbulent flow compounds this effect through the introduction of small scale eddies. These produce localized concentration disturbances that introduce what is termed turbulent diffusion. Natural systems usually are dominated by turbulent diffusion while molecular diffusion is considered negligible. Much of the turbulent diffusion theory is based on empirical results. Fischer (1968), Orlob (1959), and Taylor (1921) demonstrated that a Fickian representation of turbulent diffusion can approximate the process after sufficient time has passed allowing complete mixing across the river.

Dispersion is the process in which fluid particles undergo differential displacement due to differences in internal circulation. Fischer (1976) discusses the components of longitudinal dispersion as four factors: density distribution, inertial and frictional effects, the earth's rotation, and wind. The effect of wind and earth's rotation has not been investigated in estuary systems because it is generally believed to be small.

Variation in the density or buoyancy of water may be produced by differences in temperature, salinity, and/or other dissolved substances. The Estuarine Richardson Number (R),

$$R = \frac{\Delta\rho \, g \, Q_f}{\rho \, W \, \bar{U}^3} \qquad [2.1]$$

where ρ is density, Δρ is the density difference, g is gravity, Q_f is the freshwater discharge, W is the width, U is the rms tidal velocity, which is the ratio of the input of buoyancy per unit width to the effect of the tidal current, has been found to correspond to the state of stratification of an estuary. But the magnitude of R has not been linked to the amount of dispersion found in a system because it only describes external inputs. Mixing in estuaries is also determined by the geometry of the channels, which is not taken into account.

Inertial forces are responsible for creating the shear effect. Variation of the velocity across the cross section is responsible for this effect. Typical cross sectional views of velocity show the sides and bottom of the cross section to reflect the zero slip condition: the velocity is zero. The middle of the channel and top of the water's surface show the largest velocities. These differences in velocity disperse the dissolved/concentrated mass causing it to be stretched in the longitudinal direction. This is commonly referred to as shear flow dispersion (Fischer 1979). Taylor (1954) estimated dispersion in a pipe as D = 10.1 r u^* (where r is pipe radius and u^* is shear velocity). Later application showed this should be doubled for open channel flow (with depth replacing the radius). Bowden (1965) showed dispersion would be reduced by half when an oscillating current (u = u sin(2 π t / T) is introduced. The effect of the oscillation depends on the ratio of the period T to the time scale for cross sectional mixing.

Several methodologies of modeling the transport and dispersion of dissolved and/or suspended substances in streams and rivers have been developed over the years. The most common approach is to approximate the dissolved concentration of the substance, averaged over the cross section of the river, with the one-dimensional equation:

$$\frac{d}{dt}(AC)+\frac{d}{dx}(uAC)=\frac{d}{dx}\left(KA\frac{dC}{dt}\right) \qquad [2.2]$$

C represents the cross-sectionally averaged concentration, A the cross sectional area, u the average velocity (a function of location and time), and K is the longitudinal dispersion coefficient. x and t are downstream distance and time, respectively (Fischer 1976).

Various analytical solutions have been developed for simple cases (Maidment 1993). Numerical methods are generally required for real-life applications for flexibility and robustness. Procedures using finite difference or finite element methods experience various degrees of numerical dispersion. Other procedures have overcome this problem through use of a Lagrangian solution that incorporates a frame of reference moving with the advective component of the river. Either solution depends on the governing equation

– an averaged concentration model that simulates dispersion with one parameter (longitudinal dispersion coefficient for fixed reference models or transfer coefficient for Lagrangian models). Non-steady flows produce problems with selecting these coefficients as they may change over time and space. Averaging may be overcome by increasing to two or three dimensions, but come with a large computational burden.

Aris (1956) developed an approach for solving the diffusion equation using the method of moments. This is an analytical/numerical method that may be used to find a solution in three-dimensions. Velocity profiles are assumed for the vertical and transverse directions as well as transverse and vertical mixing parameters. Concentration may be solved for any desired accuracy, at the expense of great computational effort and the limitation of modeling a single channel. This method was used by Denton (1990) to explore the effect of dead zones on the evolution of a dispersing concentration as well as Bogle (1994) to verify the original PTM model.

An alternative approach to modeling the movement of substances through streams and rivers is a random-walk particle tracking model. In contrast with a concentration model, particle tracking simulates the movement of mass as individual, discrete particles. These models use an advective deterministic component with a random component superimposed to statistically simulate the chaotic or random nature of mixing. These particle tracking models have several advantages over concentration based models. Dimou and Adams (1993) and Bogle (1997) summarize these as: 1.) Sources are simulated more easily; concentration models have difficulty with concentration fields with spatial fields smaller than the discretized solution field; 2.) Computational effort is located only where particles are located, concentration models must make calculations at all locations for all times; 3.) Particle tracking better suits some modeling efforts where individual particles are clearly defined (such as fish larvae); 4.) Particle tracking may be more useful for aggregated properties (such as residence time) rather than concentrations; 5.) Behavior (such as mortality or settling rates) may be easier to simulate than with concentration; 6.) Global mass conservation is automatically assured; 7.) The ability to model releases without restrictions on the spatial or temporal range of validity, concentration models must wait until full cross-sectional mixing has occurred.

Sullivan (1971) used a random-walk particle tracking model to simulate the initial stages of dispersion in a two-dimensional, shear flow stream. Experimental and numerical simulations of dispersion showed the ability of this method to be used for detailed analysis. Allen (1982) showed Sullivan's work could be extended to an oscillatory tidal estuary without any theoretical difficulties. Chu and Gardner (1986) used a two-dimensional, advective particle tracking model to simulate sewage outfall into Humboldt Bay. Because diffusion was not included the results are believed to be approximate at best. Heslop and Allen (1993) applied a two-dimensional, random-walk particle tracking model to the River Severn with a logarithmic vertical profile. Simulations were compared to two tracer studies with good agreement. Dimou and Adams (1993) used a one dimensional particle tracking model for a tidally affected estuary. They concluded the average velocity of the particles movements were entirely affected by the deterministic advection component of transport. The random dispersive characteristics provided no net movement. The effects of dead zones on longitudinal dispersion have been investigated by Purnama (1988) and Denton (1990) with promising results.

Particle tracking models simulate two distinct motions: advective and random (or turbulent). Advective motion is identical to a deterministic hydrodynamic solution. The random or turbulent motion represents the diffusive and dispersive behavior. In streams and estuaries this is mainly caused by shear flow dispersion and represented by (usually) a Gaussian distribution.

Elder (1959) represented longitudinal dispersion by analyzing a logarithmic vertical velocity profile. This well known, and simple, approximation is:

$$K = 5.93\, d\, u^{*} \qquad [2.3]$$

where d is the water's depth, and u^{*} is the shear velocity, found by $u^{*} = (g\, R_h\, s)^{0.5}$, R_h is the hydraulic radius, g is gravity, and s is the slope of the energy grade line. The general form of Equation 2.3 is:

$$K = \frac{h^2\, u'^2\, I}{E} \qquad [2.4]$$

Where h is the depth of water, u'^2 is the turbulent velocity, I is a dimensionless integral representing the variation of velocity in three dimensions (usually assumed to equal 0.1), and E is a mixing coefficient. Several investigations, some by Godfrey and Frederick (1970), show that Elder's representation continuously underestimates longitudinal dispersion. Fischer (1966, 1967) shows this is due to the fact that the variation in transverse velocity across the stream is more important than the vertical velocity profile. Natural streams generally have a width to depth ratio of 10 or more. This suggests that the transverse velocity profile is two orders of magnitude more important in producing longitudinal dispersion than the vertical profile.

Fischer (1973) applied Taylor's analysis to the transverse profile and found

$$K = \frac{I\,W^2\,u'^2}{E_t} \qquad [2.5]$$

where I is a dimensionless triple integral which generally falls in the range 0.054 to 0.10, W is the channel width, u'^2 is a turbulent velocity, and E_t is the transverse mixing coefficient.

Due to the difficulties in accurately representing the longitudinal dispersion coefficient, and to the fact that Fischer (1973) found modeling results to be "insensitive" to the coefficient (the length of the dispersing cloud is proportional to the square root of the longitudinal dispersion coefficient) allows for an approximate method to work reasonably well. This starts with Equation 2.4 and makes the following assumptions: I = 0.07, h = 0.7W, the ratio u'^2/u to be 0.2. Additionally, the transverse mixing coefficient E or E_t is:

$$E_t = C_t\, d\, u^* \qquad [2.6]$$

Fischer approximates C_t as 0.6 and the ratio of the shear velocity u^* to mean velocity u as 0.1. The large amount of uncertainty in this representation is reflected in the +/- 50% accuracy reported by Fischer. Substitution of the above values into Equation 2.6 yields:

$$Et = 0.06\, d\, u^* \qquad [2.7]$$

$$= 0.006\, d\, u$$

A similar representation of the vertical mixing coefficient may be found. If the von Karman logarithmic profile is used, the vertical mixing coefficient ($kdu^*(z/d)(1-z/d)$), when averaged over the vertical depth, yields the vertical mixing coefficient:

$$E_v = C_v \, d \, u^* \qquad [2.8]$$

Where C_v is 0.067. This may be represented as:

$$E_v = 0.1 \, C_v \, d \, u \qquad [2.9]$$

$$= 0.0067 \, d \, u$$

Accuracy for this parameterization is also in the range of +/- 50% accuracy.

Combining these terms into the longitudinal dispersion coefficient equation results in

$$K = \frac{0.11 \, W^2}{d \, u^*} \qquad [2.10]$$

where W is width, d is depth, u^* is shear velocity. Inclusion of the uncertainty over the transverse mixing coefficient results in a range of coefficient values of 0.06 and 0.229.

Table 2.1 shows various values of longitudinal dispersion from a range of rivers. These serve as a guide to the range of longitudinal dispersion that may be found.

Table 2.1: Longitudinal Dispersion for Various Rivers (Fischer 1979)

Channel	Depth (m)	Width (m)	Mean Velocity (m/s)	Long. Disp (m2/s)
Clinch River, TN	0.85	47	0.32	14
Copper Creek, VA	0.40	19	0.16	9.9
Powell River, TN	0.85	34	0.15	9.5
Sacramento River	4.00	NA	0.53	15
John Day River	0.58	34	0.82	14
John Day River	2.47	34	0.82	65
Yadkin River	2.35	70	0.43	110
Sabine River	2.04	104	0.58	315

3. PTM Model

3.1 Introduction

The Delta Simulation Model 2 is the simulation model used by the DWR's Delta Modeling Section. There are three components: Hydro, Qual, and PTM. Hydro is a one-dimensional, unsteady hydrodynamic model. Hydro originated from the FourPt model developed by Lew Delong of the USGS (DeLong 1995, DWR 1999). It is a fully implicit unsteady flow model and is based on the one-dimensional Saint Venant equations:

$$\frac{d}{dt}\left(\rho M_a A\right)+\frac{d}{dx}\left(\rho Q\right)-\rho_q q=0$$

$$\frac{d}{dt}\left(\rho M_q Q\right)+\frac{d}{dx}\left(\beta\rho\frac{Q^2}{A}+\rho g I_1\right)+\rho g A\left(s_o+s_f\right)-\rho g I_2=0 \qquad [3.1]$$

where t is time, ρ is density, A is cross-sectional area, M_a is the area-weighted sinuosity coefficient, x is downstream distance, Q is the flow rate, q is the lateral inflow, ρ_q is the density of the lateral inflow, M_q is the flow weighted sinuosity coefficient, β is the momentum coefficient, g is gravity, s_o is the channel bottom slope, s_f is the friction slope, and I_1 and I_2 are integrals for averaging the depth over the cross section.

FourPt has been adapted for accommodating simulation in the Delta. These changes provide for inclusion of reservoirs, gates, and an entirely different input system. DSM2-Hydro Version 6.1 and DSM2-PTM Version 1.10 was used for this thesis. Output from the Hydro component is used by the other two modules for determination of the velocity and stage conditions throughout the delta. Thus, the water quality parameters determined by Qual and the particle movement from PTM do not affect the hydrodynamics of the

Delta system. The schematic representation of the Delta is represented in Figure 1.1 and 1.2. This representation of the Delta is modeled as a network of channel segments and open water areas. The hydro setup currently used is being updated by the Delta Modeling Section. This new calibrated Delta setup will improve on the current one with new geometric information. This is not available for implementation in this study due to time restraints.

3.2 PTM Theory

The PTM simulates the movement of particles in a channel by imposing a velocity field and random mixing across the channel. The mean channel velocity is found by the DSM2-Hydro model. The dispersive characteristics are determined by PTM. Velocity profiles are used to extrapolate the calculated one-dimensional velocity into a more realistic representation of velocity. This simulation of shear flow dispersion, along with random mixing coefficients, simulate the particle movements.

Longitudinal Dispersion

Longitudinal dispersion in the PTM is simulated by extrapolating the mean channel velocity from DSM2-Hydro into a psuedo three-dimensional velocity cross section. This representation allows the simulation of shear flow dispersion in which a particle traveling in the center of the channel (or top of the water column) will be subjected to a higher velocity than if it were at the sides of the channel (or at the bottom of the water column). This formulation does not directly use a longitudinal dispersion coefficient typically found in the literature. Instead, this is represented in the PTM as the standard deviation or variance of the distance of all the particles from the center of mass of the particles.

The transverse velocity profile is represented by a fourth order polynomial developed by Bogle (1997) of the form:

$$F_T = A + B\left(\frac{2y}{W}\right)^2 + C\left(\frac{2y}{W}\right)^4 \qquad [3.2]$$

where A, B, and C are constants, y is the depth of water, and w is the width of the rectangular channel. The three constants must be restricted such that the velocity at the sides of the channel is zero and to maintain a constant mean velocity. This is accomplished by satisfying the two equations:

$$A + B + C = 0 \qquad [3.3]$$

and

$$A + \frac{B}{3} + \frac{C}{5} = 1 \qquad [3.4]$$

When one constant value is selected, the other two are determined through solution of these two equations. Thus, selection of one constant determines the value of the others. Figure 3.1 shows the transverse velocity profile with various coefficients determined by A. The current transverse profile used by PTM is A = 1.62, B = -2.22, C = 0.6. Selection of this profile was achieved by matching the dispersion generated by these profiles to the dispersion predicted by Equation 2.10. Higher A values yield stronger peak velocity, while a lower A yields a flatter profile.

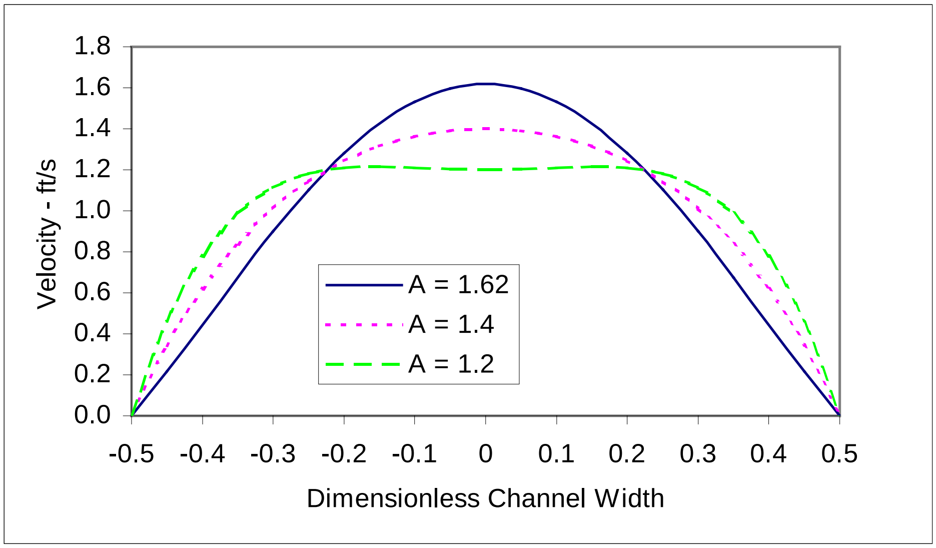

Figure 3.1: Transverse Velocity Profiles

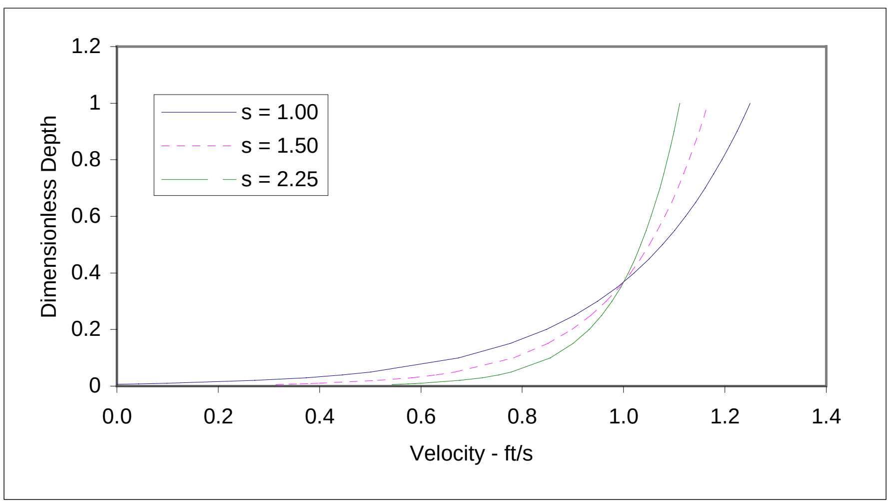

Figure 3.2: Vertical Velocity Profiles

The vertical velocity profile is represented as the Von Karmon logarithmic equation:

$$F_v = 1 + \frac{0.1}{k}\left[1 + \log\left(\frac{z}{d}\right)\right] \qquad [3.5]$$

where k is the von Karman constant, z is vertical position in the water column, and d is the depth of water. Inclusion of a shape factor s, multiplying the von Karman constant, allows the modification of the shear induced by the velocity profile:

$$F_v = 1 + \frac{0.1}{s\,k}\left[1 + \log\left(\frac{z}{d}\right)\right] \qquad [3.6]$$

Changing the shape factor yields different peak velocities. Figure 3.2 shows various vertical velocity profiles with different shape factors. The current PTM model uses an s of 1.0. Increasing this constant reduces the peak velocity.

One set of velocity profile coefficients are used for the entire Delta. They do not change with time or location. The transverse and vertical velocity profiles are scaled by the mean velocity in each channel. This results in the velocity at any point in the channel cross-section represented in Equation 3.7:

$$V(y,z) = \underline{u}\, F_T\, F_V \qquad [3.7]$$

Here V is the velocity at any point in the cross section and $\underline{u}$ is the mean velocity simulated by Hydro. The profiles used in the initial development of the model were selected purely on a theoretical basis. The coefficients will be selected based on data presented later.

Comparison of the effective dispersion generated by selection of the velocity profiles to the theoretical longitudinal dispersion predicted by Equation 2.10 is performed by determining the simulated longitudinal dispersion. The variance of the longitudinal displacement of particles is found by:

$$\sigma^2 = \frac{1}{N}\left[\sum x_i^2 - \frac{\left(\sum x_i\right)^2}{N}\right] \qquad [3.8]$$

Here σ^2 is the variance, N is the number of particles, and x_i is the longitudinal location of particle i. The effective longitudinal dispersion is then found by:

$$K(t) = \frac{\sigma^2(t) - \sigma^2(t - dt)}{2\,dt} \qquad [3.9]$$

PTM determines the position of each simulated particle as the longitudinal distance from the beginning of each channel, the vertical distance from the bottom of the channel, and the transversal distance from the centerline of the channel. The output may be modified to allow the results to be compared to concentrations of dissolved substances, such as data from a tracer study. The number of particles in a channel segment is scaled by the volume of water in that segment. This may be represented as:

$$C = f\,\frac{(\#\text{ of particles})}{AL} \qquad [3.10]$$

where A is the cross-sectional area, L is the length of the channel segment, and f is a scaling factor used to adjust to appropriate magnitude. The area changes with time as the stage and flow oscillate due to the hydrodynamics of the Delta.

4. Data

Two sets of data collected by the USGS are used for this calibration study. These consist of channel cross sectional velocity profiles and a Rhodamine WT tracer data.

4.1 ADCP

Acoustic Doppler Current Profiler (ADCP) data are used to measure the flow and velocity in the cross section of a channel. The ADCP instrument is an advanced acoustic device that sends signals into the water column. These signals reflect off particles moving with the water and return to the instrument. The ADCP measures the change in frequency in the signal and determines the velocity associated with the particles. The ADCP divides the depth of water into a series of vertical bins and returns the average velocity for each bin. The depth of each bin is approximately 0.3 meters. A series of these depth readings are made as the boat carrying the ADCP travels across the channel. The speed of the boat is removed from the velocity by using "bottom tracking." This results in a cross sectional view of the velocity field (RD Instruments 1996).

ADCP data were collected at sixteen sites in the Delta over a period of three years starting in 1997. The typical pattern of collection consists of between two to seven hours of cross section transverses at one location. This enables the collection of data to include a portion of the tidal motion. One transverse takes between five to fifteen minutes, depending on width of cross section. Table 4.1 lists the locations and dates of this data.

Table 4.1: Location and Dates of Collected ADCP Data

	1997			1999					
Location	April	May	June	March	April	May	June	July	August
Connection Slough					x	x	x	x	
Dutch Slough below Jersey Island Road @ Jersey Point									x
False River					x	x	x	x	
Grantline Canal @ Tracy Roud	x	x	x			x	x	x	
Middle River @ Middle River									x
Middle River South of Columbia Cut	x	x	x		x	x	x	x	
Old River @ Bacon Island									x
Old River @ Clifton Court Ferry	x	x	x						
Old River Near Webb Tract						x	x		
Sacramento River above Delta Cross Channel									x
San Joaquin River @ Jersey Point									x
San Joaquin River bet. Columbia & Turner Cuts	x	x	x						
San Joaquin River below Garwood Bridge @ Stockton				x					
Threemile Slough @ San Joaquin River						x			
Turner Cut	x	x	x		x	x			
Victoria Canal	x	x	x						

Figures 4.1 and 4.2 show the measured data for Turner Cut. Figure 4.2 shows the transverse and vertical velocity profiles measured on April 9, 1997 at 1:30pm. Figure 4.1 shows the tidal influence on the flow at this location. Averaging the velocity profile data allows the irregular data (due to turbulence) to be smoothed as Figure 4.2 shows. The averaging was done as a running mean of 5 to 15 data points. The general trend of the velocity profiles does correlate with the vertical and transverse profiles assumed in the PTM model. Comparisons with the PTM profiles are presented in a later section.

Similar characteristics are found at the San Joaquin River between Columbia and Turner Cuts. Figures 4.3 and 4.4 show the flow and ADCP velocity profile data on April 4, 1997 at 10:30am.

Additional locations showing cross sectional velocity magnitudes are shown in Appendix I in Figures I-1 to I-48 for different stages in the tidal sequence. The stage data corresponding with these times are also provided. Inspection of these figures shows a great deal of heterogeneity in the channel cross-section and velocity magnitudes.

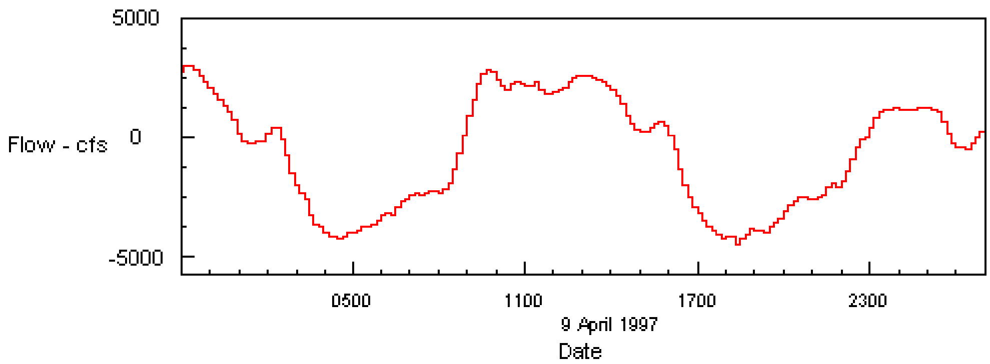

Figure 4.1: Historical Flow at Turner Cut

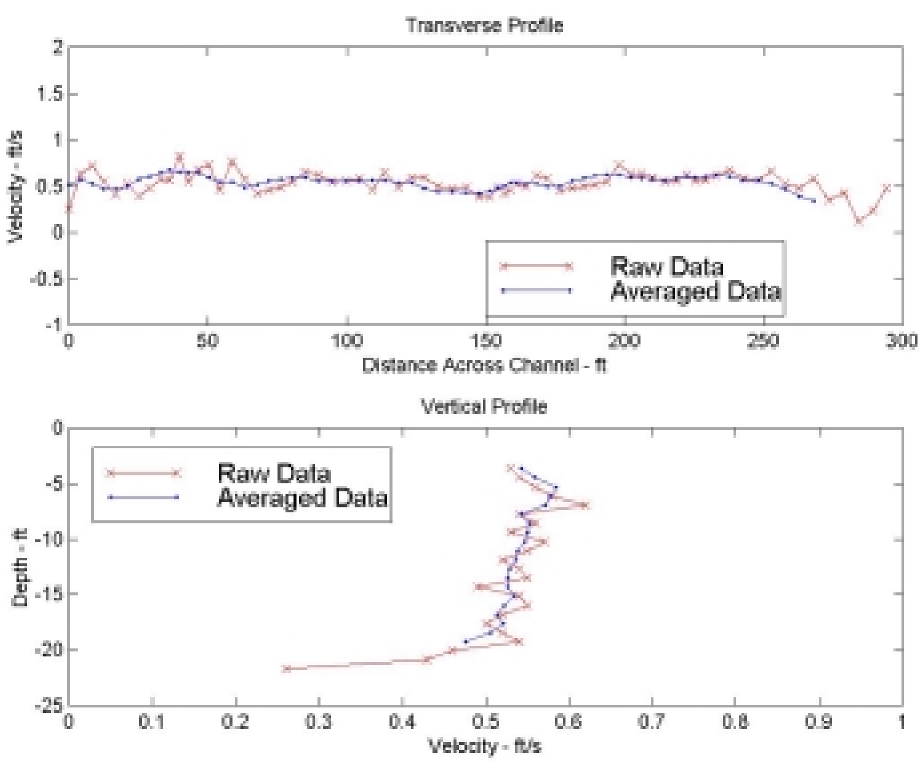

Figure 4.2: Turner Cut ADCP Profile Data (April 9,1997 1:30pm)

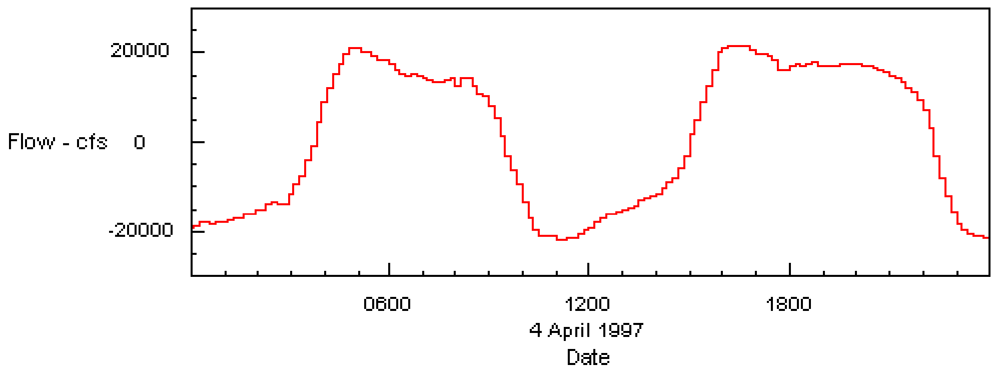

Figure 4.3: Historical Flow for SJR between Turner and Columbia Cuts

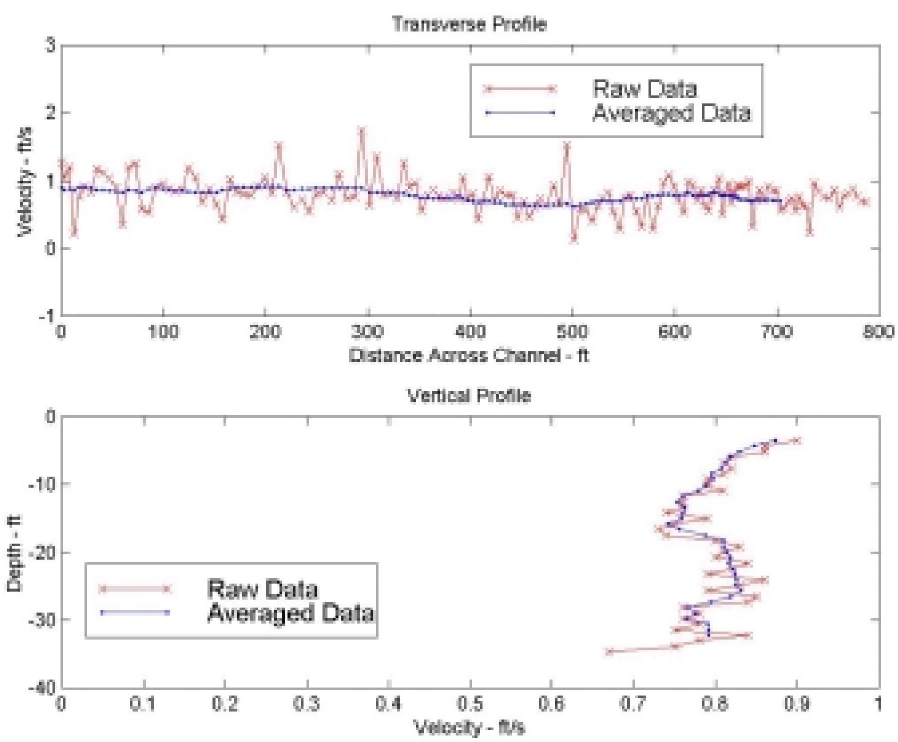

Figure 4.4: SJR between Turner and Columbia Cuts ADCP Profile Data

(April 4,1997 10:30pm)

4.2 Tracer

The tracer study used in this project was conducted and presented by Oltmann (1998) and is summarized here. A Rhodamine WT tracer study was performed in April and May of 1997 to track the movement of water into which tagged salmon smolts were released. The tracer was released at noon on April 28, 1997 near Mossdale on the San Joaquin River one hour prior to the release of 50,000 salmon smolts by the U.S. Fish and Wildlife Service and California Department of Fish and Game. 48 liters of 20% Rhodamine WT was released over a fifteen minute period. Nine automatic sampling measurement sites in the Delta were used to record the concentration of the tracer. These took samples on an hourly basis and were retrieved and transported to a laboratory where a fluorometer was used to measure the tracer concentration. Figure 4.5 shows the locations of the tracer data collection sites; the locations are Grantline Canal at Tracy Blvd bridge, Jersey Point, Middle River at Middle River, Middle River South of Columbia Cut, Old River at Bacon Island, Old River at Clifton Court Ferry, Turner Cut, San Joaquin River at Stockton UVM site, and San Joaquin River at Mandeville Ranch.

The tracer was released during the Vernalis Adaptive Management Plan's (VAMP) pulse-flow period on April 28, 1997. The flow on the San Joaquin River near Mossdale is shown in Figure 4.7. The tracer traveled from the release point to the Stockton UVM sampling site (about 13 miles) in about 10 hours (mean velocity of 1.9 ft/sec). Figure 4.6 shows the tracer concentration for the Stockton UVM site. This shows the peak concentration reached 10.5 ug/L and took about four hours to pass the site.

Turner Cut tracer concentration and flow are shown in Figures 4.8 and 4.9. Turner Cut is approximately 10 miles downstream from the Stockton UVM site. Travel time for the tracer to reach Turner Cut was about 25 hours (mean velocity 0.6 ft/sec). As Figure 4.9 shows, this portion of the Delta is influenced much more by tidal forces than the Stockton UVM site resulting in the tracer taking more time to pass this site due to the reversing flow conditions. The peak concentration reached about 0.8 ug/L and the tracer took just over two days to pass the site.

Figure 4.5: Location of Tracer Study Data Collection Sites

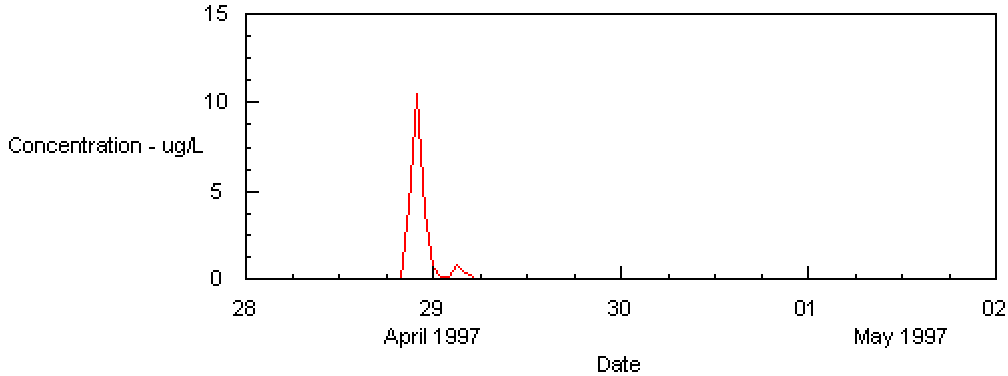

Figure 4.6: Tracer Concentration at Stockton UVM Site.

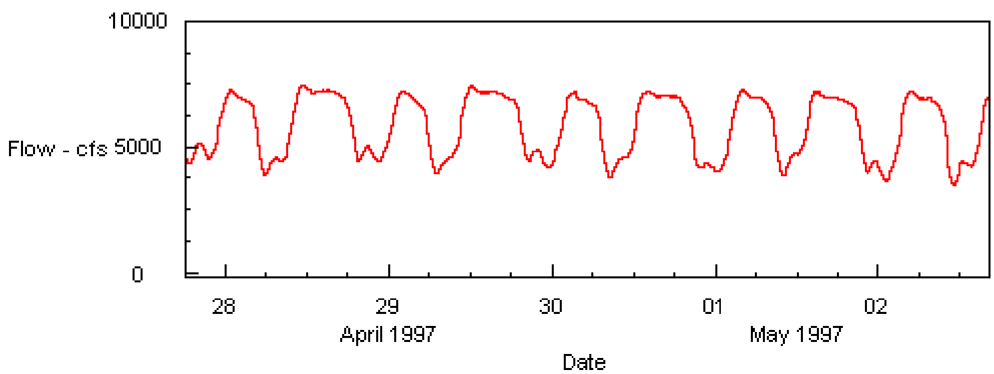

Figure 4.7: Measured Flow at Stockton UVM Site.

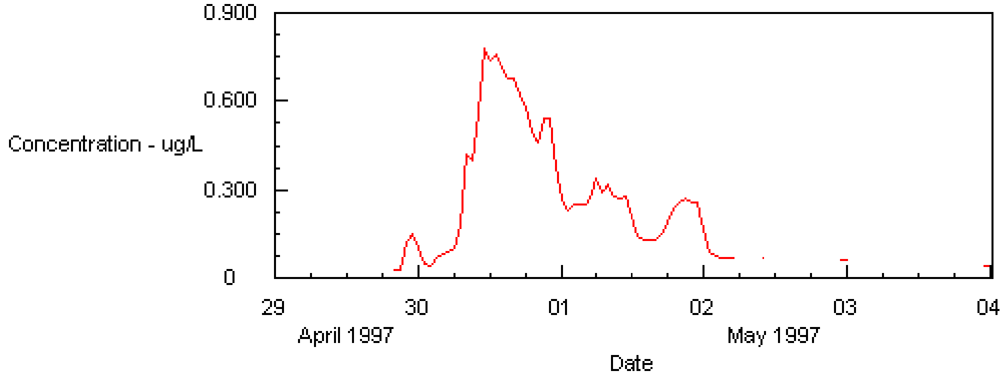

Figure 4.8: Tracer Concentration at Turner Cut.

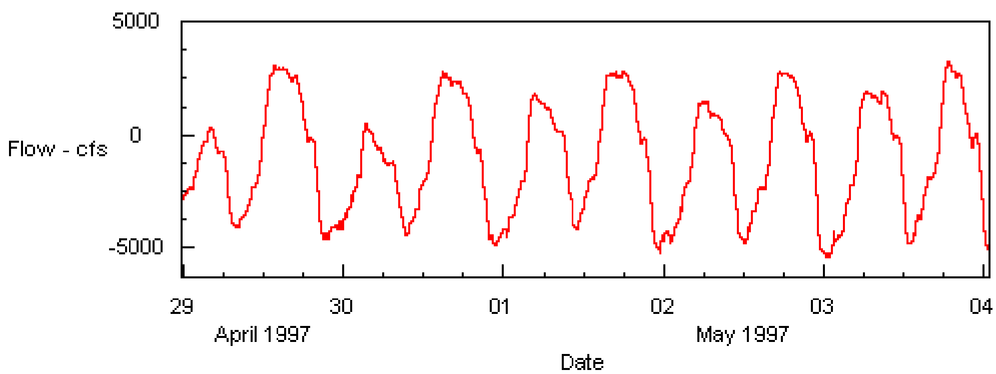

Figure 4.9: Measured Flow at Turner Cut.

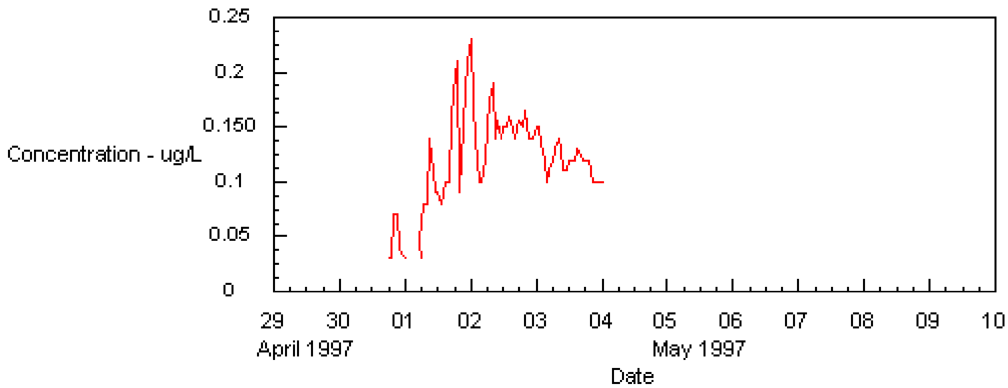

Figure 4.10: Tracer Concentration at San Joaquin River near Mandeville Ranch.

Figure 4.10 shows the tracer concentration at San Joaquin River near Mandeville Ranch. No measured flow data were available for this location. The peak concentration is reduced and the length of time passing the site is increased compared to the previous two locations. This is due to the increased mixing caused by tidal forces in the Delta. Similar results were found at Middle River South of Columbia Cut, shown in Figures 4.11 and 4.12.

Figures 4.13 and 4.14 show the tracer and measured stage at Grantline Canal near the Tracy Blvd Bridge. This shows some flow was able to pass through the barrier and culverts installed at the Head of Old River. The concentrations measured at Grantline are fairly small compared to the other locations.

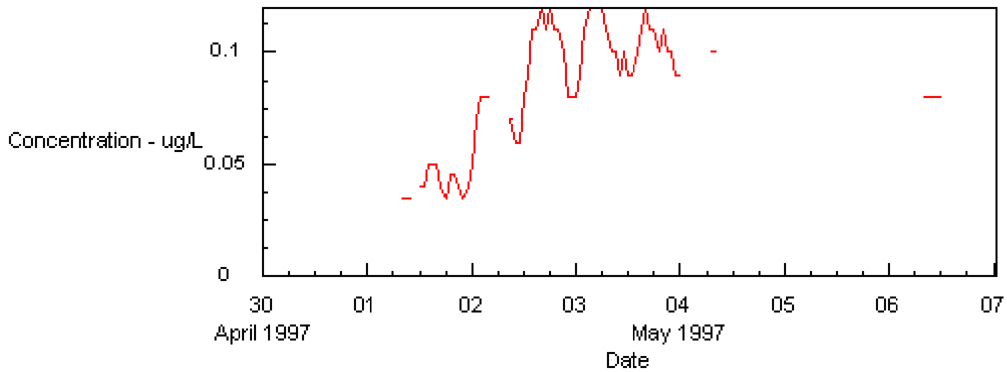

Figure 4.11: Tracer Concentration at Middle River near Columbia Cut.

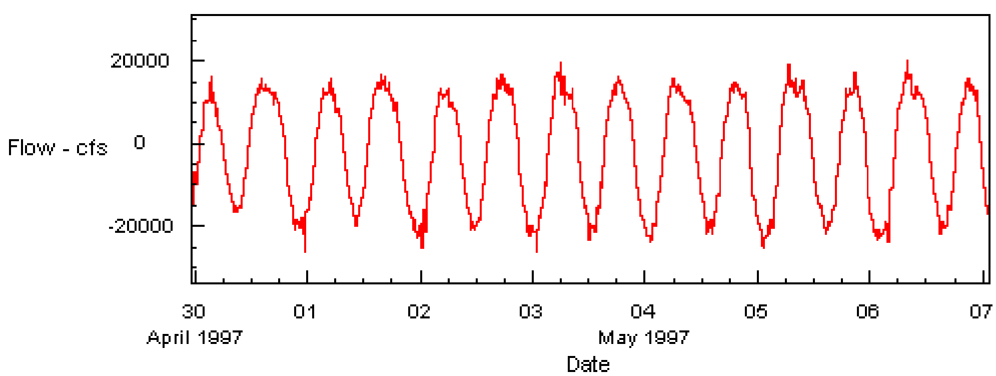

Figure 4.12: Measured Flow at Middle River near Columbia Cut.

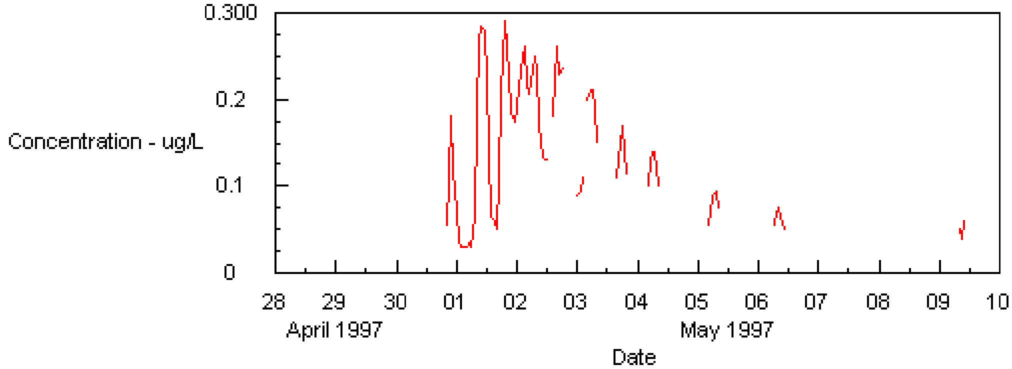

Figure 4.13: Tracer Concentration at Grantline Canal near Tracy Blvd Bridge.

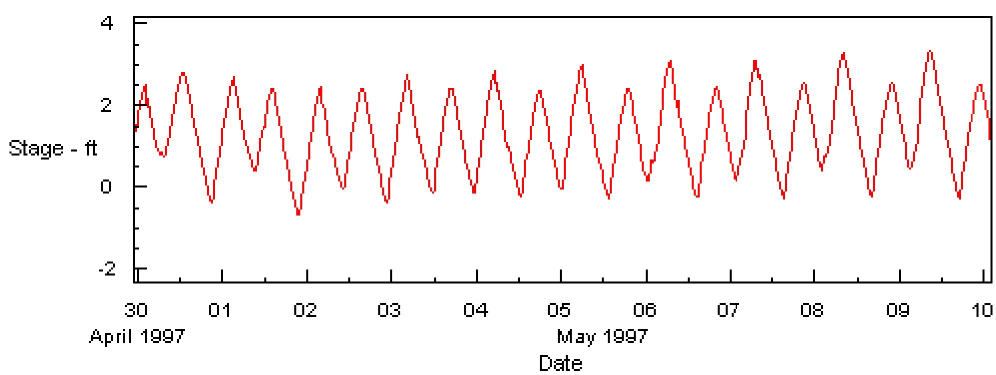

Figure 4.14: Measured Stage at Grantline Canal near Tracy Blvd Bridge.

Other locations where tracer samples were recorded experienced difficulties making the data inapplicable for the purpose of this project. All collected at Old and Middle River UVM sites showed concentrations no higher than background concentrations (about 0.04 ug/L). The Old River UVM (near Clifton Court Forebay) measured the tracer arriving prior to the arrival at Grantline Canal – this shows something was interfering with the measurement. The Jersey Point station did not record any data.

5. Modeling Results

5.1 Profile Comparisons

Comparison of velocity profiles between the ADCP data and those used by the original PTM profiles show some inconsistencies. The profiles used by the PTM model have the same mean velocity, but consistently over predict variation in peak velocity across the channel. This leads to the overestimation of shear flow dispersion calculated by PTM. Modification of the velocity profile coefficients yields an improved representation of the velocity fields.

Adjustments of the coefficients for the transverse and vertical velocity profiles make it possible to improve the representation of these idealized profiles to better approximate the profiles measured by the ADCP data. Figures 5.1 and 5.2 show the velocity data for Turner Cut shown previously. These now have additional information including the original and modified profiles. The modified profiles, obtained by inspection, were found to better represent the transverse and vertical velocities. Coefficients selected for the transverse profile are A = 1.2 and for the vertical profile the shape factor s = 1.25. Figures 5.3 and 5.4 show similar graphs for San Joaquin River between Columbia and Turner Cuts.

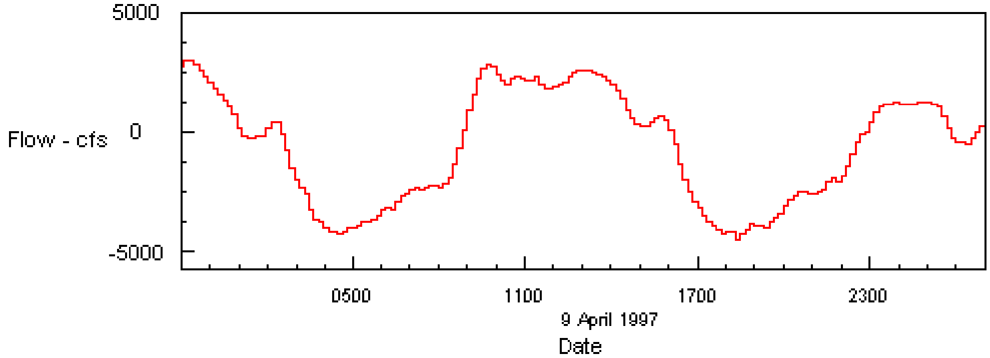

Figure 5.1: Turner Cut Flow

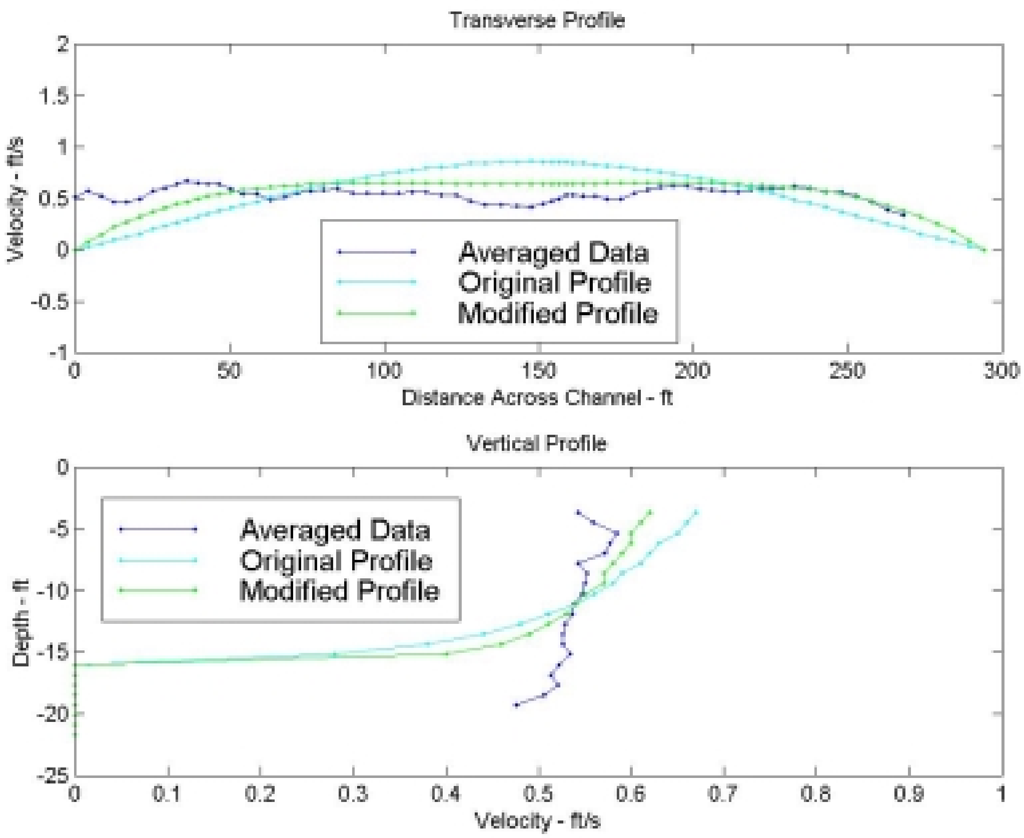

Figure 5.2: Turner Cut Profile – ADCP Comparison (April 9, 1997 1:30pm)

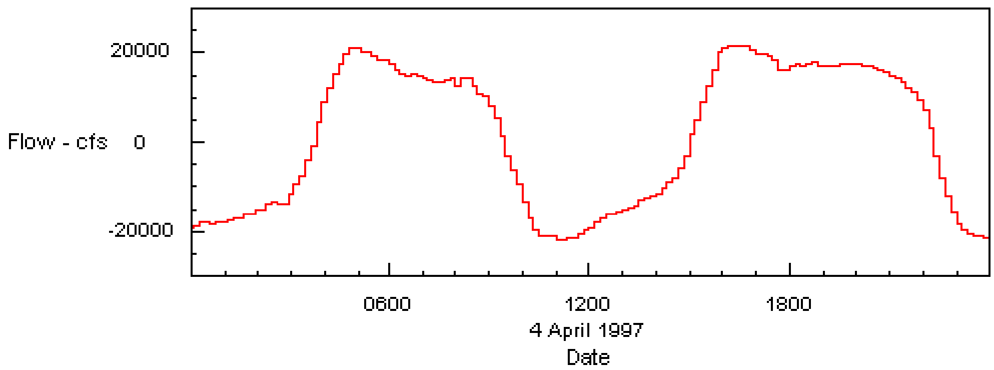

Figure 5.3: SJR between Columbia and Turner Cuts, Flow

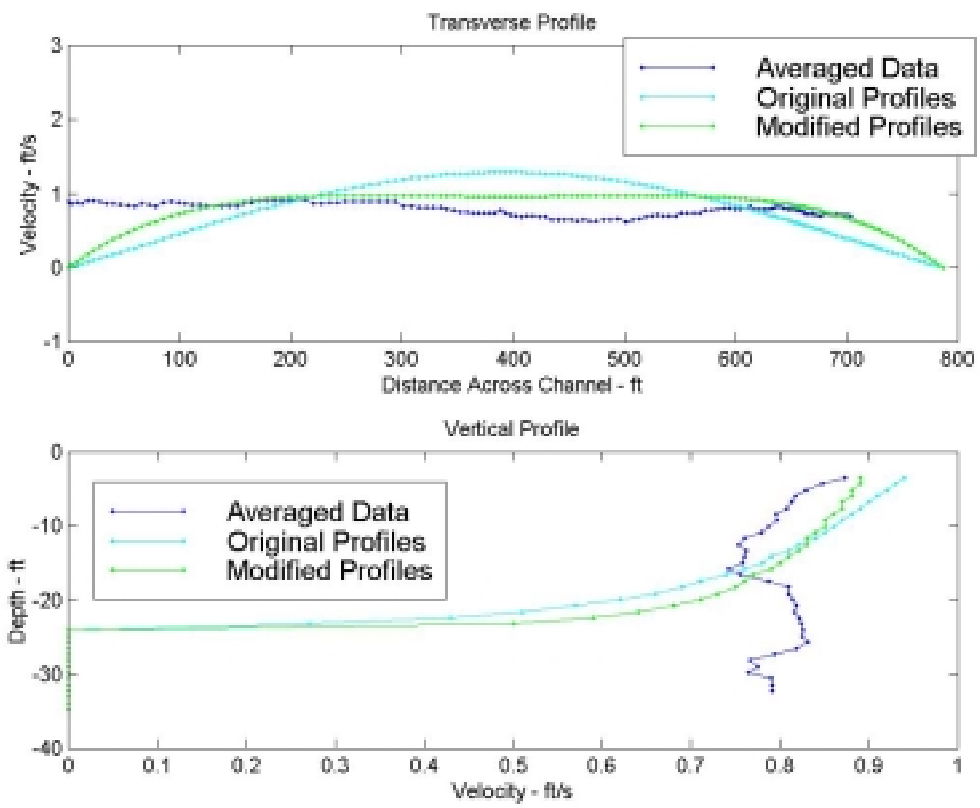

Figure 5.4: SJR between Columbia and Turner Cuts, Profile and ADCP Comparison (April 4, 1997 10:30pm)

Additional figures presented in Appendix I show the comparisons between the ADCP data and the theoretical transverse and vertical velocity profiles for both the original and the modified profile coefficients. The vertical velocity profile shows more inconsistencies when compared to the ADCP data than the transverse profile. Several of the figures show a uniform vertical velocity profile may better represent the observed data. In a later section a uniform vertical velocity profile, as well as a uniform transverse velocity profile, will be compared to the modified velocity profiles shown in the figures.

5.2 Longitudinal Dispersion

A single hypothetical channel was represented in DSM2 in order to investigate the behavior of the Particle Tracking Model's implementation of longitudinal dispersion. Modification of the velocity profile coefficients controls the amount of dispersion superimposed on the advection of mass of particles. Velocity profile coefficients used for this simulation were both the original (A = 1.6, s = 1.0) and the modified profiles (A = 1.2, s = 1.25). The channel has width 500 feet, average depth of 40 feet, and average velocity of 1.6 ft/sec. 10,000 particles were inserted instantaneously at the furthest upstream location.

Figure 5.5 shows the particle concentration for the original and modified velocity profiles. Three locations are shown (at 5, 20, and 35 miles downstream of the beginning of the channel) which demonstrate how, under steady flow conditions, the different dispersion scenarios transport the particles. The original profiles produce more dispersion. This is shown in the figure by the smaller peak concentration and the longer time it takes to pass a single site. The modified profiles, having less dispersion, have higher concentrations and behave more advectively.

Equation 2.10 may be used to predict theoretical longitudinal dispersion. The range of theoretical longitudinal dispersion for this channel is 165 to 4900 ft2/sec as determined by the uncertainty of Equation 2.10. Figure 5.6 shows the variance for the longitudinal displacement of particles produced by the original velocity profiles. The linear nature, once dispersion has fully developed, reflects the steady state condition. Figure 5.7 shows the effective longitudinal dispersion coefficient based on the original profiles. The steady state range approaches 1200 ft^2/s, which is in the range of theoretical dispersion in Equation 2.10. This figure shows the first 3 hours of simulation time. A period of about two hours is needed for the dispersion to fully develop. The fluctuations in the curve are due to the randomness of the random mixing coefficients.

Figure 5.8 and 5.9 show the variance of longitudinal displacement and the effective longitudinal dispersion coefficient using the modified velocity profiles. The steady-state value of dispersion for the modified profiles is about 300 ft^2/s, which is also in the range of theoretical longitudinal dispersion. The modified velocity profiles yield a smaller longitudinal dispersion coefficient. This value is still within the range of acceptable values, as compared to those from Table 2.1.

Inclusion of a tidal influence at the downstream end of the channel allows for the investigation of how longitudinal dispersion behaves in the Delta. A repeating 25-hour oscillating stage was added to the downstream boundary condition. Figure 5.10 shows a segment of the historic tide used for this example. Predicting a longitudinal dispersion coefficient by Equation 2.10 in a tidally influenced system becomes difficult because a steady state condition never develops – the dispersion coefficient is always changing. Additionally, in real systems with many branches, such as the Delta, the mass of particles becomes separated into different channels as the tide forces the flow throughout the system. Each channel typically experiences different flow and tidal conditions at different times, producing different dispersion coefficients for each.

Figure 5.11 shows the tidal influence on the stage for different locations in the channel. The upper reaches (5 and 20 miles downstream) are slightly influenced while the lower reaches (34 and 45 miles downstream) are significantly affected by the tide. Figure 5.12 shows the particle concentration for three locations in the channel. The tide at the various locations has delayed the arrival time of the particle cloud by almost 12 hours and reduced the peak concentrations.

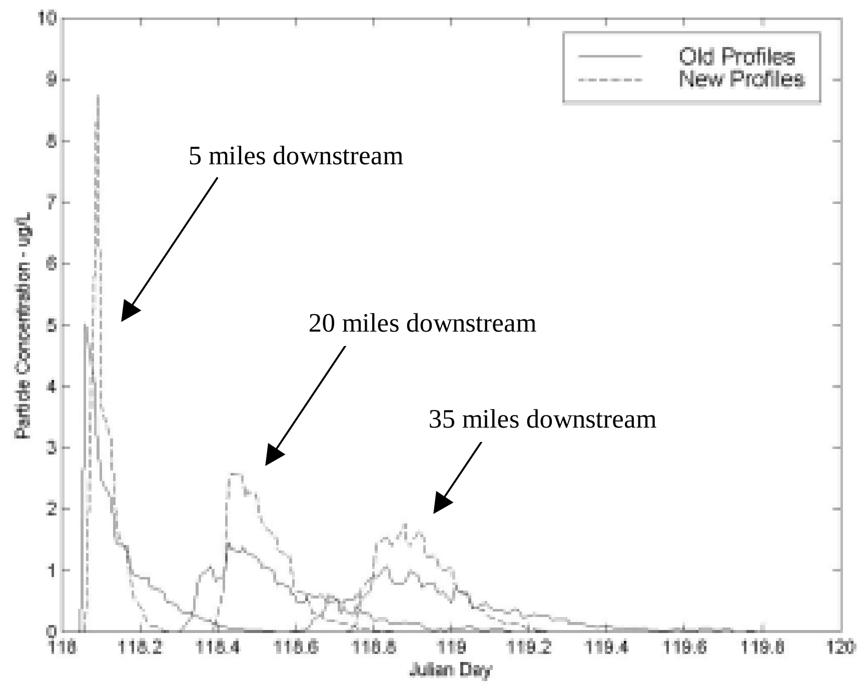

Figure 5.5: Particle concentrations for a Single Long Channel

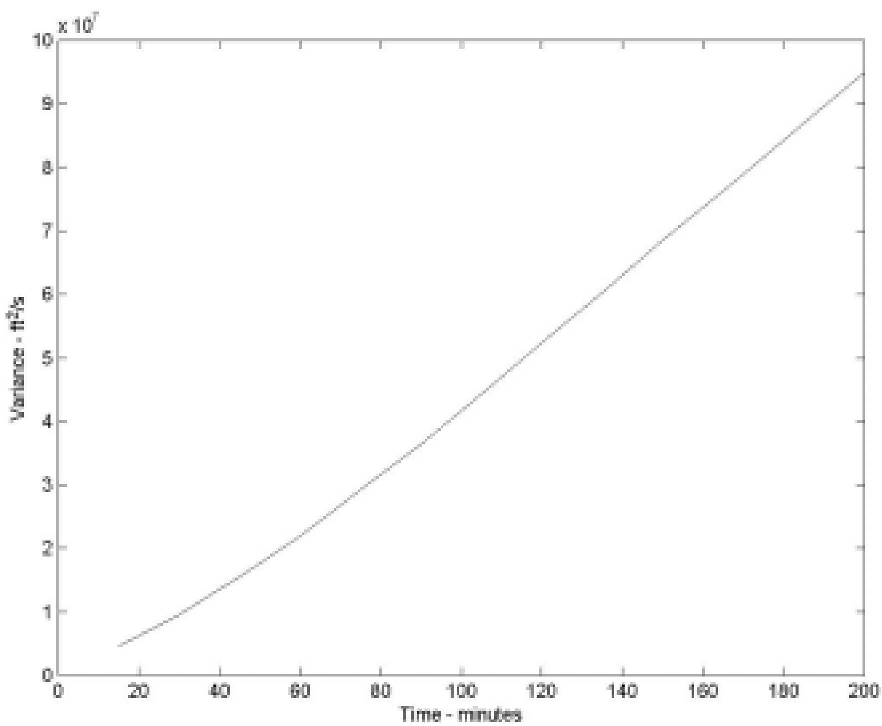

Figure 5.6: Variance of Longitudinal Displacement for Original Profiles.

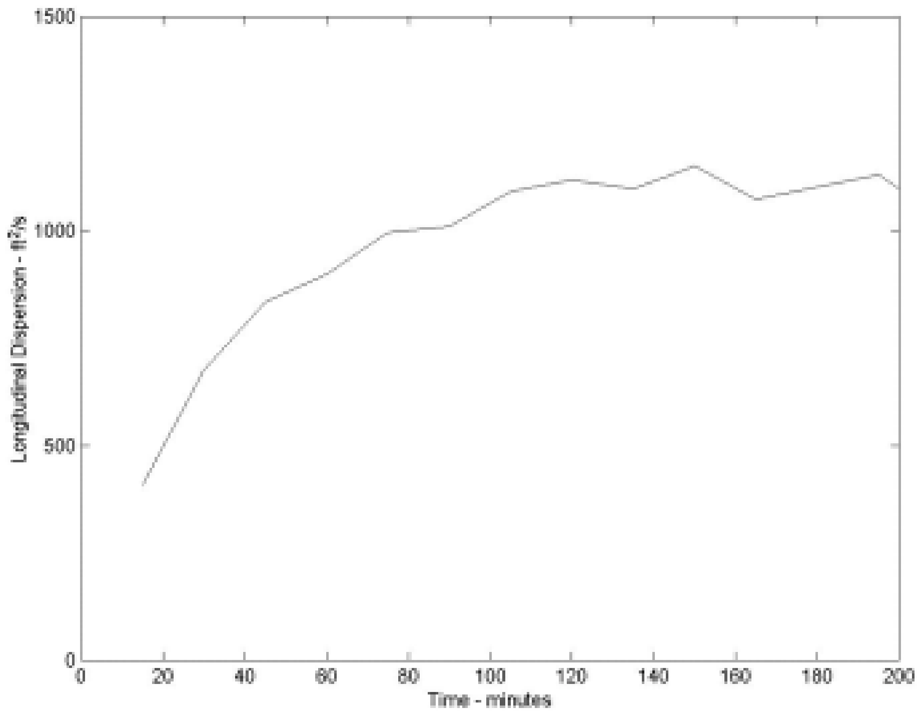

Figure 5.7: Effective Longitudinal Dispersion for Original Profiles.

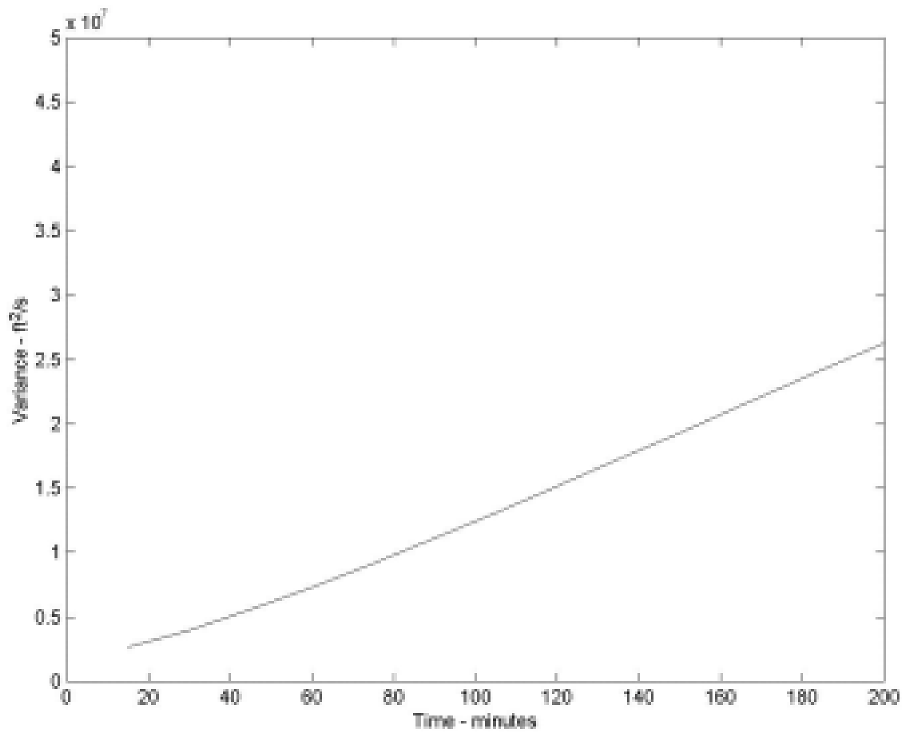

Figure 5.8: Variance of Longitudinal Displacement for Modified Profiles.

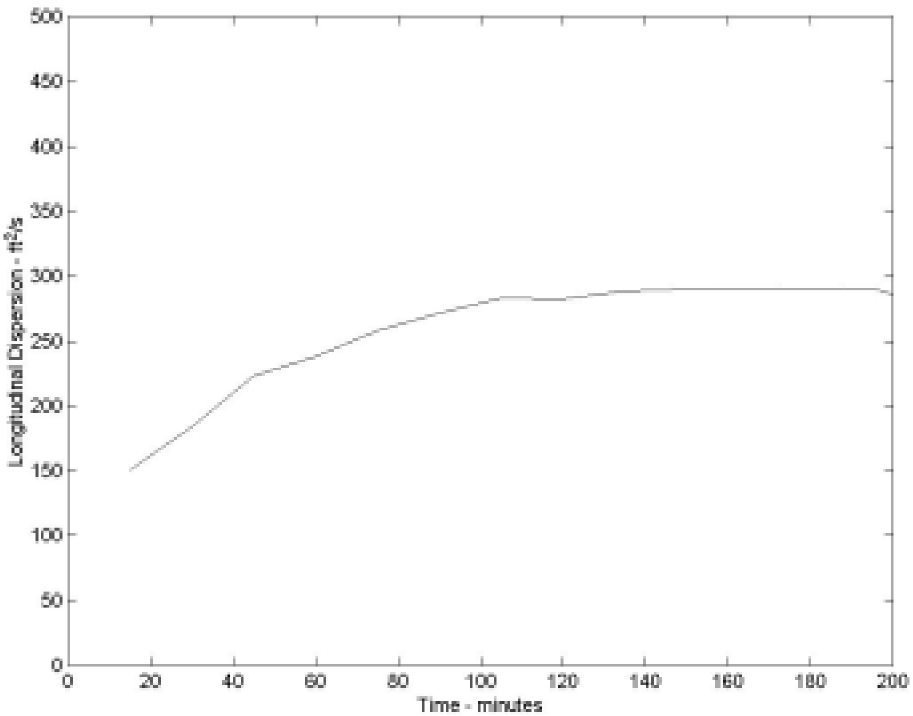

Figure 5.9: Effective Longitudinal Dispersion for Modified Profiles.

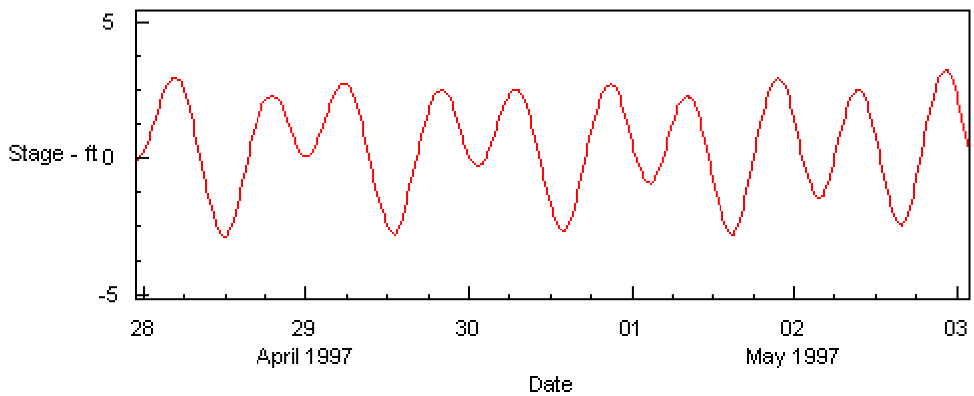

Figure 5.10: Stage Boundary Condition for Long Channel.

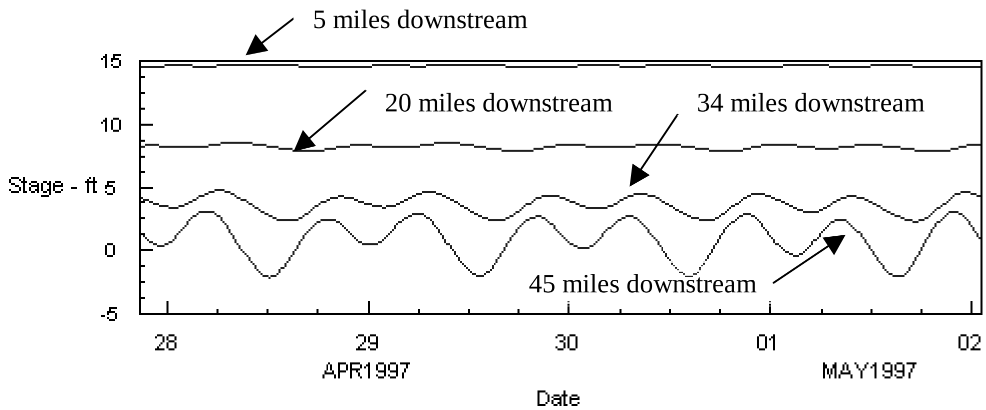

Figure 5.11: Stage at Various Locations influenced by Tidal Boundary Condition.

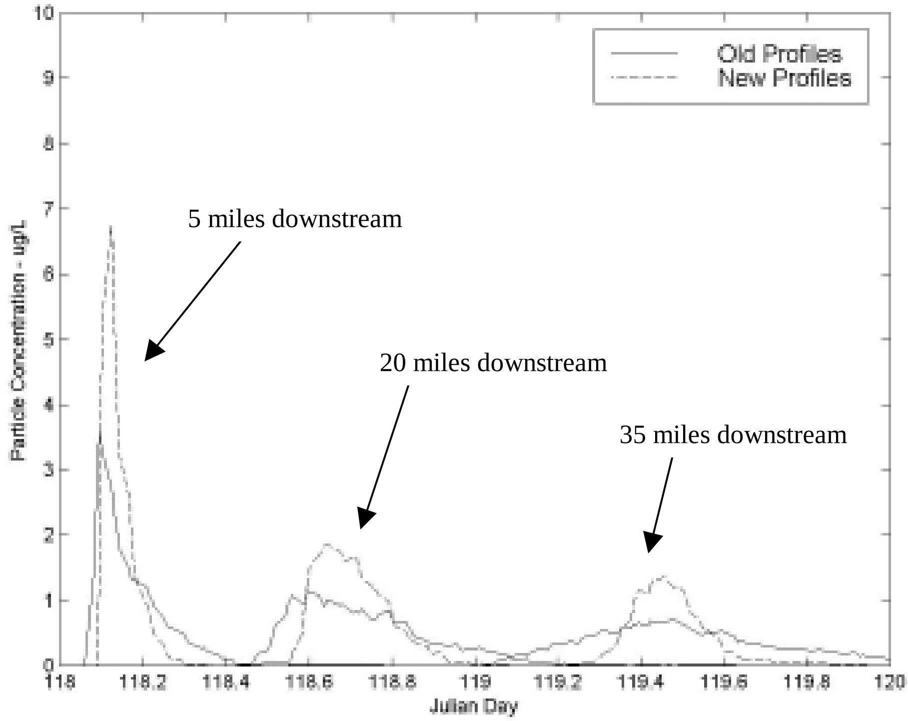

Figure 5.12: Particle Concentration for Long Channel with Tidal Boundary Condition.

5.3 DSM2 Results

5.3.1 Hydrodynamics

The hydrodynamics of the delta are important to represent accurately in order for the PTM model to give accurate results. While the hydrodynamics are not the focus of this investigation, they are presented here for completeness.

The simulations use an historical real tide for the western-most boundary at Martinez. The stage used as a boundary condition is shown in Figure 5.13 for the duration of the tracer study. There is a 25-hour repeating tide sequence. This includes a 12.5-hour period between each high tide (also for low tide).

Gate operations are accounted for in such places as the Delta Cross Channel and temporary barriers at Head of Old River. Documented gate installation and operations come from DWR (Aug 1998).

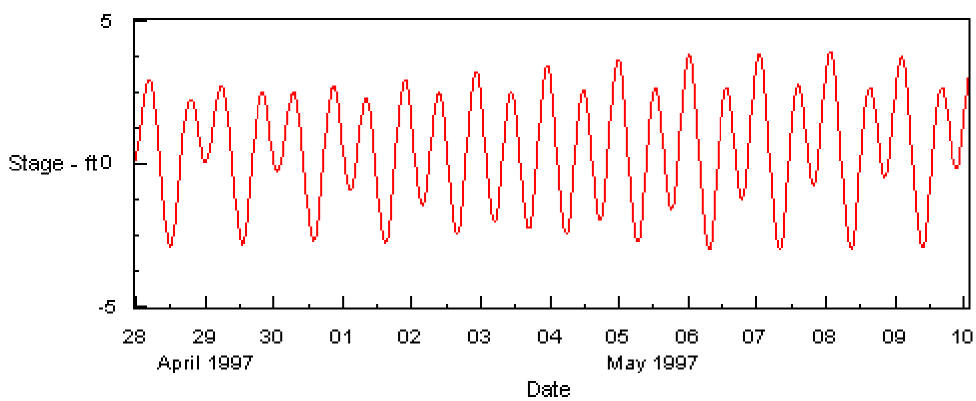

Figure 5.13: Martinez Stage Boundary Condition.

Stage and Flow results are presented with historical data at various locations. Locations of interest for the tracer study are shown. Figures 5.14 – 5.17 show Hydro simulation results with historical data for Turner Cut, Jersey Point, Old River near Bacon Island, and Middle River at Middle River.

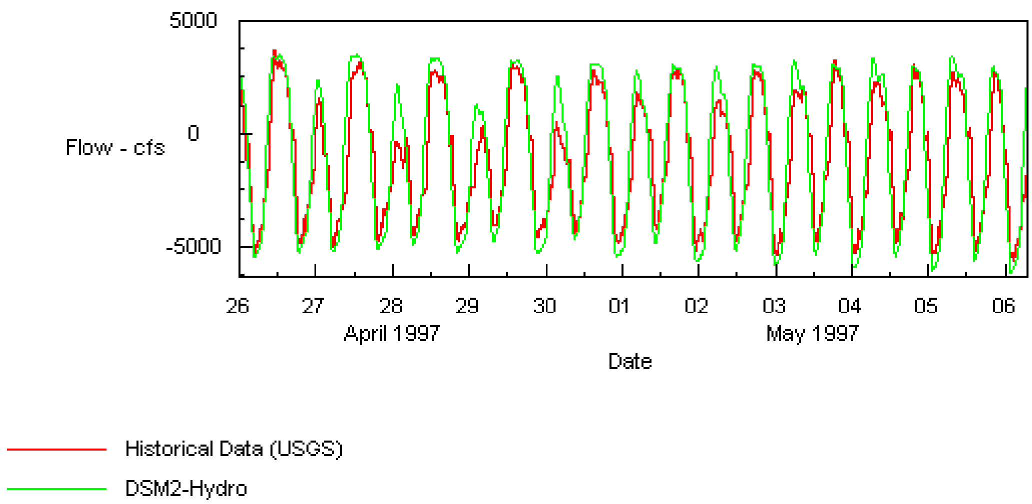

Figure 5.14: DSM2 and Measured Flow, Turner Cut

Figure 5.14 shows the simulated flow at Turner Cut. Hydro represents fairly well the measured flow. The extreme magnitudes on the tidal oscillation show the greatest amount of problems for this and other sites. The largest inconsistencies are about 600 cfs, while the majority of the time these measure less than 200 cfs.

Figure 5.15 shows the simulated and measured flow for Jersey Point. This also shows the majority of the inaccuracies with Hydro have to do with simulating the peak flows. Due the magnitude of the flow at Jersey Point the small differences shown on the figure are approximately 2,000 cfs.

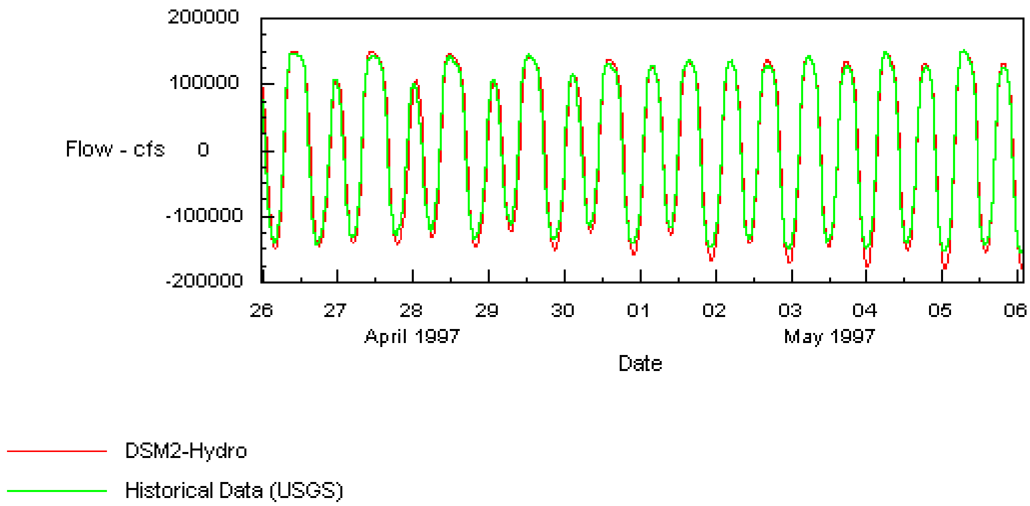

Figure 5.15: DSM2 and Measured Flow, Jersey Point

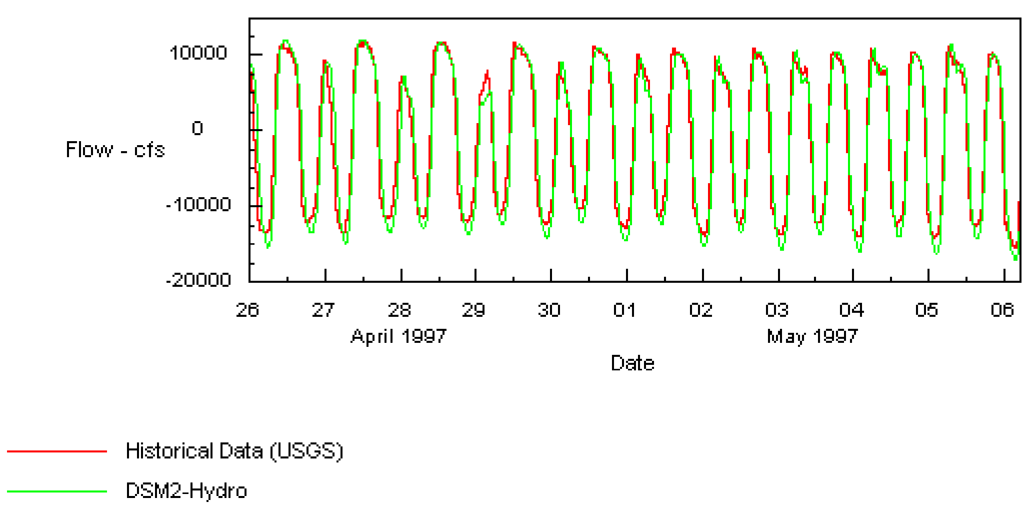

Figure 5.16: DSM2 and Measured Flow at Old River near Bacon Island

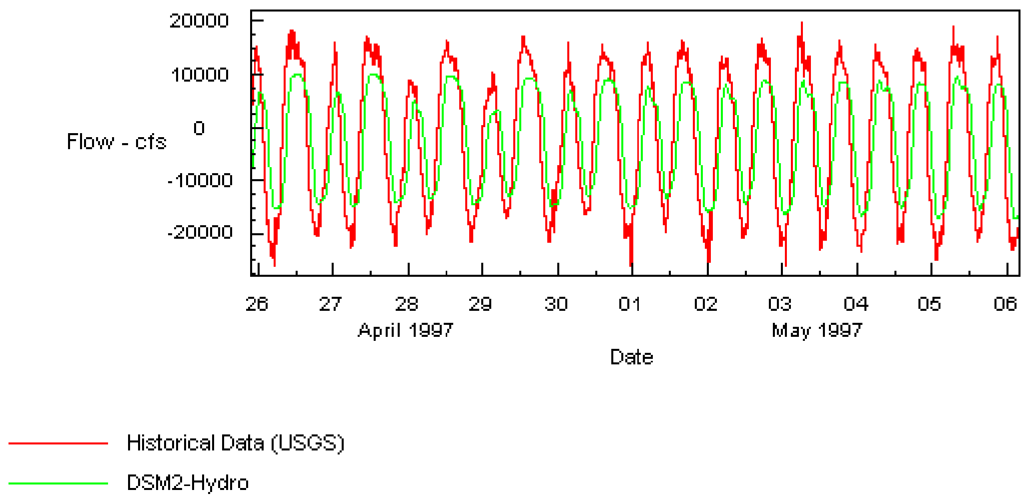

Figure 5.17: DSM2 and Measured Flow, Middle River South of Columbia Cut

Flow at Old River near Bacon Island is shown in Figure 5.16. Similar results are found comparing the measured and simulated flow. Differences between the two are less than 1,000 cfs.

Comparing simulated and measured flow for Middle River South of Columbia Cut shows a rather large amount of disagreement. Figure 5.17 shows differences of nearly 10,000 cfs. This mismatch is probably due to poor representation of the bathymetry.

5.3.2 PTM – Tracer Comparisons

The original velocity profiles are used in the first simulation to compare it to the collected tracer data. An additional simulation was performed with modified velocity profiles that more accurately represent the velocity profiles found in the ADCP data.

As discussed earlier, the concentrations for the tracer study are reliable at only a few sites. The PTM simulations and tracer data are compared at these locations only. Three locations in particular have high enough concentrations to be used in testing the PTM model; these are Turner Cut, Mandeville Ranch, the UVM site near Stockton, and Middle River South of Columbia Cut.

The PTM simulations compared here use the velocity profile coefficients listed in Table 5.1. The PTM results (position of each particle) are converted to a concentration through use of Equation 3.10. The factor used to scale the particles to micro-grams per liter is 318,000.

Table 5.1: PTM Velocity Profile Coefficients

	A	B	C	Shape Factor
Original Profile	1.62	-2.22	0.6	1.0
New Profile	1.2	0.3	-1.5	1.25

The first location, Stockton UVM, is shown in Figure 5.18. This figure shows the tracer data, and PTM simulation results with original and modified profile configurations. It appears the original profiles more accurately represent the tracer data. It should be kept in mind that the distance of the Stockton UVM site is close to the particle injection point. The modified profiles do not mix across the channel to simulate full mixing of particles.

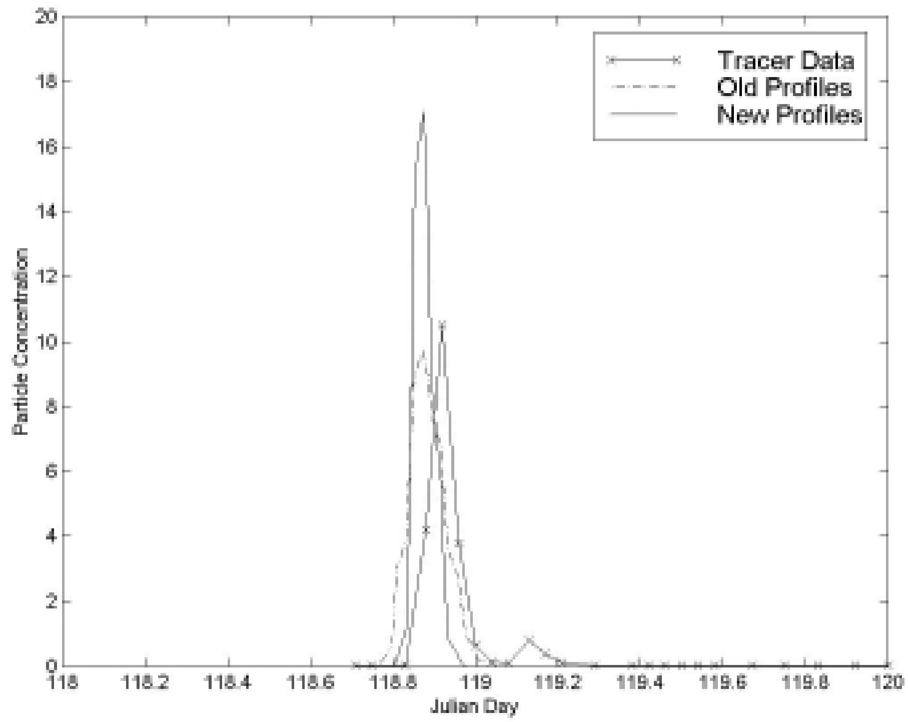

Figure 5.18: PTM and Tracer Comparison, Stockton UVM Site

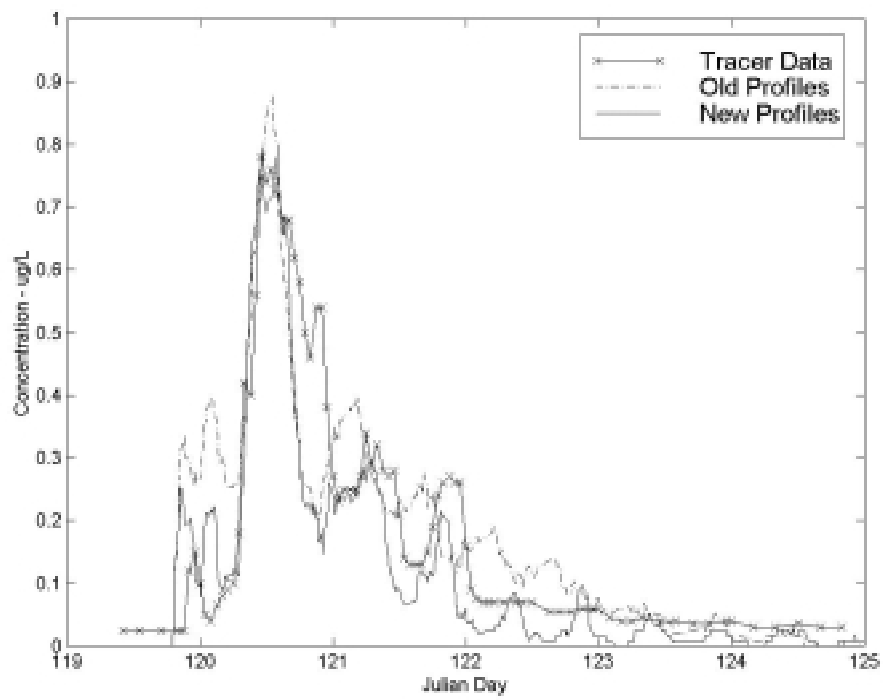

Figure 5.19: PTM and Comparison, Turner Cut

Figure 5.19 shows the tracer data and PTM results for the Turner Cut location. This shows the clearest difference between the two sets of profiles in their effects on the particle dispersion. While both profiles simulate the main peak concentration (at time 120.5) the new profiles better simulate the arrival of particles at the first (time 120), third (120.2), and fourth (120.9) peaks. The new profiles simulate a lower concentration at the first spike and arrives closer to the time the tracer data does. The original profiles do a poorer job at predicting the arrival time of these particles. Following the fourth concentration spike both PTM profiles predict more oscillations in the concentration than exist in the data. This is possibly due to inaccuracies in the hydrodynamics or to recording of tracer at low concentrations close to background levels.

Figure 5.20 shows the same PTM – tracer comparisons at the San Joaquin River near Mandeville Tract. This location experiences much more oscillations, in both PTM and in the tracer data, than the other locations. Both profiles demonstrate they over predict as well as under predict the concentrations at different times. Because of this it is difficult to determine which one simulates the tracer data more accurately. The causes of these extreme oscillations are possibly due to hydrodynamic problems or to the method of converting the PTM output to concentrations.

Figure 5.21 shows different results for Middle River South of Columbia Cut. The PTM model does not simulate the tracer movement through this location very accurately. It is believed the problem is associated with the hydrodynamic model not properly simulating the flow, as shown in Figure 5.17.

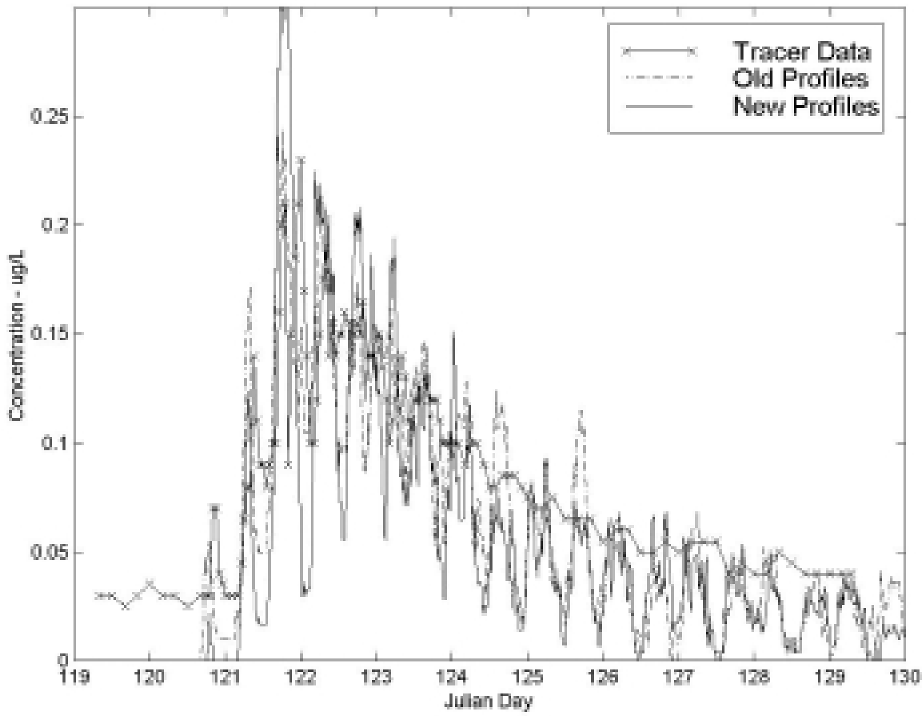

Figure 5.20: PTM and Tracer Comparison, SJR at Mandeville Reach

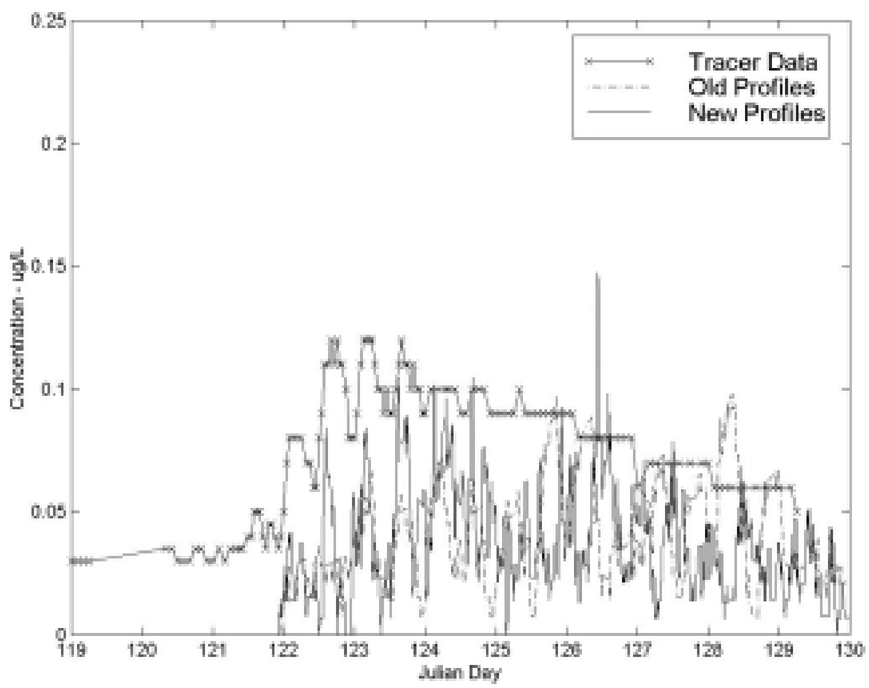

Figure 5.21: PTM and Tracer Comparison, Middle River South of Columbia Cut

5.3.3 No Dispersion

Investigation of the importance of dispersion to the movement of particles throughout the Delta is now investigated with comparisons to the new velocity profiles discussed earlier. The first condition compared is the case where the system is only subjected to advective forces. The flow in both the vertical and transverse directions are uniform, thus the velocity across the entire channel is equivalent to the mean velocity.

Figure 5.22 displays the tracer study data, the simulated tracer concentration using the new profiles, and the no-dispersion condition at Turner Cut. The arrival time of particles under the no-dispersion case matches fairly well with both the tracer and new profiles. This suggests the dominance of advection in the Sacramento – San Joaquin Delta over the effects of dispersion. However, it is obvious the no-dispersion condition does a poorer job at simulating the tracer concentration than either the original or modified velocity profiles used for representation of dispersion. While the general timing of particles is similar to the previous results, the large oscillations in particle concentration are unrepresentative of the tracer data. The movement of particles with this advection-only situation shows how the particles do no spread longitudinally – they maintain their original distribution and are controlled by the hydrodynamics of the Delta.

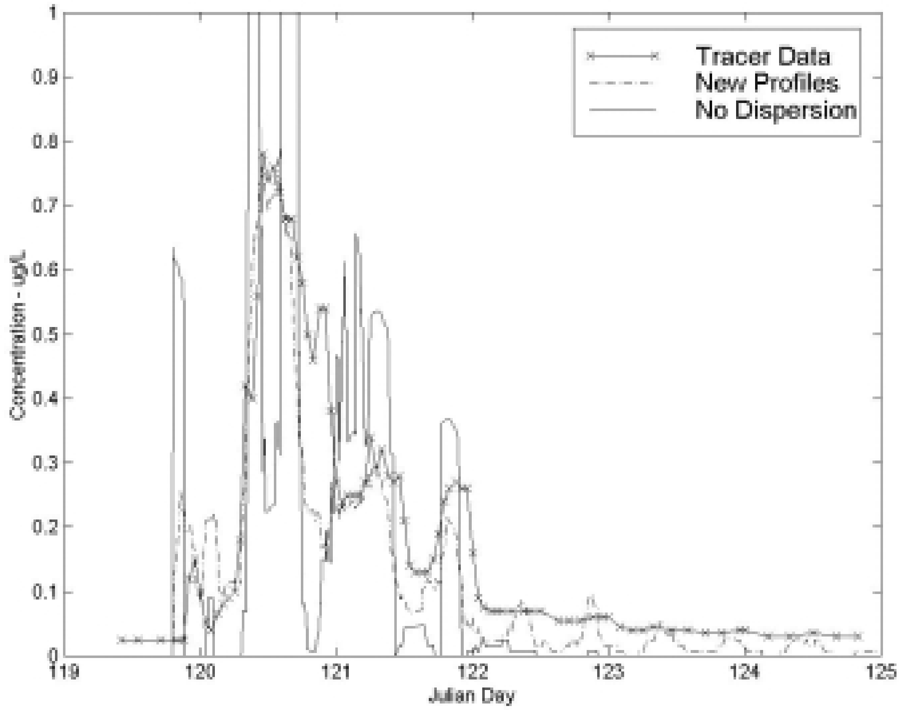

Figure 5.22: PTM and Tracer Comparison with No Dispersion, Turner Cut

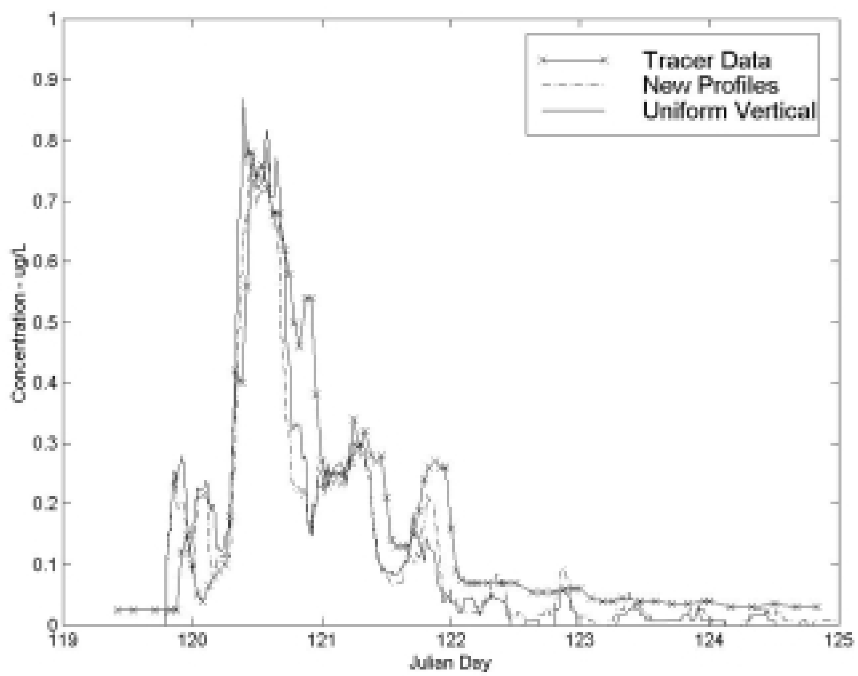

Figure 5.23: PTM and Tracer Comparison with Uniform Vertical Velocity Profile, Turner Cut

5.3.4 No Vertical Shear

Removal of the vertical velocity profile from the "best fit" PTM simulation shows how particles travel with a uniform vertical profile. All dispersion with this scenario is generated from the transverse velocity profile. Figure 5.23 shows the results of this simulation for Turner Cut. This shows a slight difference between the "best" profiles and the uniform vertical profile. The trend shows the particle arrival time as slightly earlier than the "best" profile results. While the differences are slight, it does not compare well with the tracer data. Without the vertical distribution, dispersion is slightly underestimated.

5.3.5 No Transverse Shear

Following a similar examination of a uniform vertical velocity profile, removal of the transverse velocity profile is now presented. The dispersion generated with this condition is only from that produced by the vertical velocity profile. Figure 5.24 shows the PTM results with the tracer data for Turner Cut. This shows the PTM model, without the transverse velocity profiles, predicts a much more advective particle movement than the tracer and "best" fit profiles. This also may be compared to the uniform vertical velocity profile. These show the transverse velocity profile is more important to the dispersion process than the vertical velocity profile. This observation was discussed by Fischer (1979) and supported here with the PTM results.

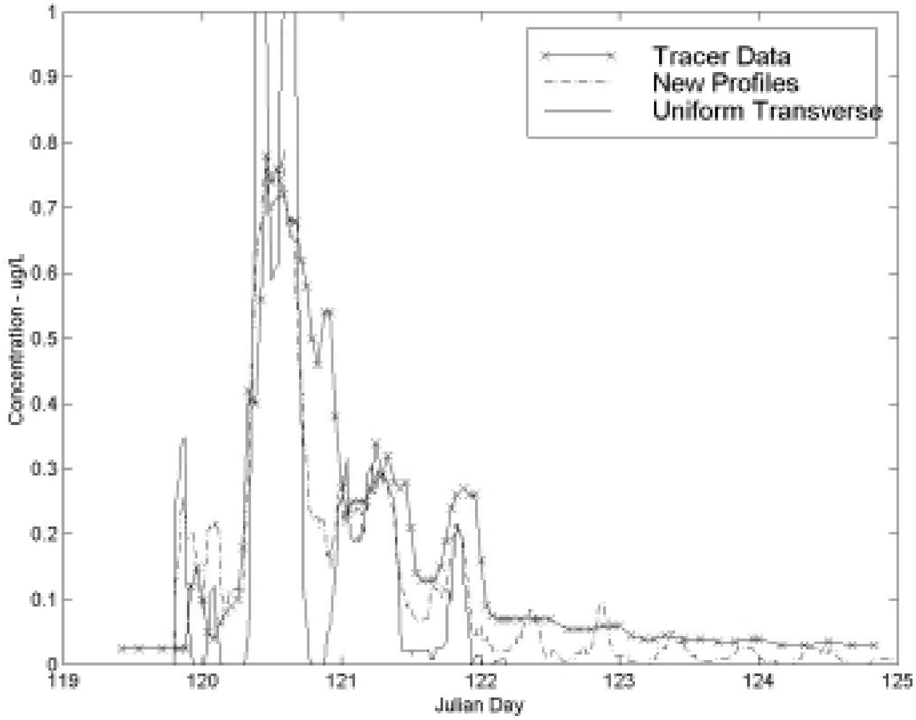

Figure 5.24: PTM and Tracer Comparison with Uniform Transverse Velocity Profile, Turner Cut

6. Conclusions

The following conclusions may be made based upon the previous discussion and analysis:

- As discussed in the literature, the dispersal cloud is proportional to the square-root of the longitudinal dispersion coefficient. Addition of an oscillating flow condition reduces the dispersion by about one half. These lead to the conclusion that the modeling results are rather insensitive to slight changes in the mechanisms causing dispersion.
- The existing velocity profiles used in the Particle Tracking Model consistently over predict the peak velocities found in the ADCP data. The mean velocity is accounted for, but the shear created by the excessive velocity profiles overestimates the dispersion in the system.
- Modification of the transverse and vertical velocity profile coefficients allow for an improved representation of the velocities found by the ADCP data. Channel irregularity can be attributed to the inconsistencies between the idealized profiles and those shown in the data.
- Simulation of the tracer study conducted by the USBR with the Particle Tracking Model yields fair results with the original profiles. Even though the original profiles over predict the peak velocities, the movement of particles is rather insensitive to the dispersive processes.
- Incorporation of the modified velocity profile coefficients into the Particle Tracking Model results in improved simulation of the tracer study. While the

particle movement is rather insensitive to the amount of dispersion in the system, it is nonetheless an important process and cannot be ignored.

- The "no-dispersion" simulation by PTM shows the importance of including dispersion in the model. The overall dominance of advection in the system is shown by the fairly accurate arrival time of particles corresponding with peak tracer concentrations. The lack of dispersion, however, produces particle distributions that do not correspond to the tracer data.
- The comparison between the uniform vertical velocity profile and the uniform transverse velocity profile show the relative importance of the transverse profile to the production of dispersion in the Delta.
- The vertical velocity profile plays a minor role in the development of dispersion in the Delta. Two very different approximations of the vertical velocity profile, uniform and either the original or modified von Karman representations, result in fairly similar simulations of the tracer study. This lessens the concerns about inconsistencies between the von Karman approximation of the vertical velocity profile and the ADCP data.
- Inspection of the Hydro and PTM results show the importance for accurate simulation of the hydrodynamics of the Delta prior to the simulation of PTM. If any error exists in Hydro, it will be carried through to the PTM model results.

7. Suggestions for Further Work

The following suggestions are made based upon the previous discussion and analysis:

- Incorporate the new geometry files used for the DSM2-Hydro simulation. These include updated bathymetry data for most of the Delta. More accurate determination of the hydrodynamics of the Delta will improve the simulations of PTM. The process of calibrating these new geometry files has yet to be completed. A similar investigation of the PTM simulation of the 1997 tracer study should be performed once the calibration process is completed.
- Improvement of the tracer study to compare the PTM simulations. The number of locations useful for this simulation study was limited to four. The data collection stations should include more stations located throughout the entire Delta. Also, the concentration levels should be high enough as to not become lost to background noise to ensure the collected data is valid.

8. References

1. Allen, C.M. "Numerical simulation of contaminant dispersion in estuary flows." *Proc. Roy. Soc.* A 381:179-194. 1982.
2. Aris, R. "On the dispersion of a solute in a fluid flowing through a tube." *Proc. R. Soc. London Ser. A.* Vol. 235, p. 67-77. 1956.
3. Bogle, G. "Stream Velocity Profiles and Longitudinal Dispersion." *J. Hyd. Eng. ASCE.* Vol. 123 No. 9. 1997.
4. Bogle, Gilbert V. "Simulation of Dispersion in Streams by Particle Tracking, Draft". 1994
5. Bowden, K.F. "Horizontal mixing in the sea due to a shearing current." *J. Fluid Mech.* 21:83-95. 1965.
6. Bugliarello, G. and Jackson, E.D.III. "Random walk study of convective diffusion." *Journal of Engineering Mechanics Division, ASCE.* 90,(EM4), 49-77, 1964.
7. Chatwin, P.C. and Allen, C.M. "Mathematical models of dispersion in rivers and estuaries." *Ann. Rev. Fluid Mech.* Vol. 17, p. 119-149. 1985.
8. Chu and Gardner. "2D PTM Estuarine Transport." *Water Resources Bulletin.* V22, No. 2, p.183-189. April 1986.
9. DeLong, L.L., Thompson, D.B. and Lee J.K. "FourPt: A model for simulating one-dimensional, unsteady, open-channel flow." Water-Resources Investigations Report 95-XXXX. U.S. Geological Survey, 1995.
10. Department of Water Resources. <u>Delta Simulation Model 2 Training Manual</u>. July 1999.
11. Department of Water Resources. <u>Methodology for Flow and Salinity Estimates in the Sacramento – San Joaquin Delta and Suisun Marsh. Nineteenth Annual Progress Report to the State Water Resources Control Board</u>. July 1998.
12. Department of Water Resources. <u>Temporary Barriers Project: Fishery, Water Quality, and Vegetation Monitoring, 1997</u>. August 1998.

13. Dimou, K. Nadia, and Adams, E. Eric. "A Random-walk, Particle Tracking Model for Well-mixed Estuaries and Coastal Waters." *Estuarine, Coastal and Shelf Science. 37:99-110.* 1993.
14. Denton, R.A. "Analytical asymptotic solutions for longitudinal dispersion with dead zones." *Journal of Hydraulic Research.* Vol. 28, No. 3, 1990.
15. Elder, J.W. "The dispersion of marked fluid in turbulent shear flow." *J. Fluid Mech.* Vol. 5, p. 544-560. 1959.
16. Fischer, H.B., List, E.J., Koh, R.C.Y. Imberger, J., Brooks, N.H. Mixing in Inland and Coastal Waters. New York, Academic, 1979.
17. Fischer, H.B. "Mixing and dispersion in estuaries." *Ann. Rev. Fluid Mech*. 8:107-133. 1976.
18. Fischer, H.B. "Longitudinal dispersion and turbulent mixing in open-channel flow." *Ann. Rev. Fluid Mech*. 5:59-78. 1973.
19. Fischer, H.B. "Dispersion Predictions in natural streams." *J. of the Sanitary Eng. Division, ASCE*. No. SA5, 927-943. 1968.
20. Fischer, H.B. "The mechanics of dispersion in natural streams." *J. of Hydraulics Division, ASCE*. Vol. 93, No. HY6, 187-216. 1967.
21. Godfrey, R.G. and Frederick, B.J. "Dispersion in Natural Streams." U.S. Geological Survey Professional Paper 433-K. 1970.
22. Hyslop, S.E. and Allen, C.M. "Modeling contaminant dispersion in the River Severn using a random-walk model." *J. Hydraul. Res.* Vol. 31 No. 3, 323-331. 1993.
23. Maidment, David R. Handbook of Hydrology. McGraw-Hill, Inc. 1993.
24. Oltmann, Richard N. Measured Flow and Tracer – Dye Data Showing Anthropogenic Effects on the Hydrodynamics of South Sacramento – San Joaquin Delta, Calfornia, Spring 1996 and 1997. United States Geological Survey, Open File Report 98-285. 1998.
25. Orlob, G.T. "Eddy diffusion in Homogeneous turbulence." *J. of Hydraulics Division, ASCE*. Vol. 85, No. HY9, p. 75-101.
26. Purnama, A. "The effect of dead zones on longitudinal disperson in streams." *J. Fluid Mech.* Vol. 186, p. 351-377. 1988.

27. RD Instruments. Transect User's Manual. 1994.
28. RD Instruments. ADCP Principles of Operation: A Practical Primer. 1996.
29. Sullivan, P.J. "Longitudinal dispersion within a two-dimensional turbulent shear flow." *Journal of Fluid Mechanics.* V.49, p.551-576.1971.
30. Taylor, G.I. "Diffusion by continuous movements." *Proc. London Math. Soc., Ser. 2, 20, 196-212.*
31. Taylor, G.I. "The dispersion of matter in turbulent flow through a pipe." *Proc. R. Soc. London. Ser. A* 223: 446-468. 1960.
32. Thackston, E.L. and Schnelle, K.D.,Jr. "Predicting effects of dead zones on stream mixing." *J. Sanitary Engineering Div. ASCE*. Vol. 96, p319-331. 1970.
33. Tompson, A.F.B. and Gelhar, L.W. "Numerical simulation of solute transport in three-dimensional randomly heterogeneous porous media." *Water Resources Research* 26:2541-2562. 1990.

9. Appendices

Table of Contents:

9.1 Appendix 1

ADCP Profiles

Table of Contents:

	Flow	May 30, 1997		I-37	84
	Profile	May 30, 1997	8:10 am	I-38	84
	Flow	May 30, 1997		I-39	85
	Profile	May 30, 1997	11:10 am	I-40	85
Victoria Canal	Flow	April 3, 1997		I-41	86
	Profile	April 3, 1997	12:42 pm	I-42	86
	Flow	April 3, 1997		I-43	87
	Profile	April 3, 1997	3:20 pm	I-44	87
	Flow	May 29, 1997		I-45	88
	Profile	May 29, 1997	2:10 pm	I-46	88
	Flow	May 29, 1997		I-47	89
	Profile	May 29, 1997	2:30 pm	I-48	89

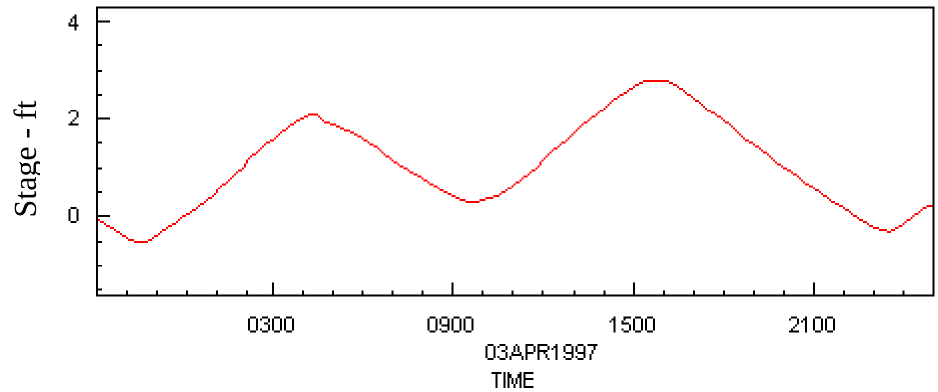

Figure I-1: Historical Grantline Canal Stage

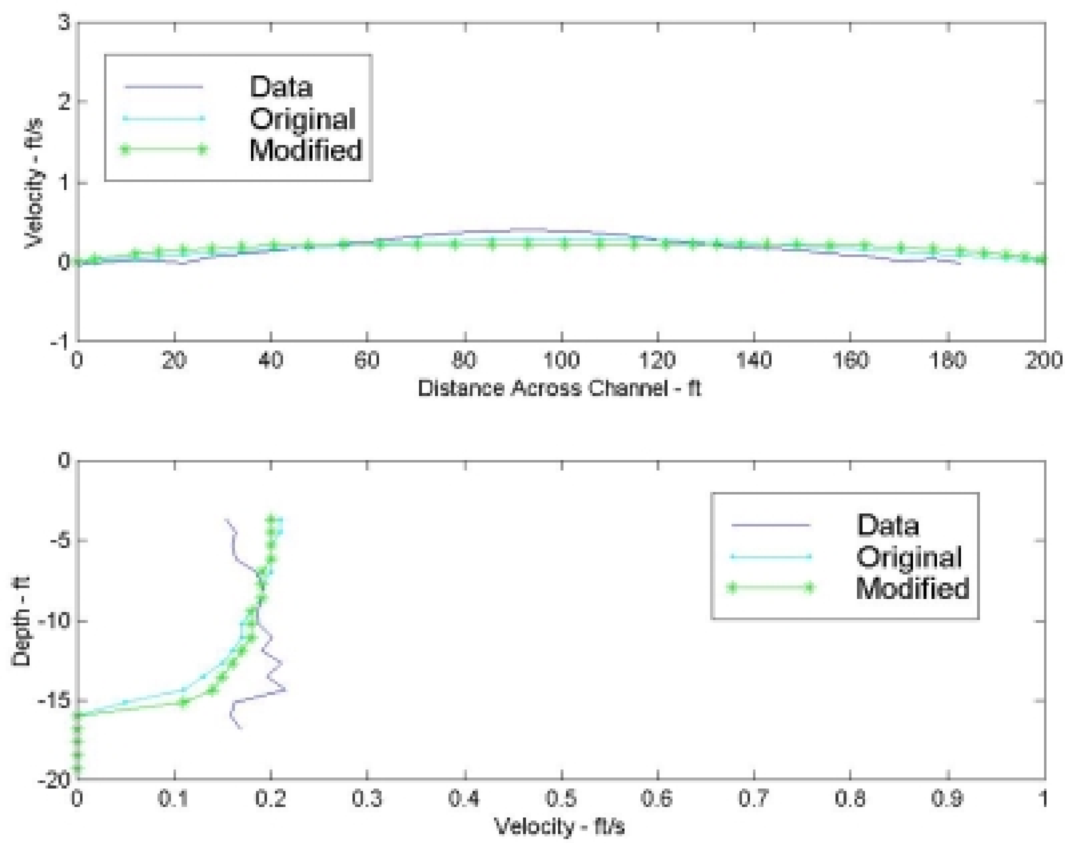

Figure I-2: ADCP and PTM Velocity Profiles, Grantline Canal (April 3, 1997 16:30)

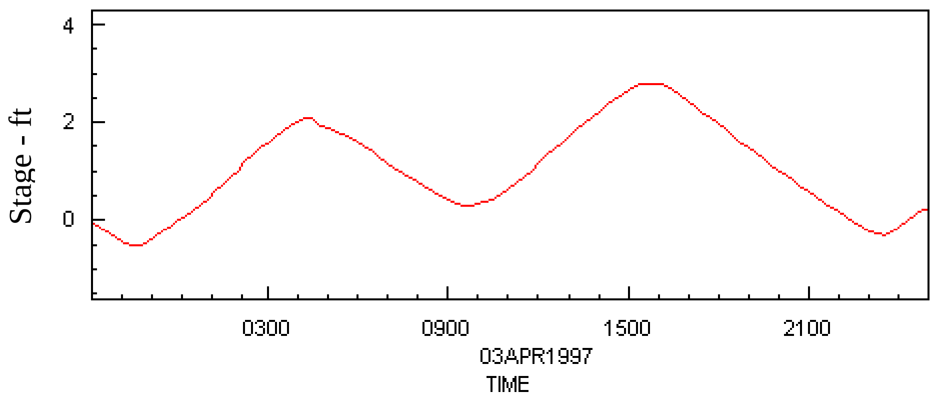

Figure I-3: Historical Grantline Canal Stage

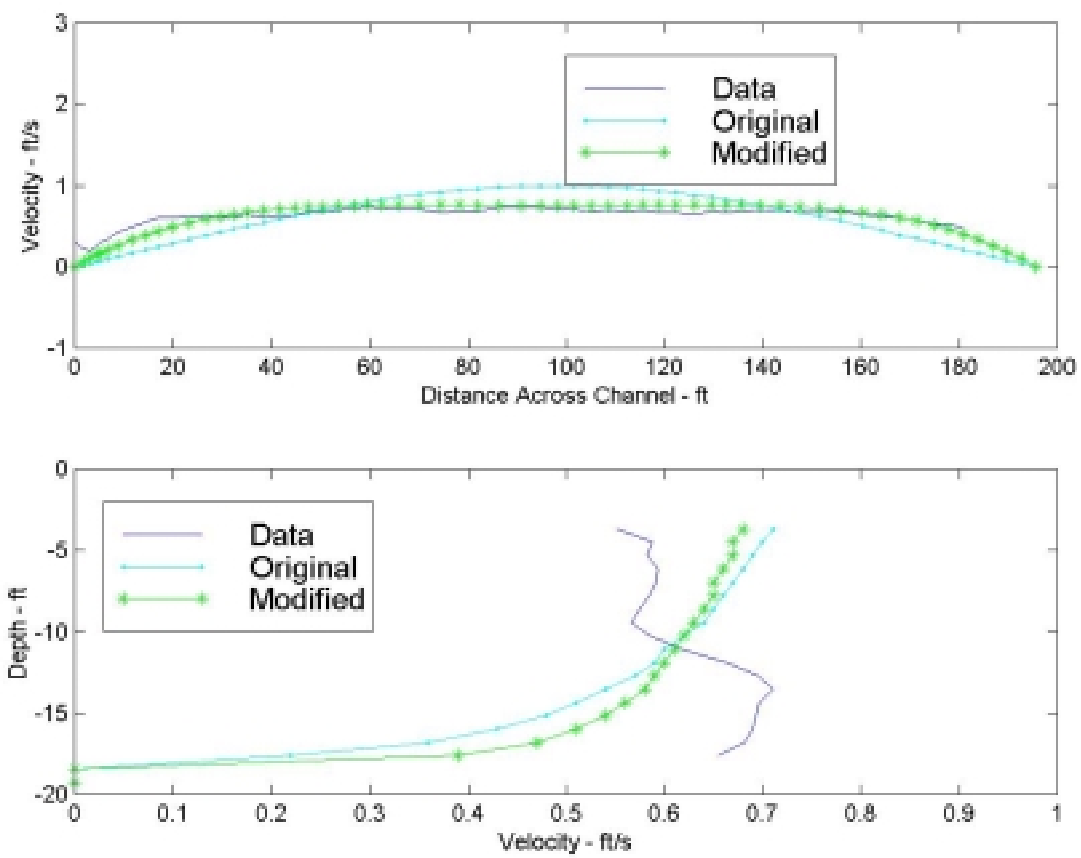

Figure I-4: ADCP and PTM Velocity Profiles, Grantline Canal (April 3, 1997 11:10)

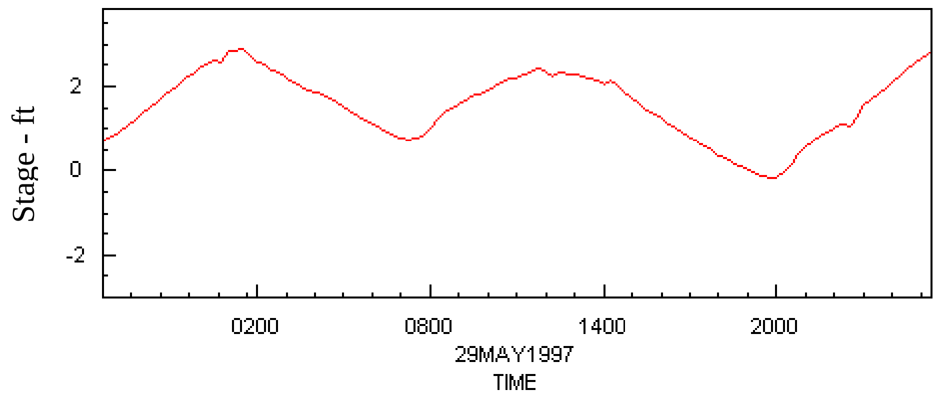

Figure I-5: Historical Grantline Canal Stage

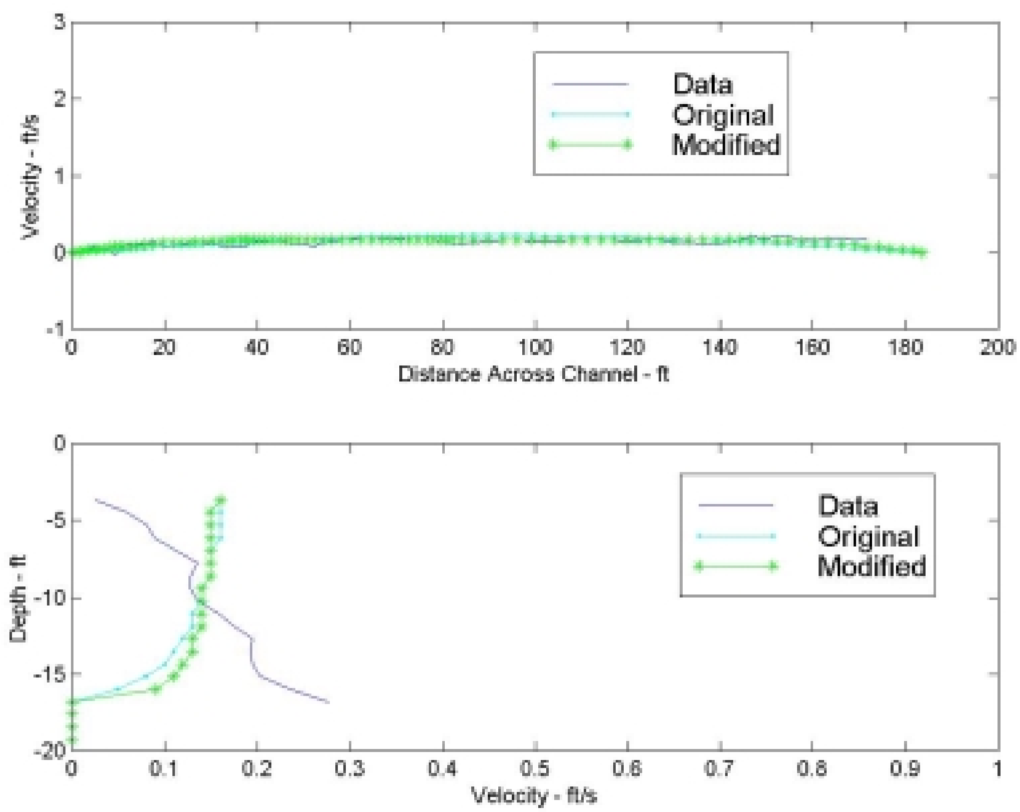

Figure I-6: ADCP and PTM Velocity Profiles, Grantline Canal (May 29, 1997 12:00)

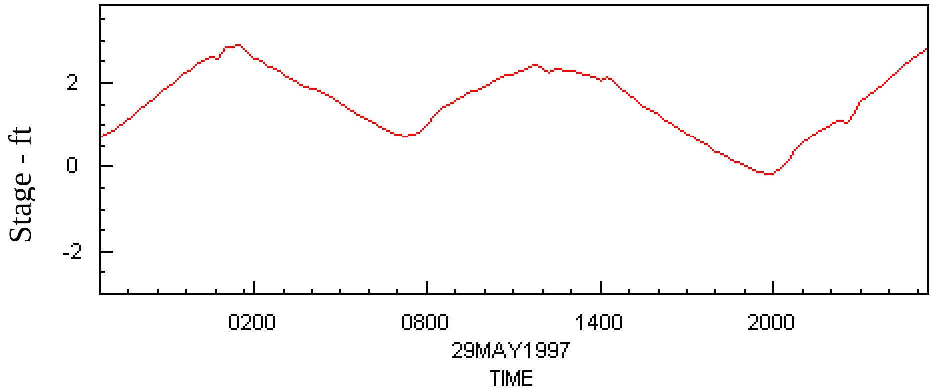

Figure I-7: Historical Grantline Canal Stage

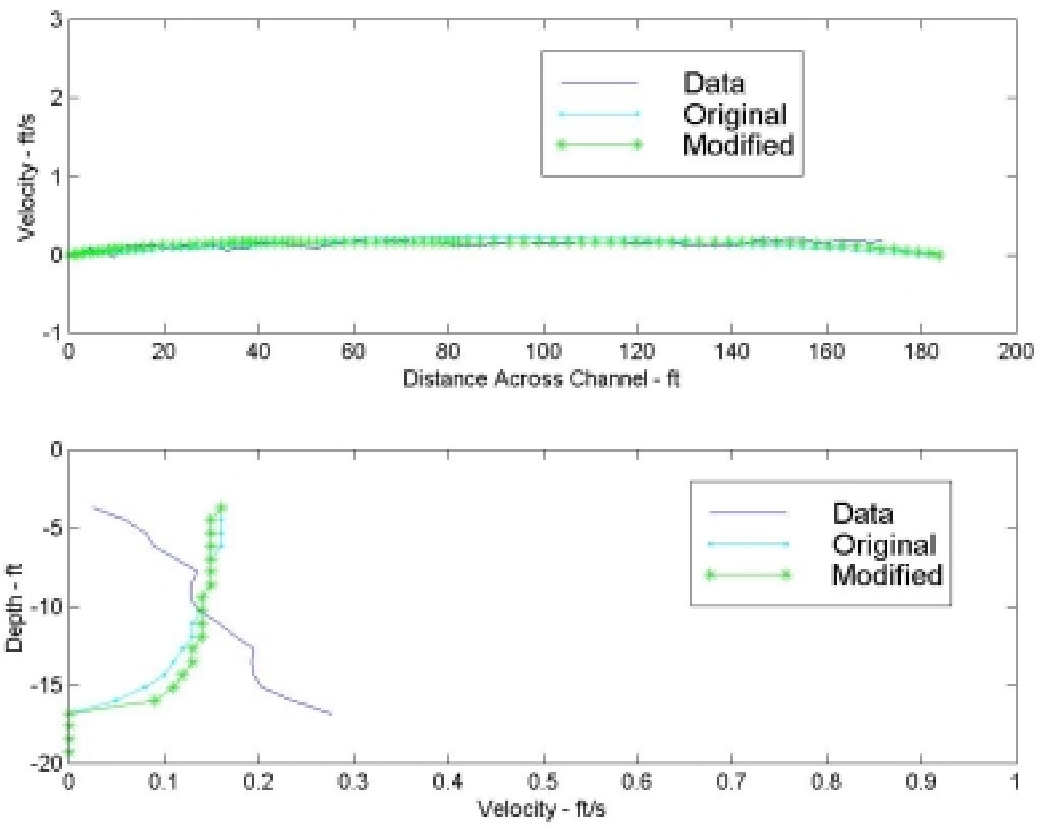

Figure I-8: ADCP and PTM Velocity Profiles, Grantline Canal (May 29, 1997 15:30)

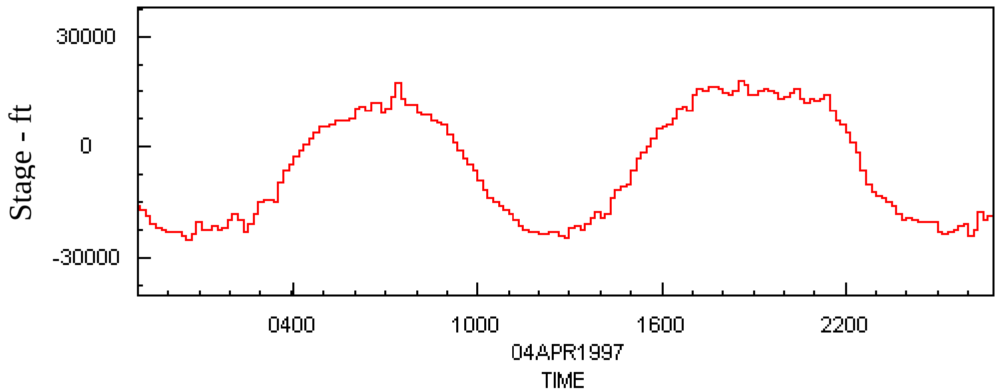

Figure I-9: Historical Middle River South of Columbia Cut Flow

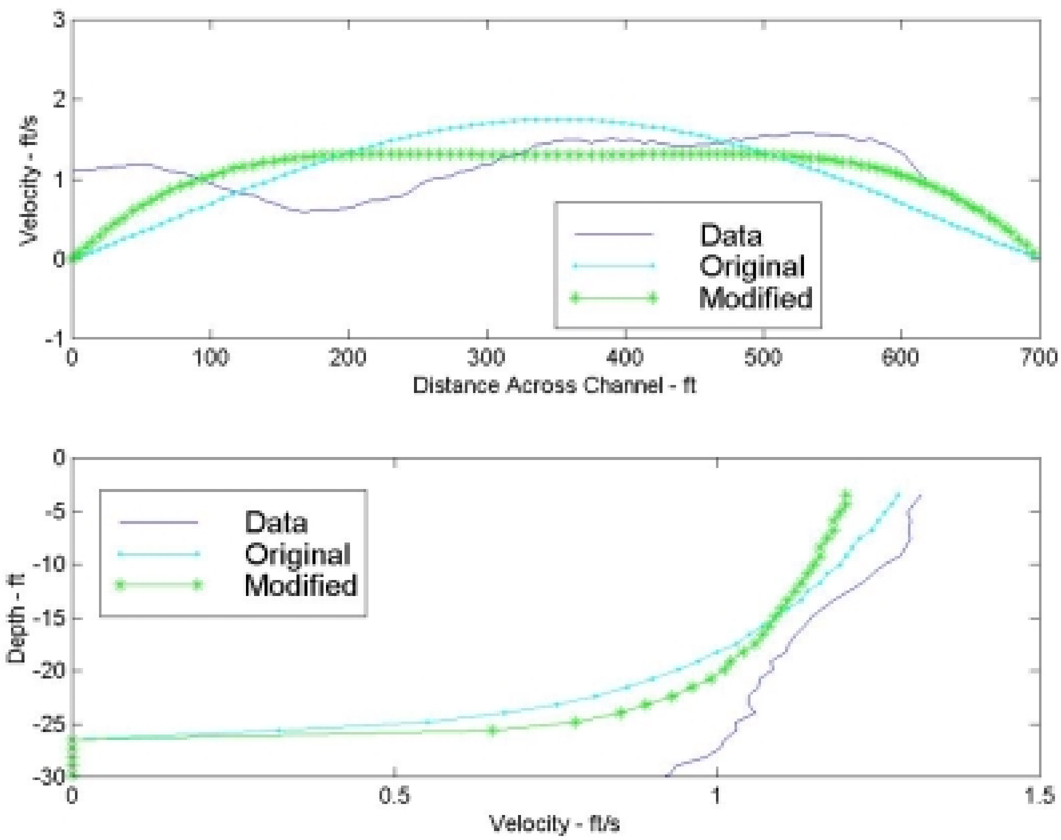

Figure I-10: ADCP and PTM Velocity Profiles, Middle River (April 4, 1997 12:50)

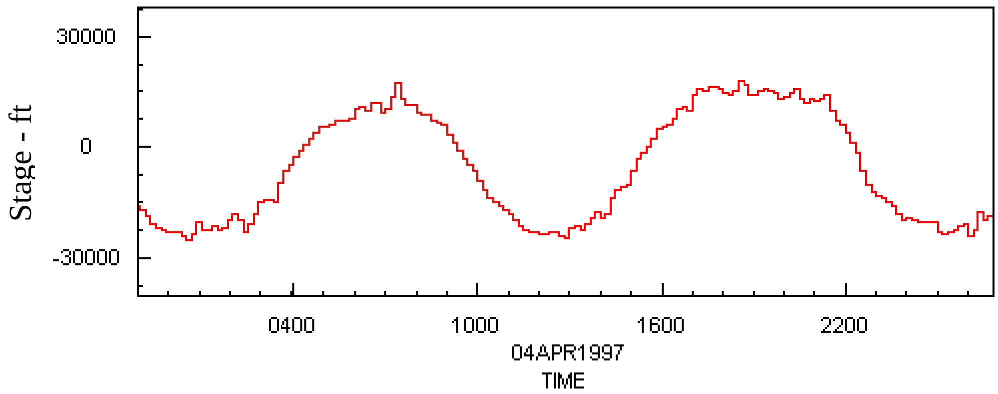

Figure I-11: Historical Middle River South of Columbia Cut Flow

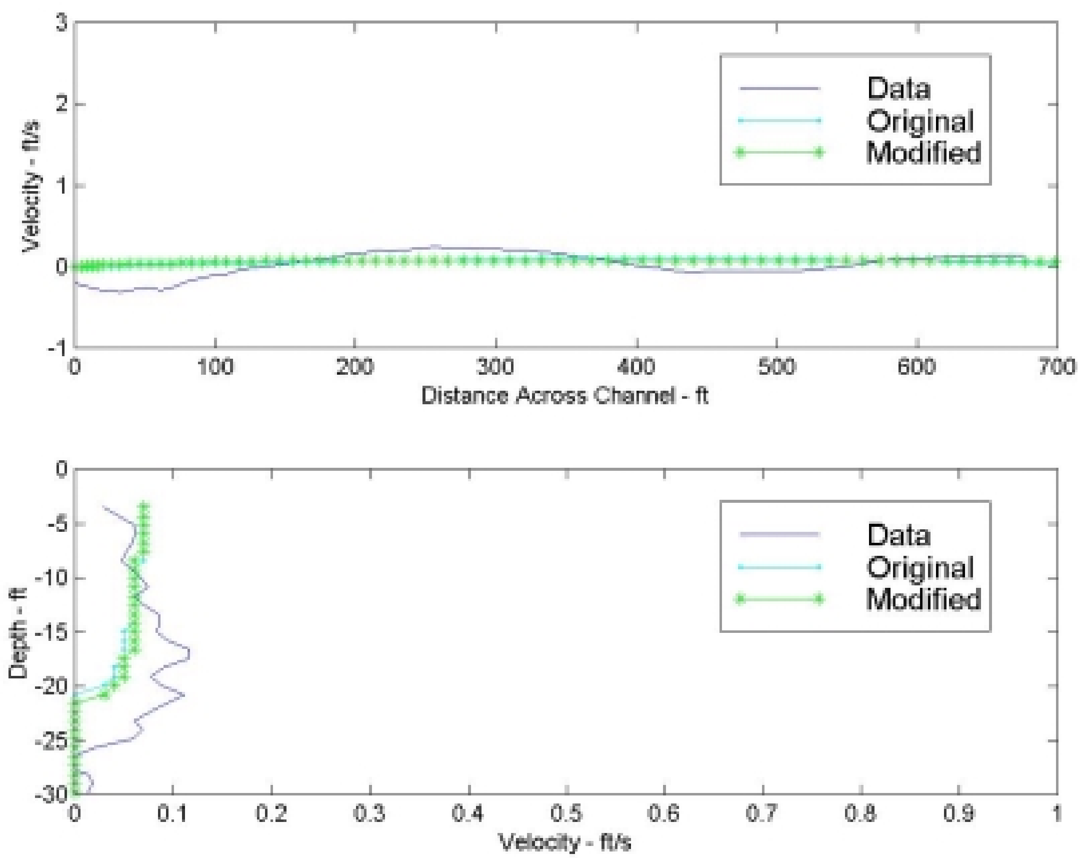

Figure I-12: ADCP and PTM Velocity Profiles, Middle River (April 4, 1997 15:30)

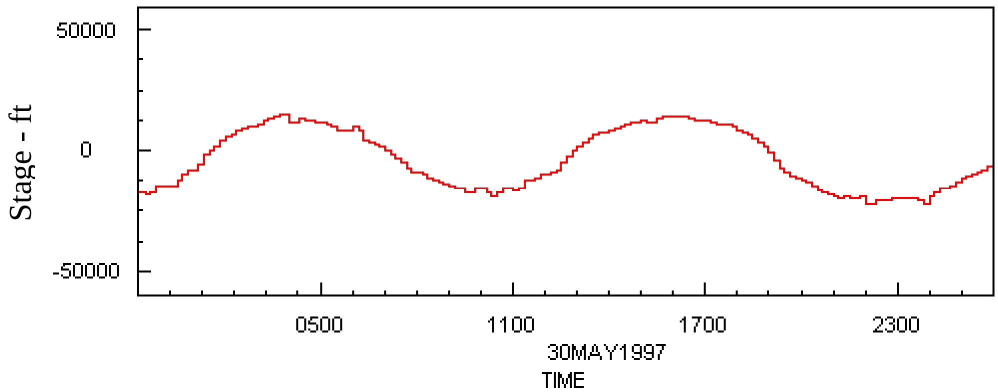

Figure I-13: Historical Middle River South of Columbia Cut Flow

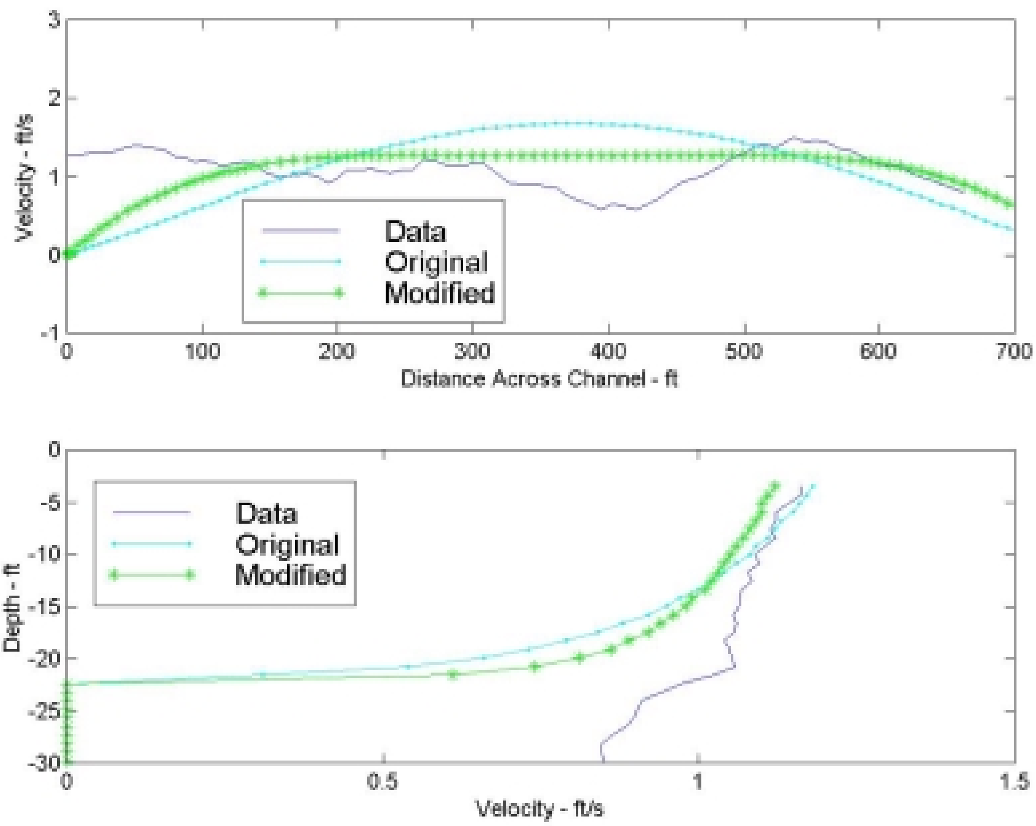

Figure I-14: ADCP and PTM Velocity Profiles, Middle River (May 30, 1997 9:50)

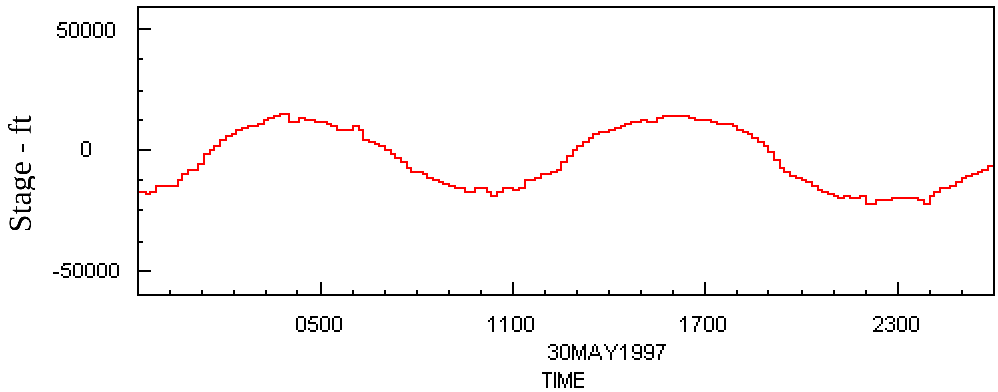

Figure I-15: Historical Middle River South of Columbia Cut Flow

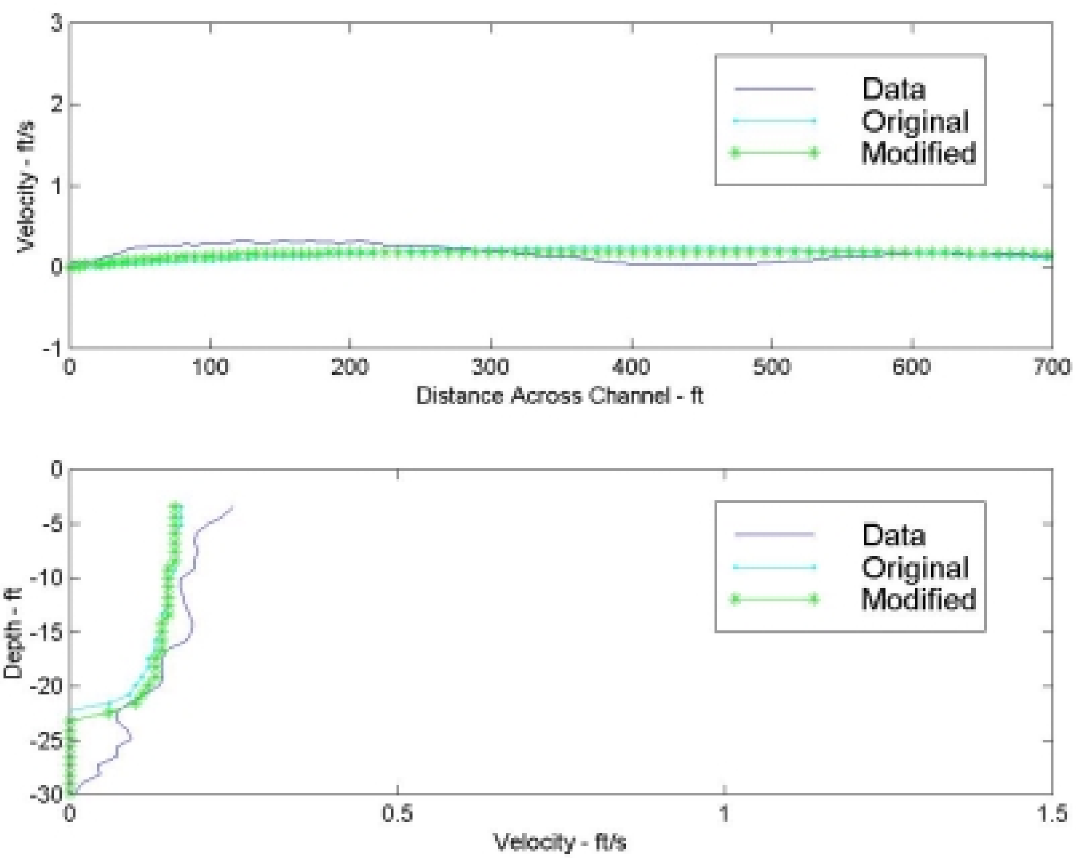

Figure I-16: ADCP and PTM Velocity Profiles, Middle River (May 30, 1997 12:50)

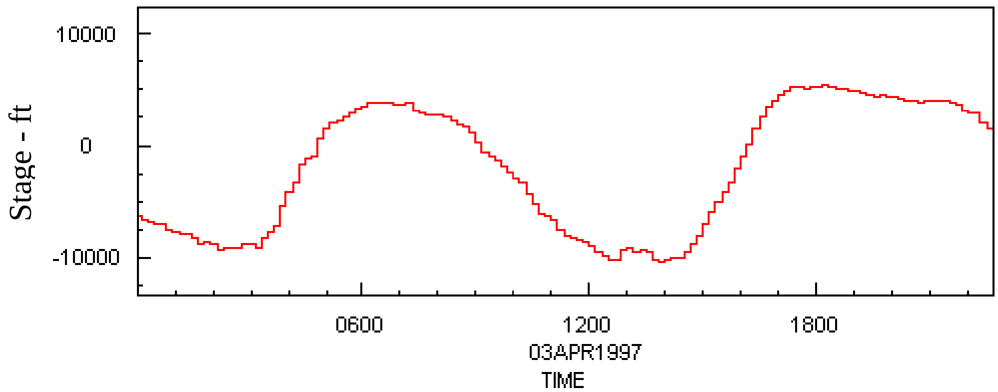

Figure I-17: Historical Flow at Old River near Clifton Court Ferry

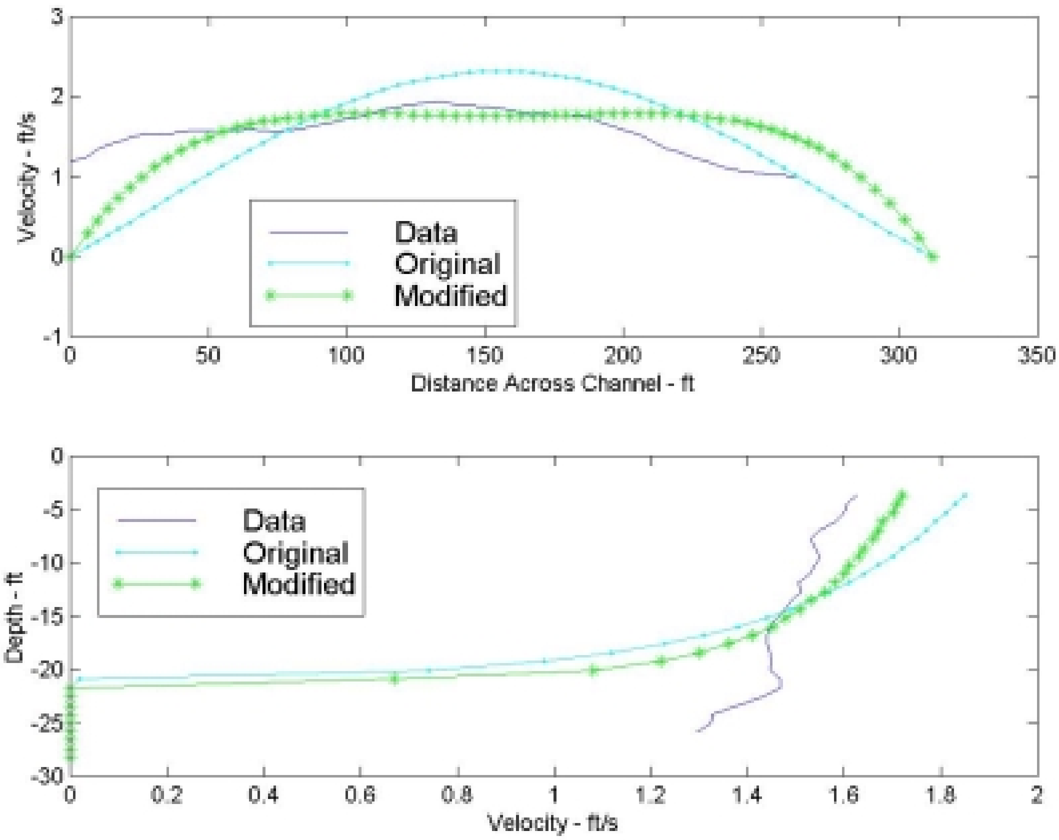

Figure I-18: ADCP and PTM Velocity Profiles, Old River (April 3, 1997 13:20)

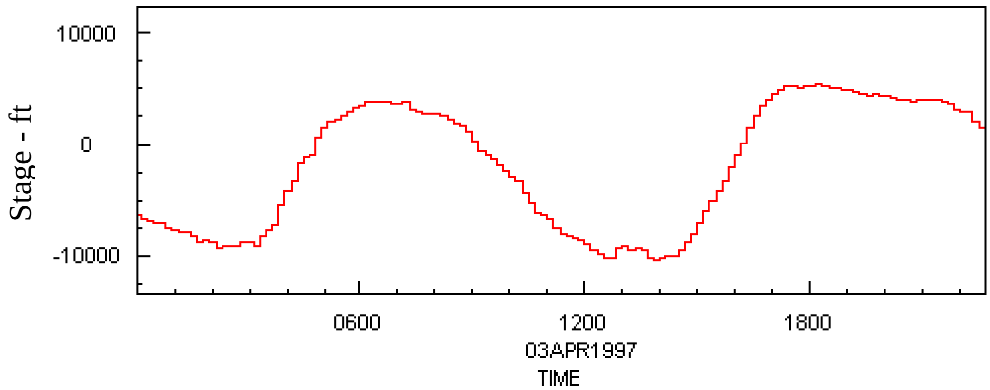

Figure I-19: Historical Flow at Old River near Clifton Court Ferry

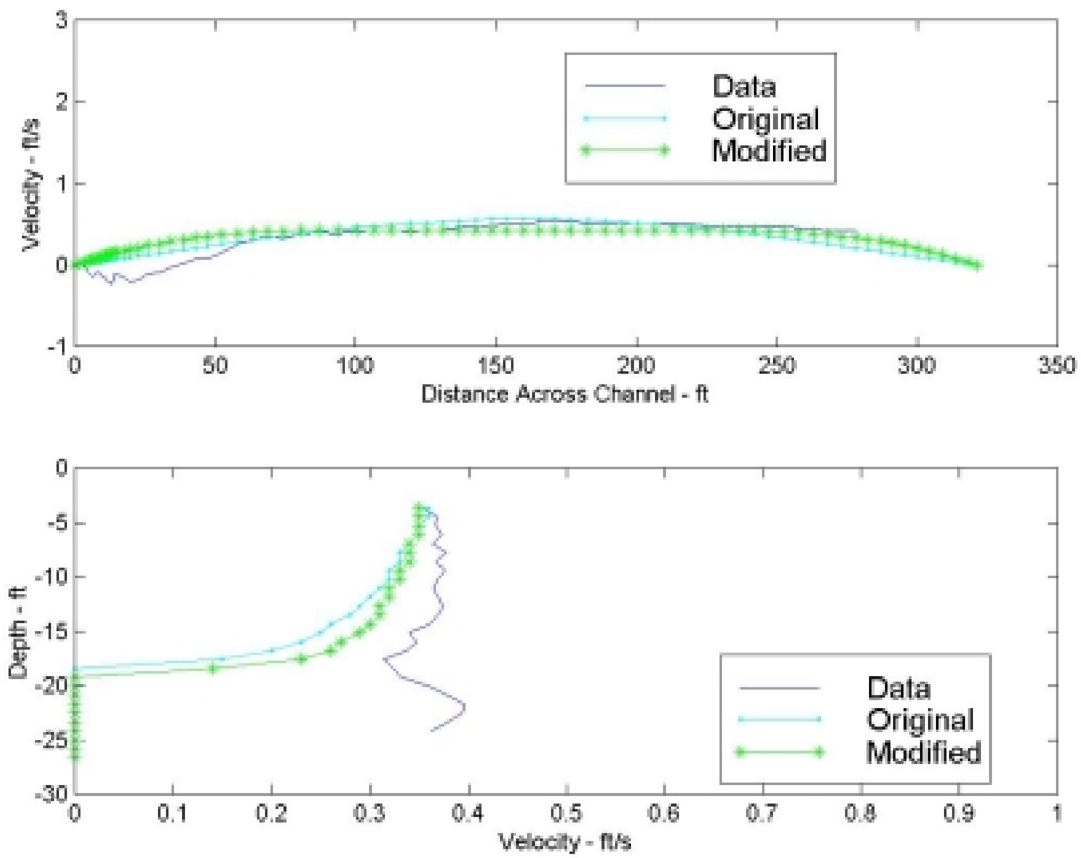

Figure I-20: ADCP and PTM Velocity Profiles, Old River (April 3, 1997 16:00)

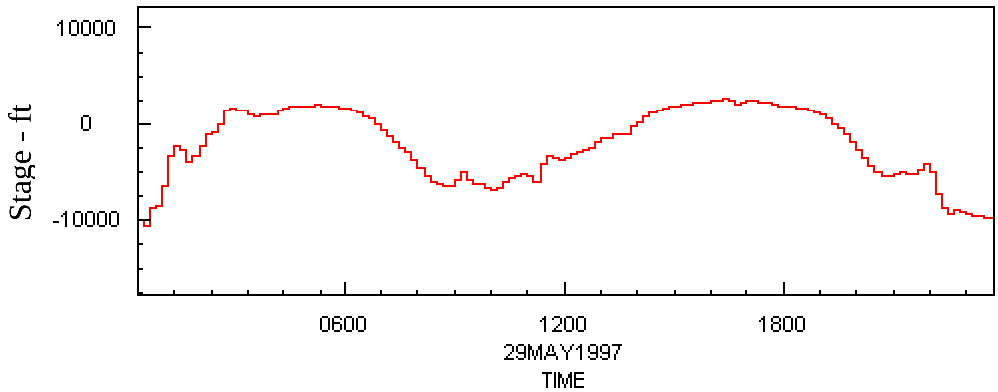

Figure I-21: Historical Flow at Old River near Clifton Court Ferry

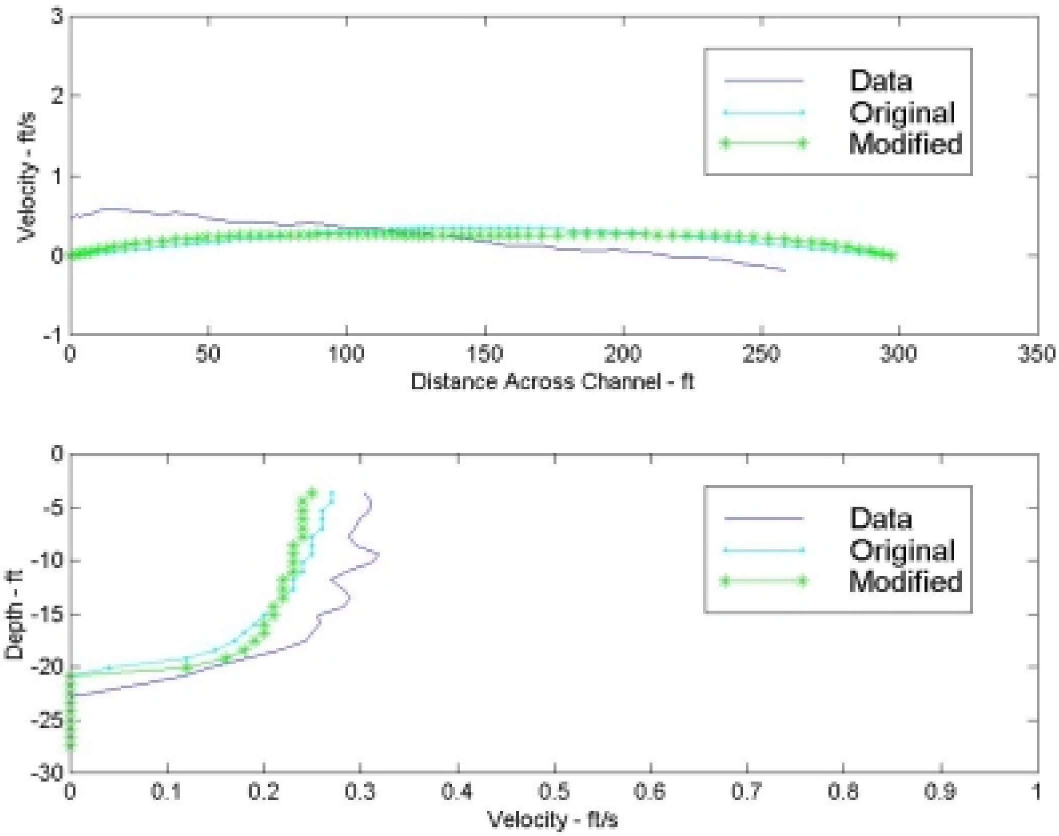

Figure I-22: ADCP and PTM Velocity Profiles, Old River (May 29, 1997 13:10)

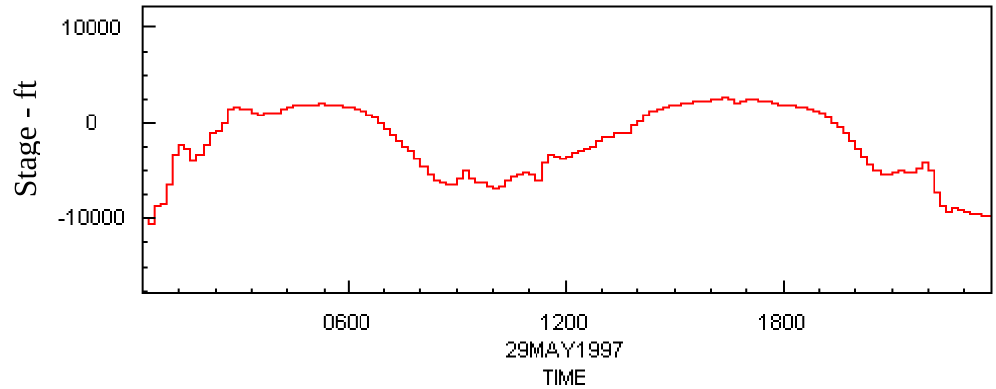

Figure I-23: Historical Flow at Old River near Clifton Court Ferry

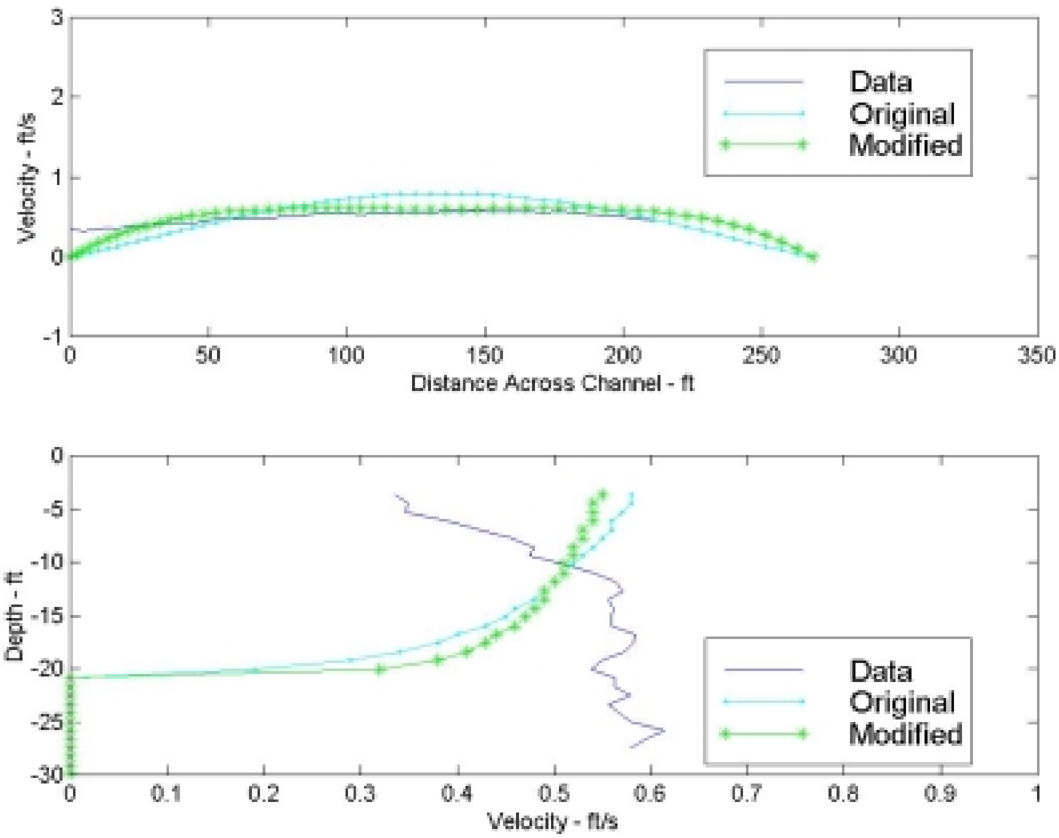

Figure I-24: ADCP and PTM Velocity Profiles, Old River (May 29, 1997 16:10)

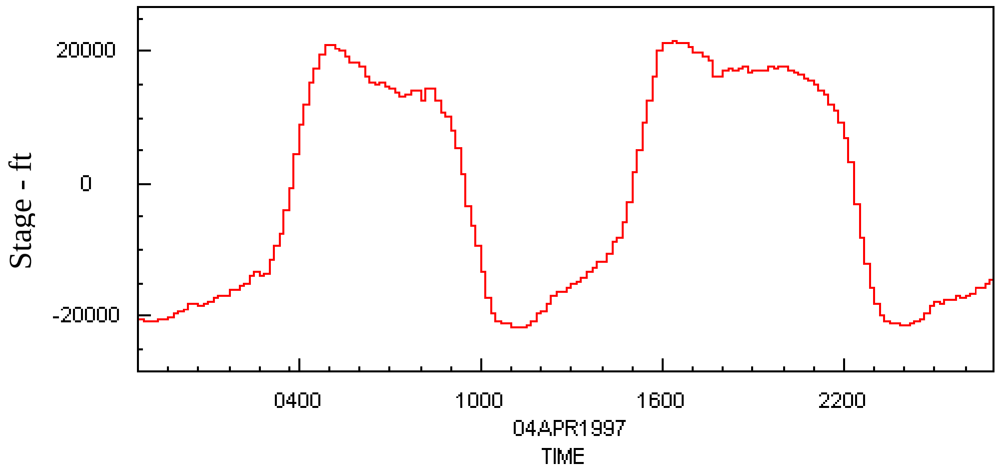

Figure I-25: Historical Flow at San Joaquin River Between Col. And Turner Cut

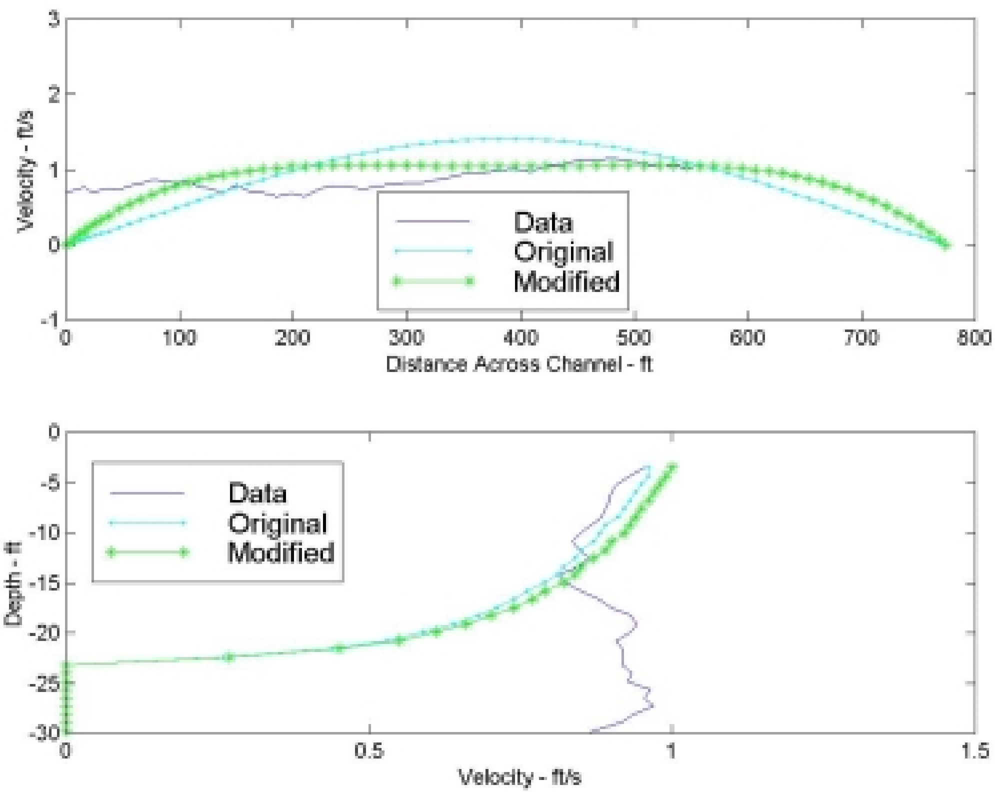

Figure I-26: ADCP and PTM Velocity Profiles, SJR (April 4, 1997 10:30)

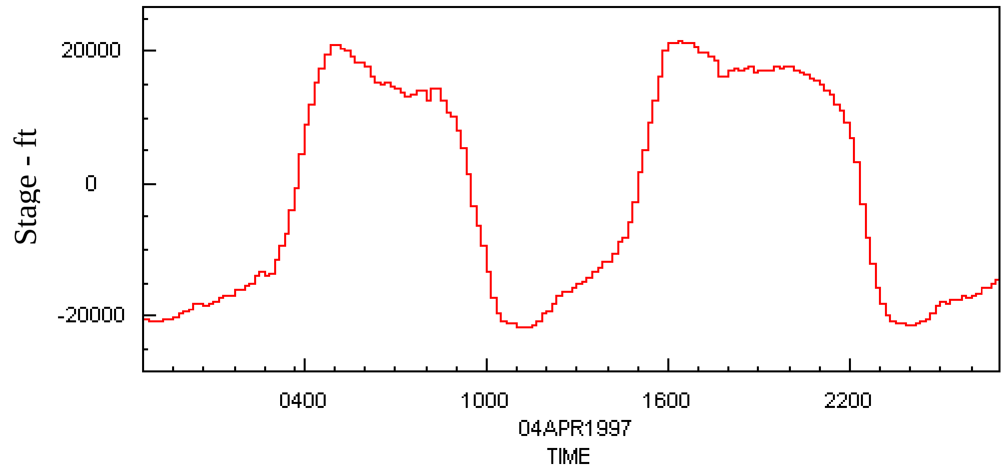

Figure I-27: Historical Flow at San Joaquin River Between Col. And Turner Cut

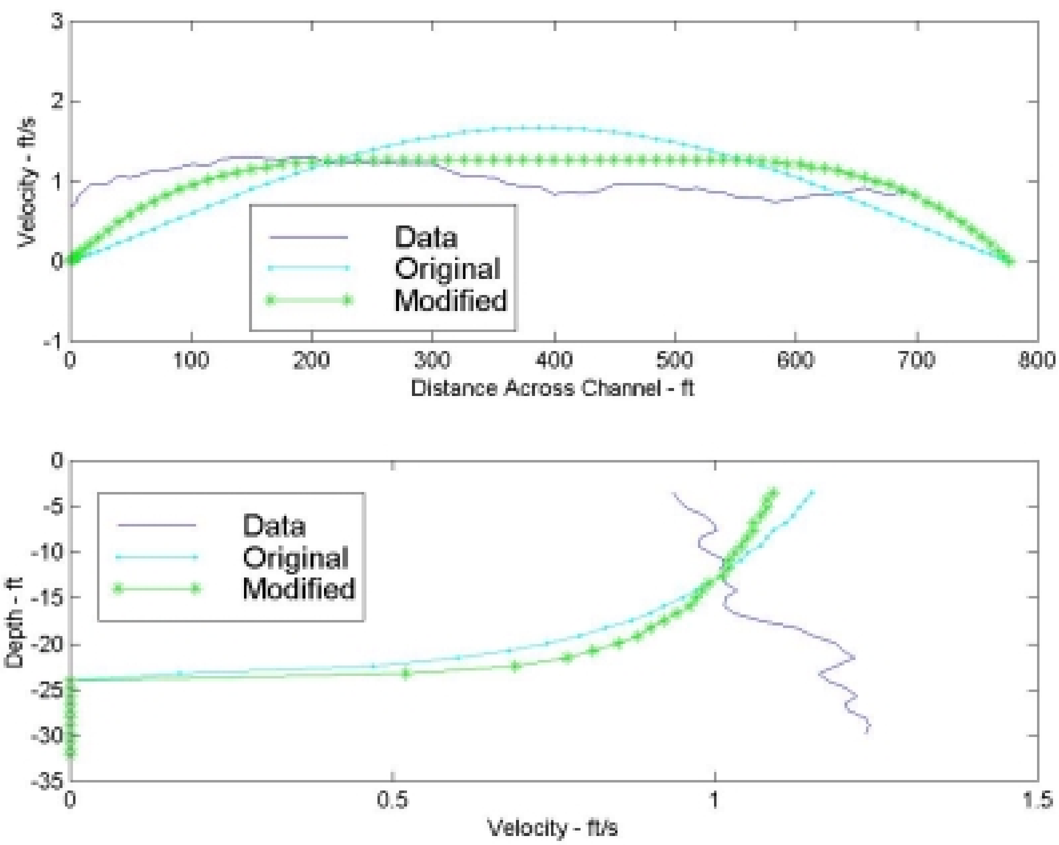

Figure I-28: ADCP and PTM Velocity Profiles, SJR (April 4, 1997 16:40)

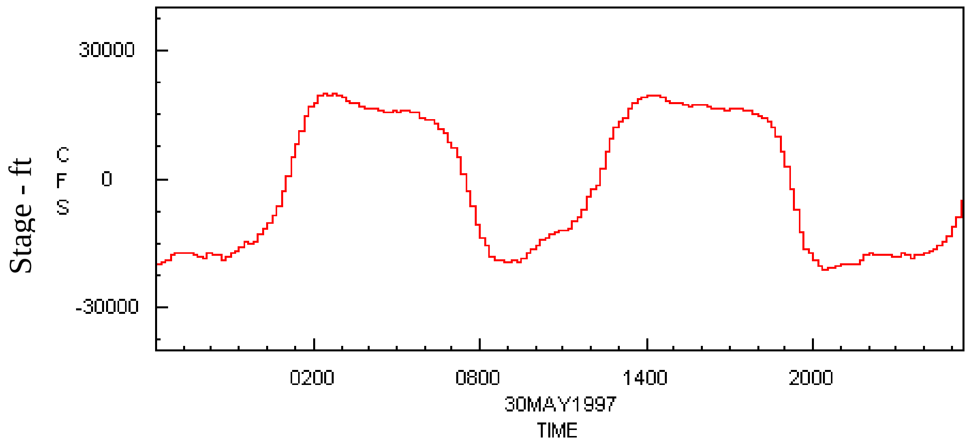

Figure I-29: Historical Flow at San Joaquin River Between Col. And Turner Cut

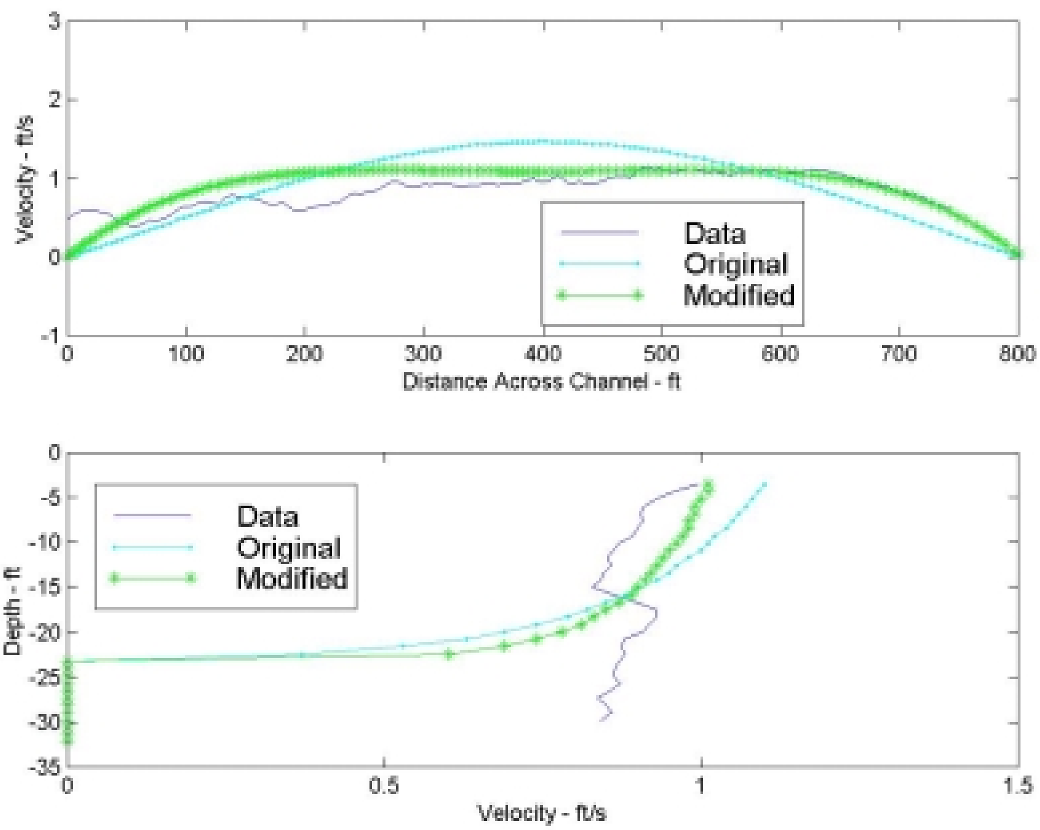

Figure I-30: ADCP and PTM Velocity Profiles, SJR (May 30, 1997 9:00)

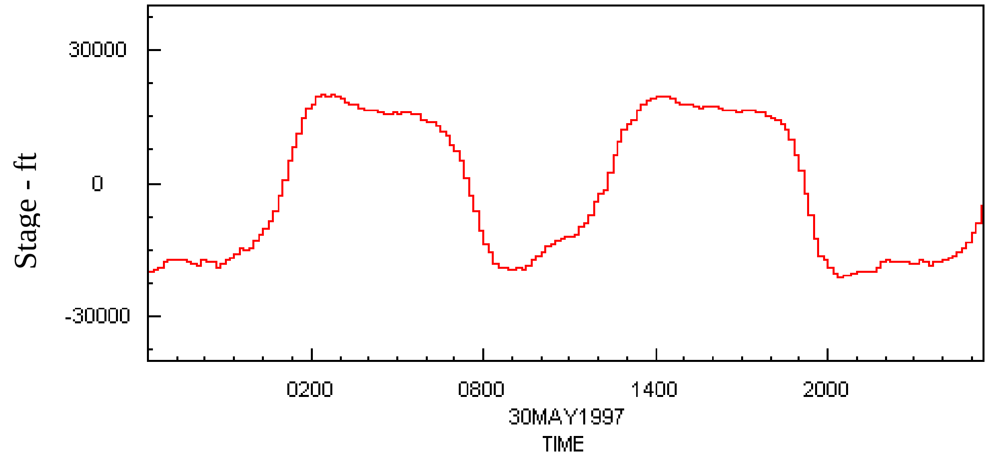

Figure I-31: Historical Flow at San Joaquin River Between Col. And Turner Cut

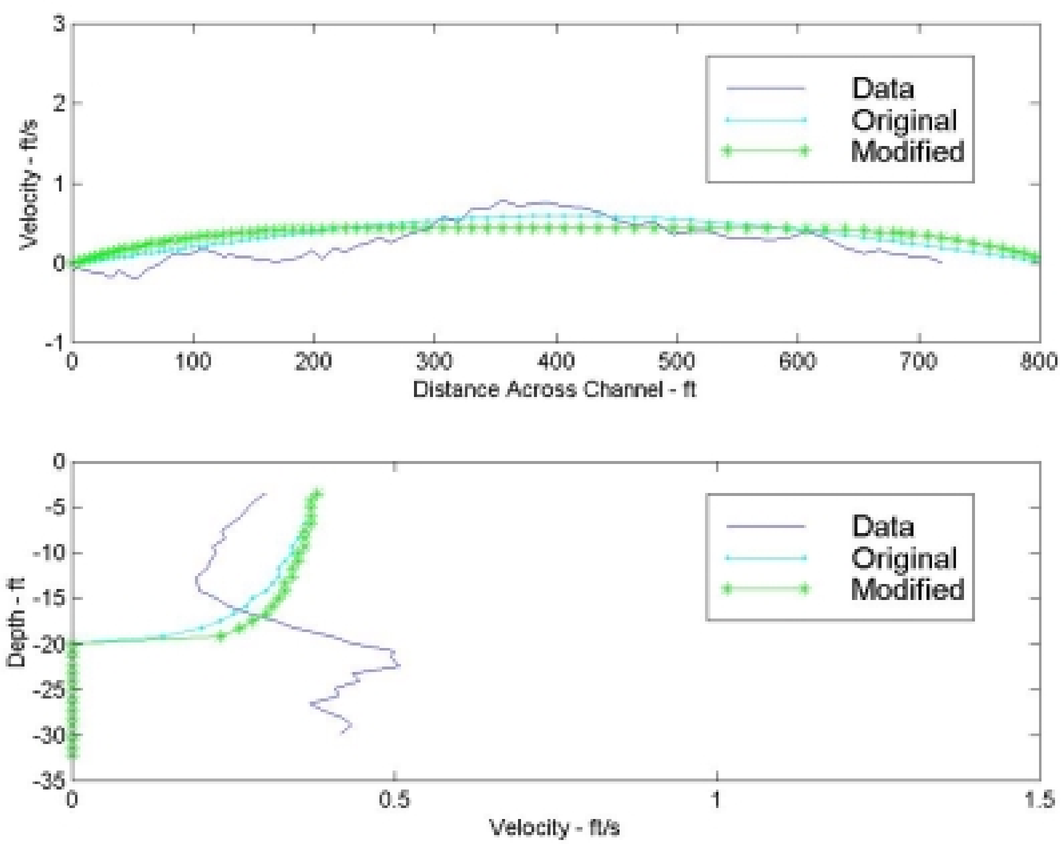

Figure I-32: ADCP and PTM Velocity Profiles, SJR (May 30, 1997 12:10)

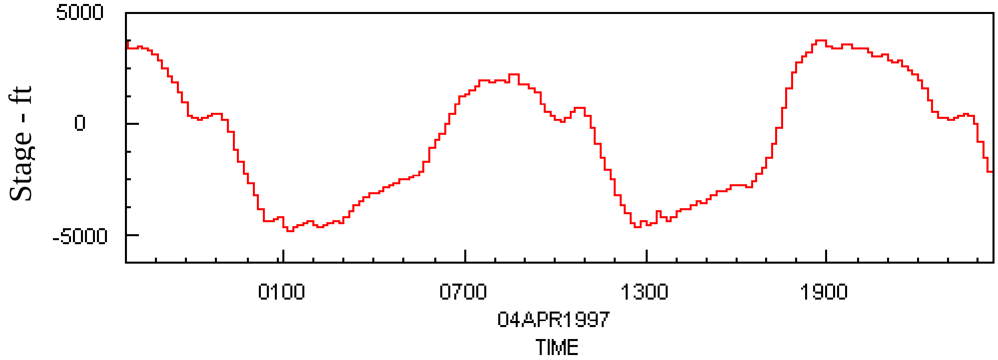

Figure I-33: Historical Flow at Turner Cut

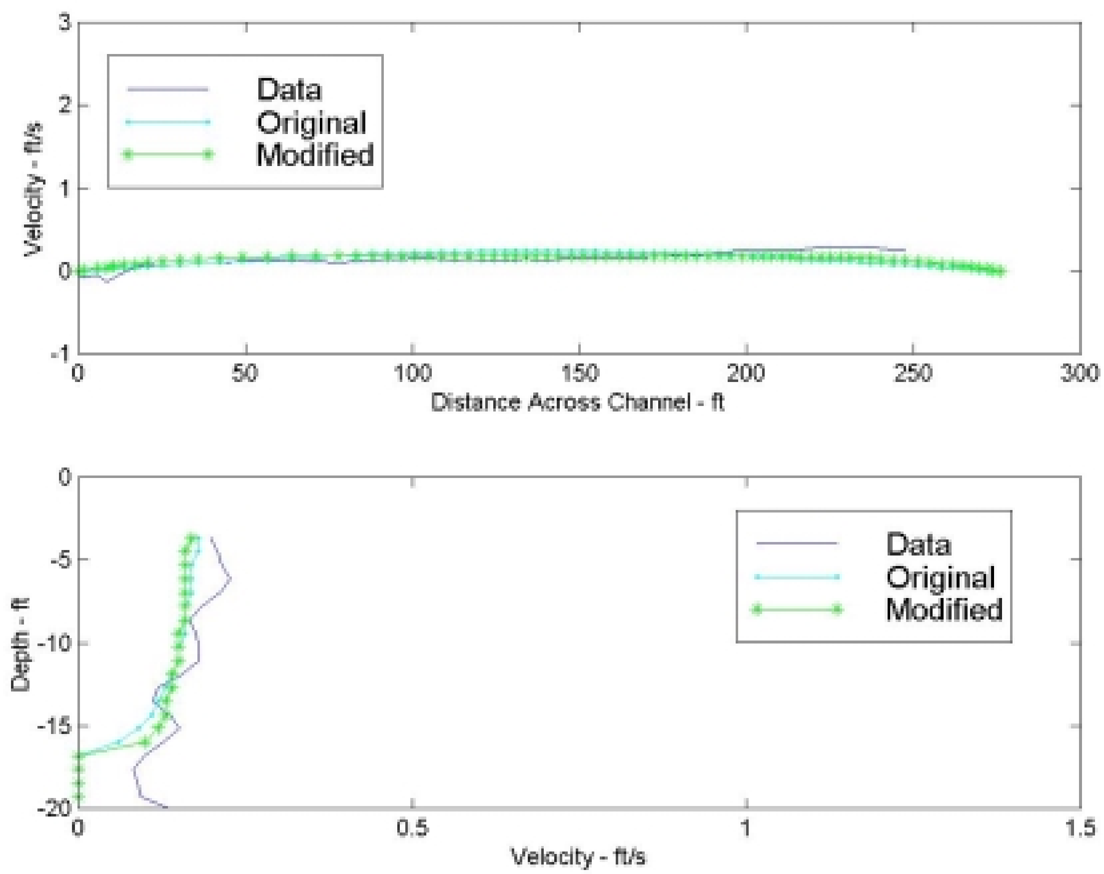

Figure I-34: ADCP and PTM Velocity Profiles, Turner Cut (April 4, 1997 11:30)

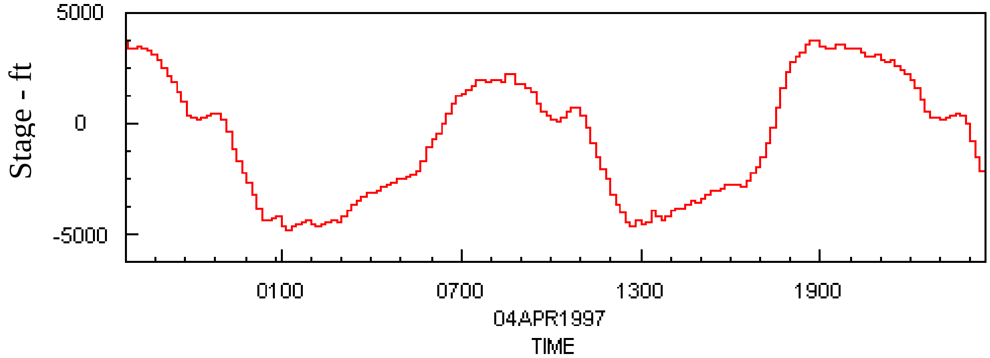

Figure I-35: Historical Flow at Turner Cut

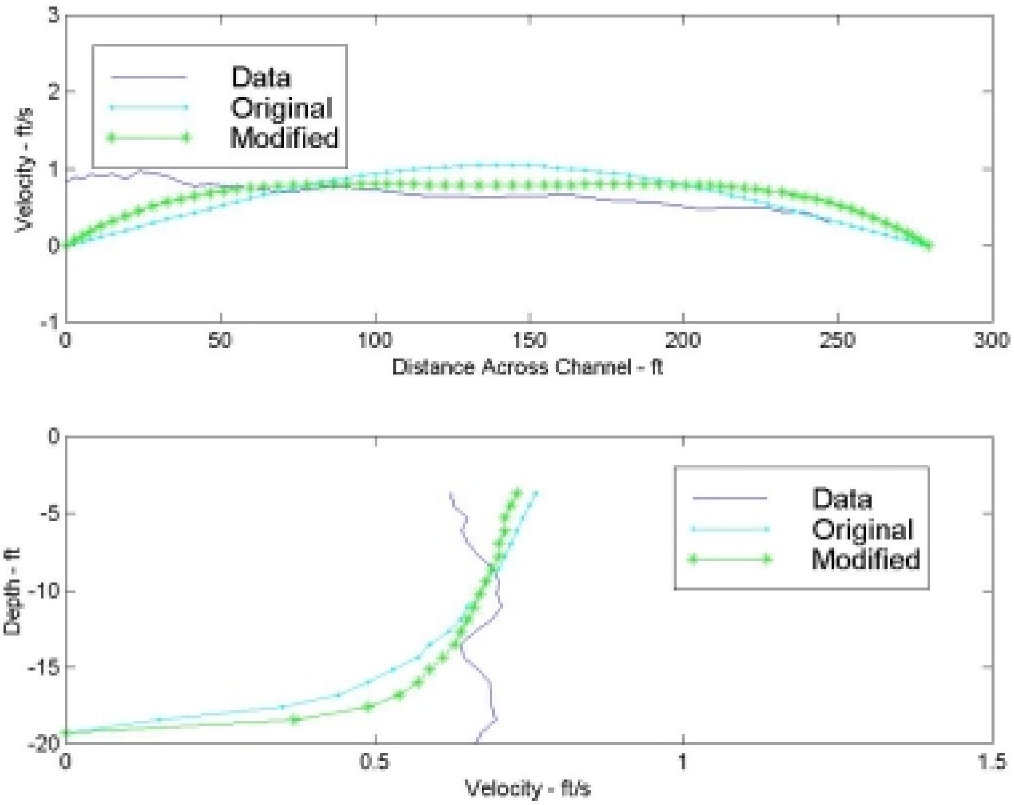

Figure I-36: ADCP and PTM Velocity Profiles, Turner Cut (April 4, 1997 14:30)

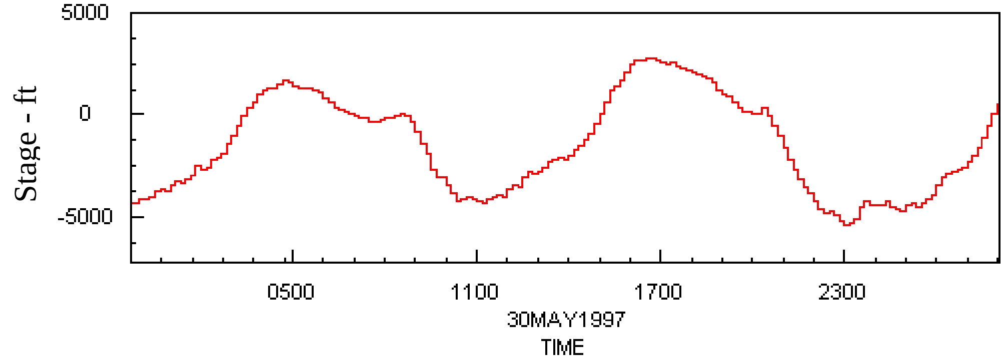

Figure I-37: Historical Flow at Turner Cut

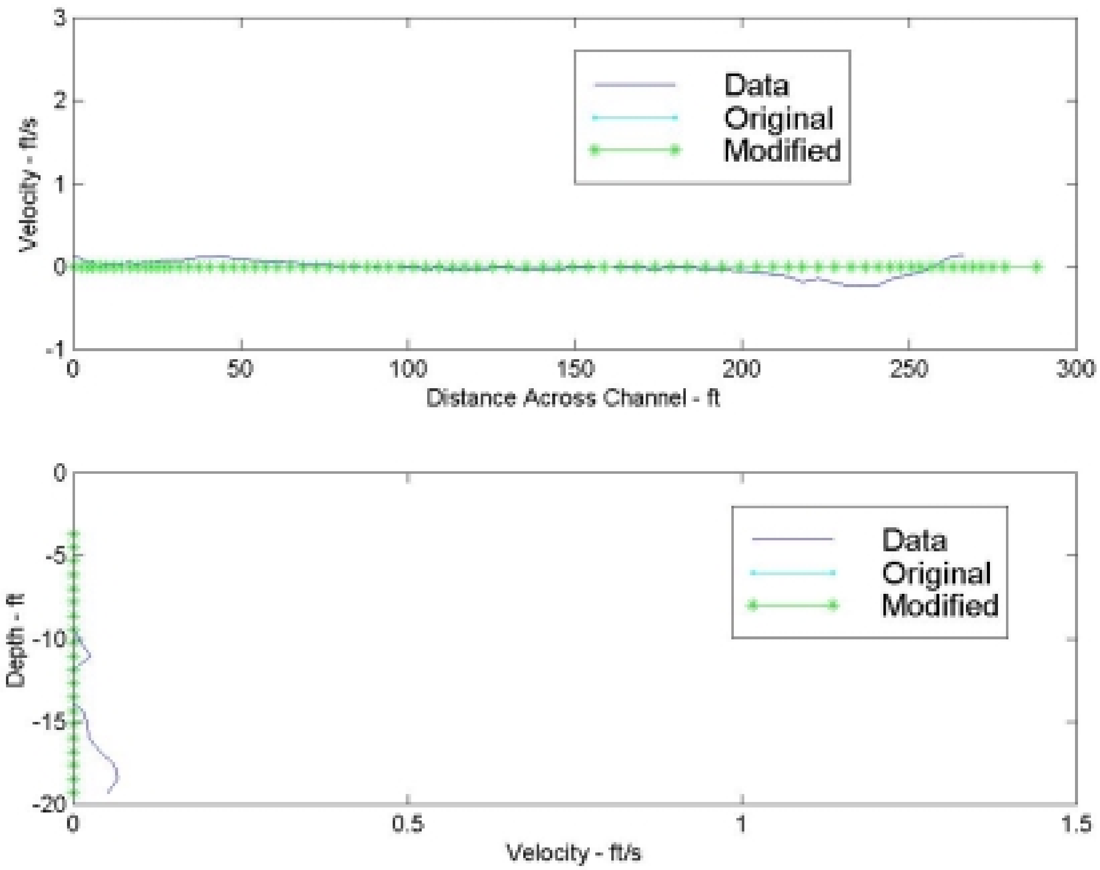

Figure I-38: ADCP and PTM Velocity Profiles, Turner Cut (May 30, 1997 8:10)

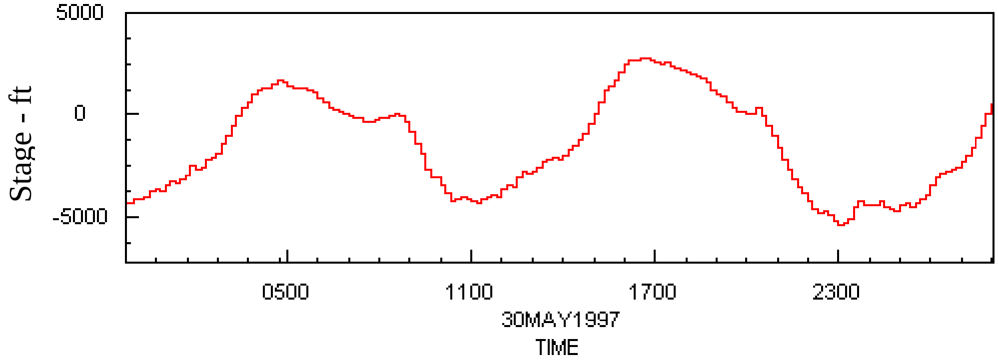

Figure I-39: Historical Flow at Turner Cut

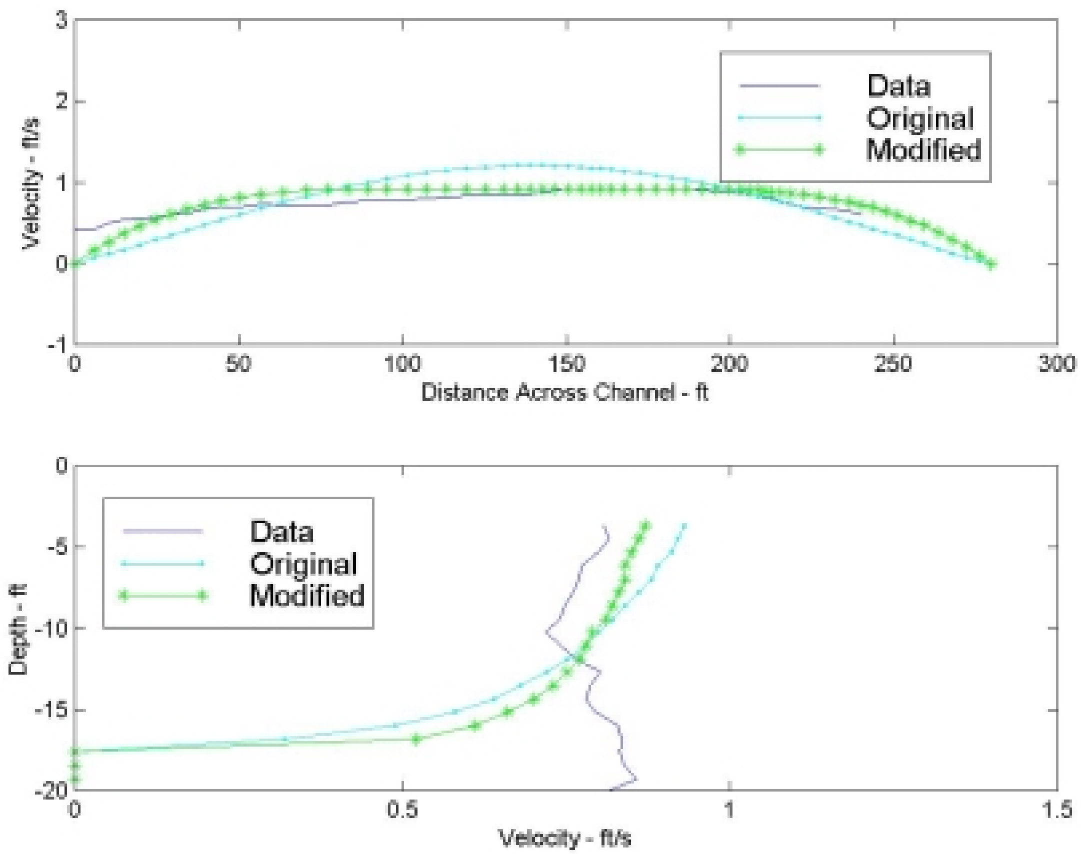

Figure I-40: ADCP and PTM Velocity Profiles, Turner Cut (May 30, 1997 11:10)

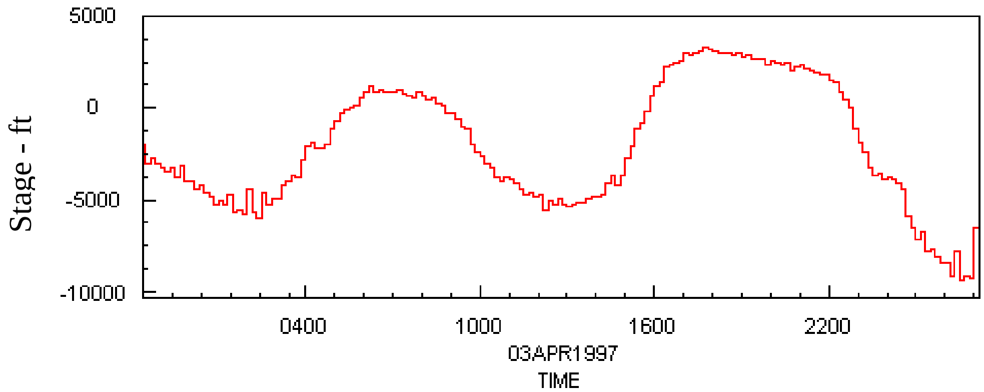

Figure I-41: Historical Flow at Victoria Canal

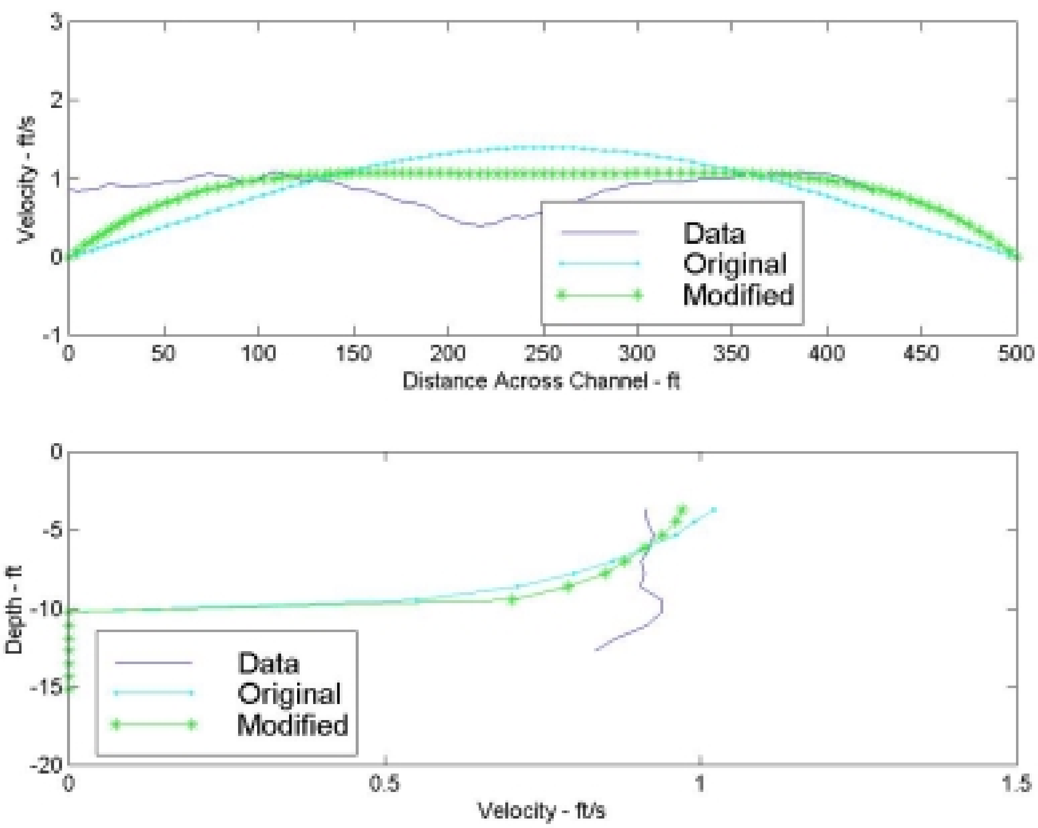

Figure I-42: ADCP and PTM Velocity Profiles, Victoria Canal (April 3, 1997 12:40)

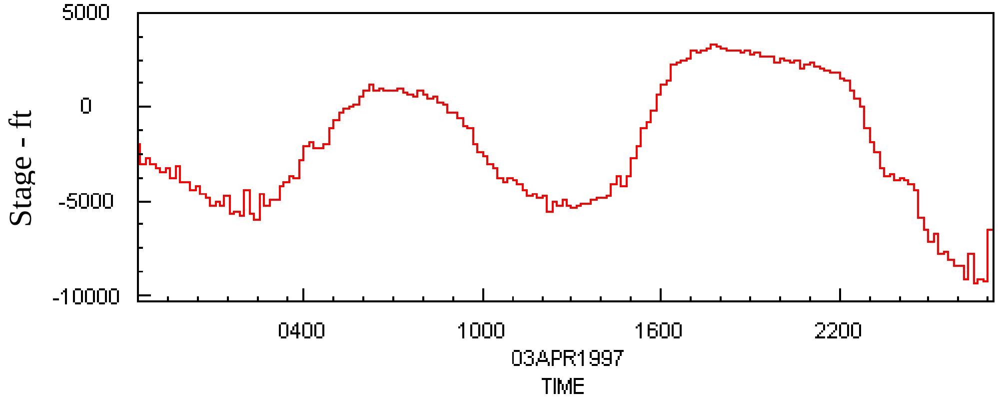

Figure I-43: Historical Flow at Victoria Canal

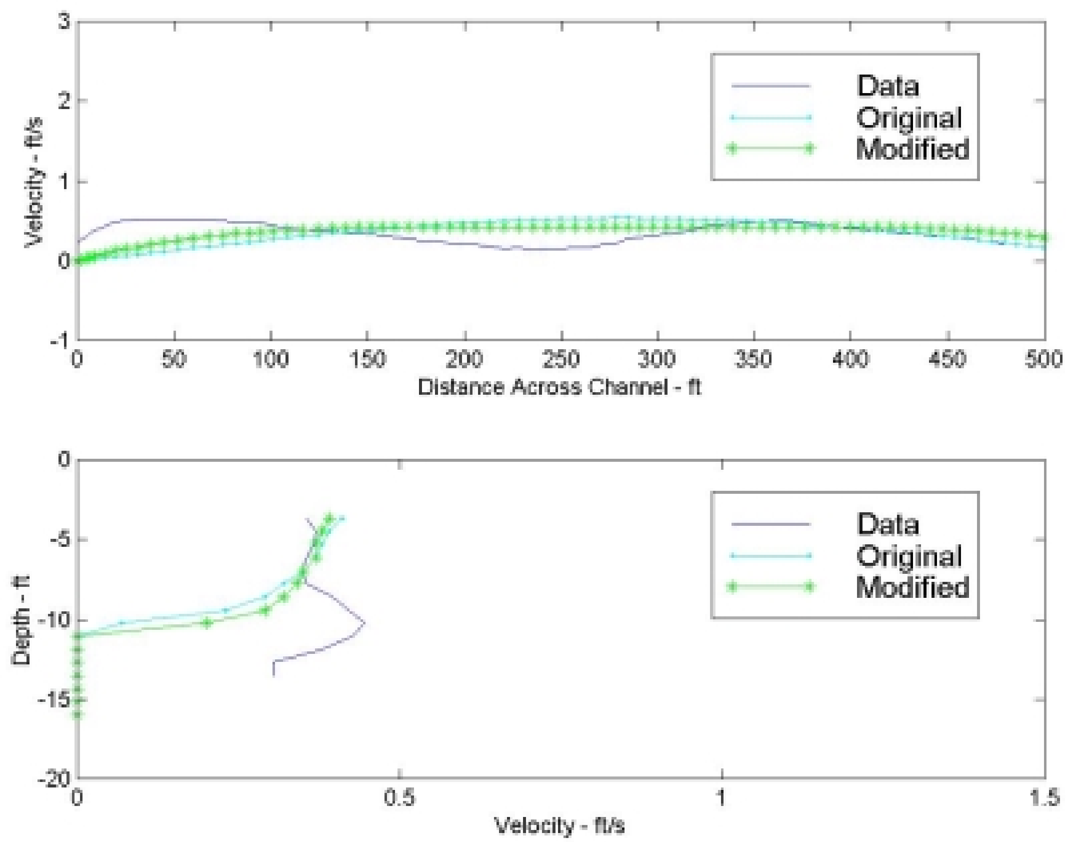

Figure I-44: ADCP and PTM Velocity Profiles, Victoria Canal (April 3, 1997 12:40)

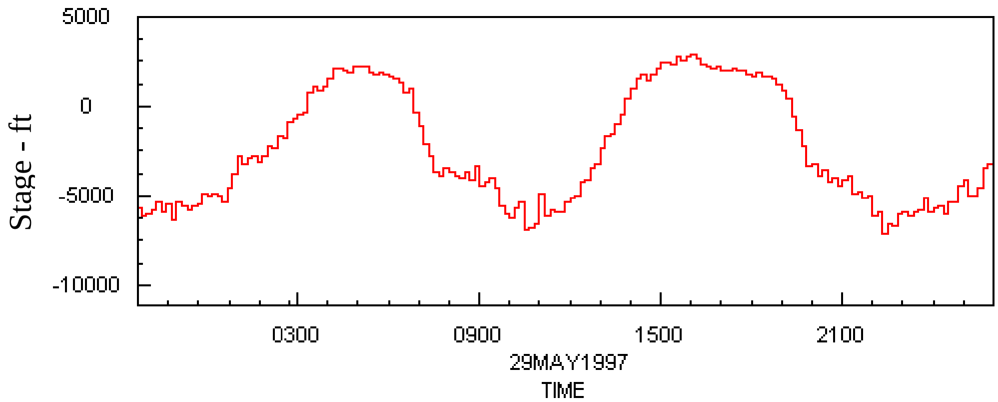

Figure I-45: Historical Flow at Victoria Canal

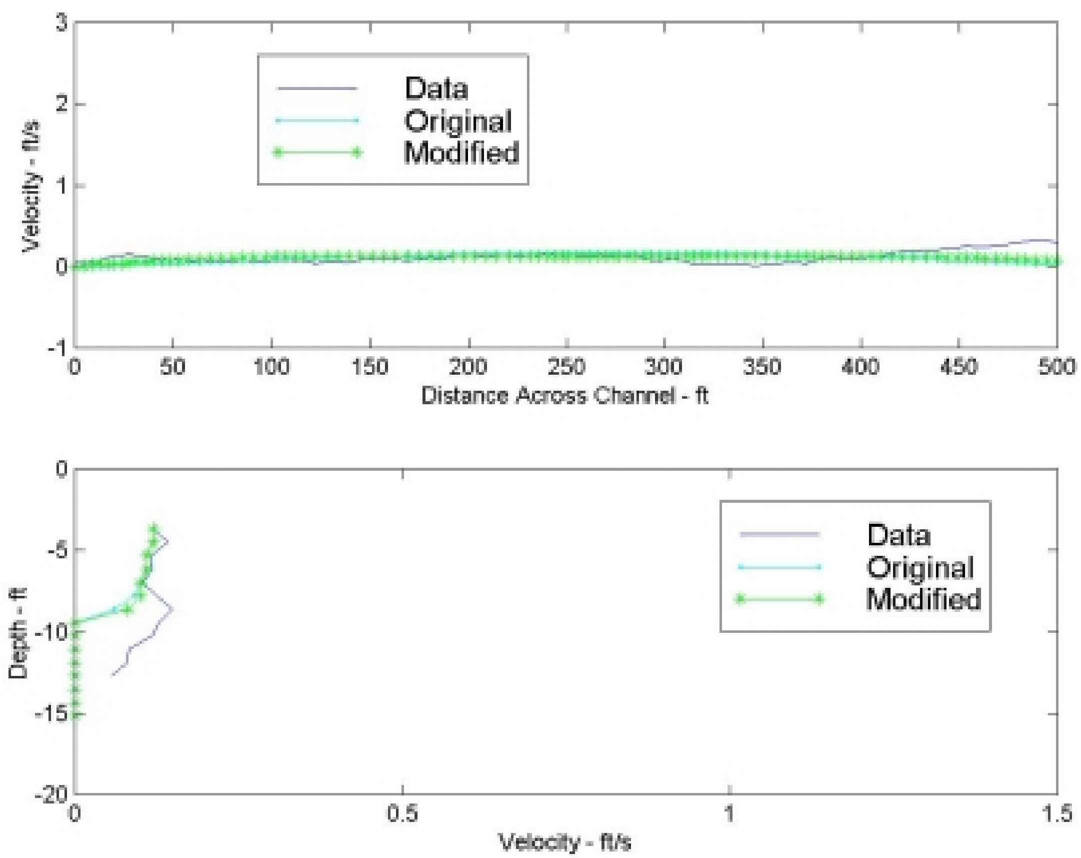

Figure I-46: ADCP and PTM Velocity Profiles, Victoria Canal (May 29, 1997 13:10)

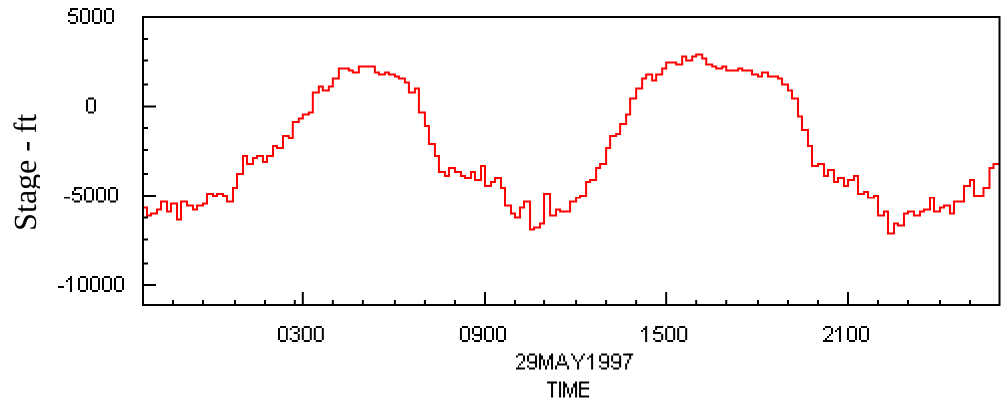

Figure I-47: Historical Flow at Victoria Canal

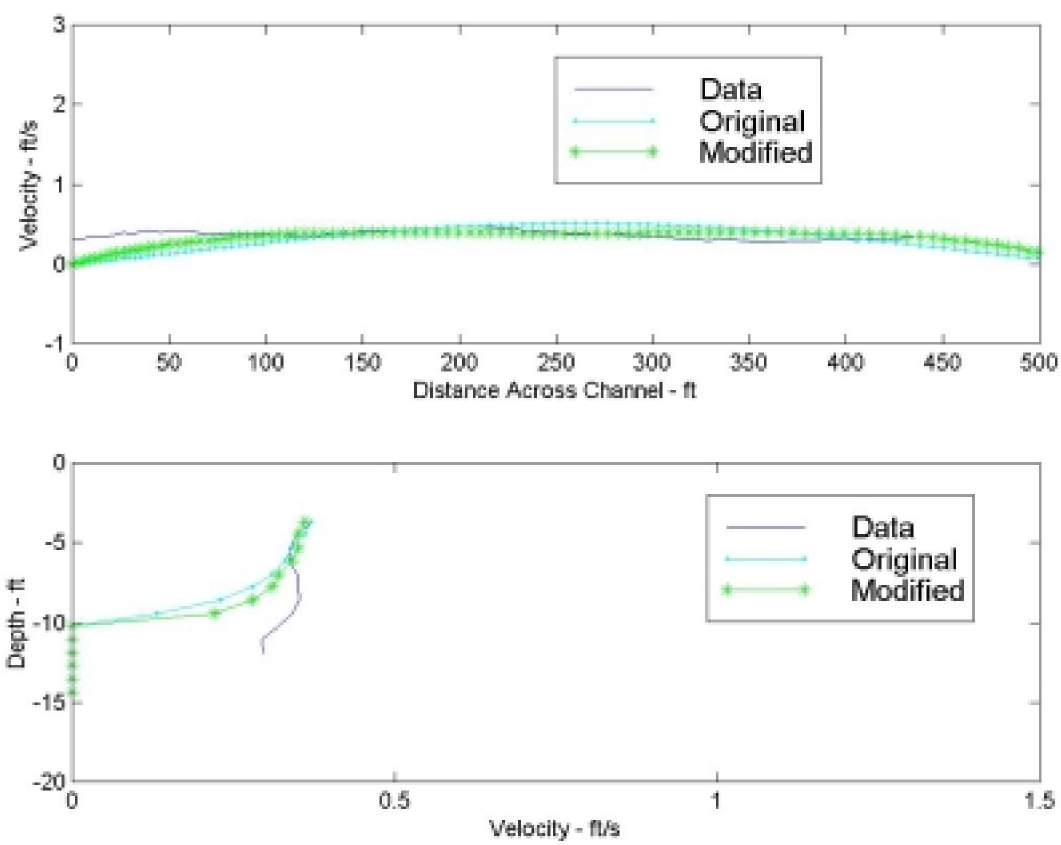

Figure I-48: ADCP and PTM Velocity Profiles, Victoria Canal (May 29, 1997 16:10)

9.2 Appendix 1I

Tracer Study Data

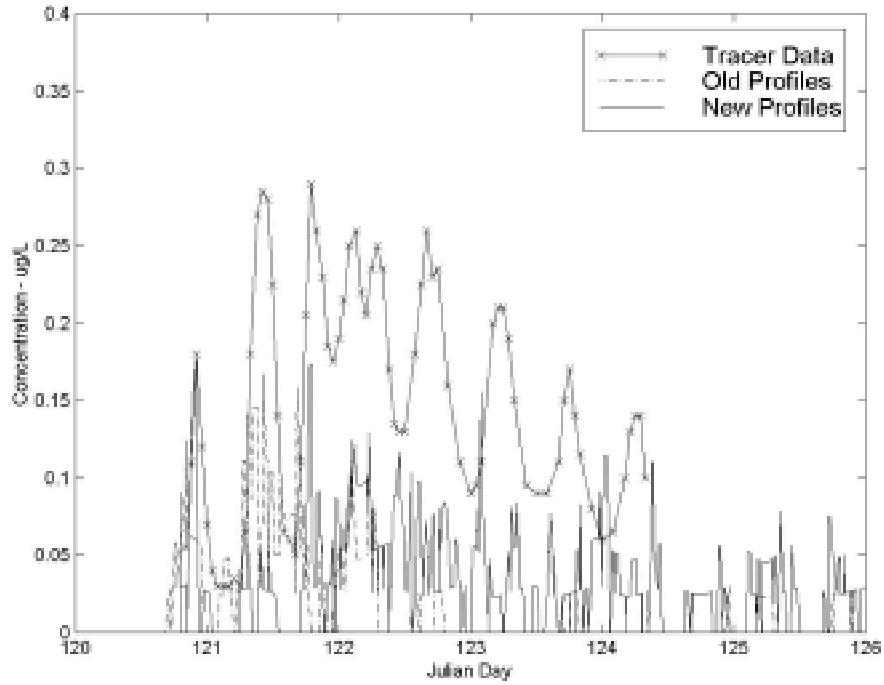

Figure II-1: PTM and Tracer, New Profiles, Grantline Canal

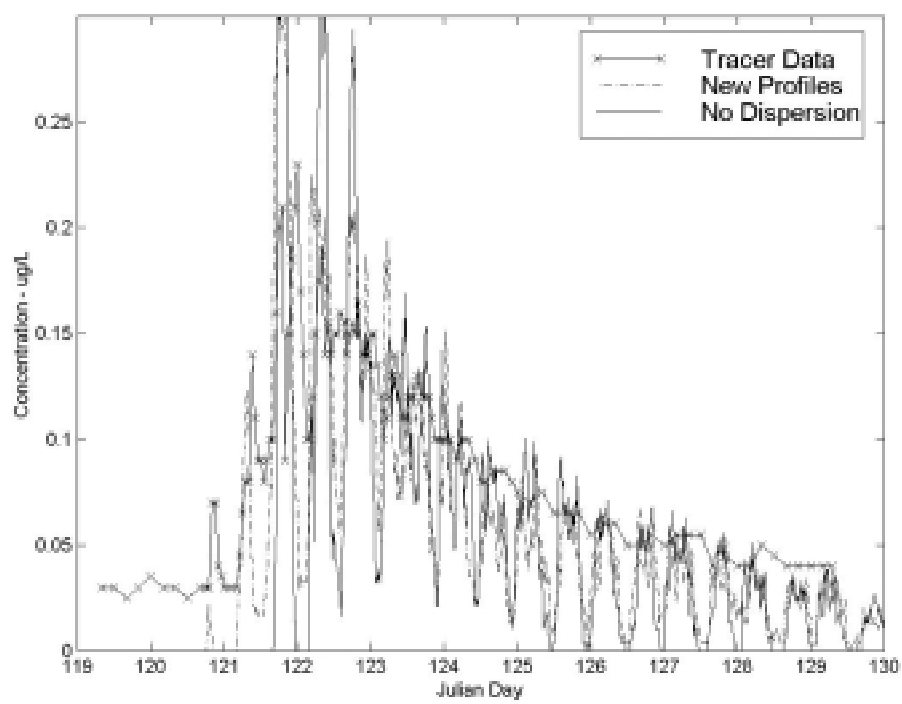

Figure II-2: PTM and Tracer, No Dispersion, Mandeville

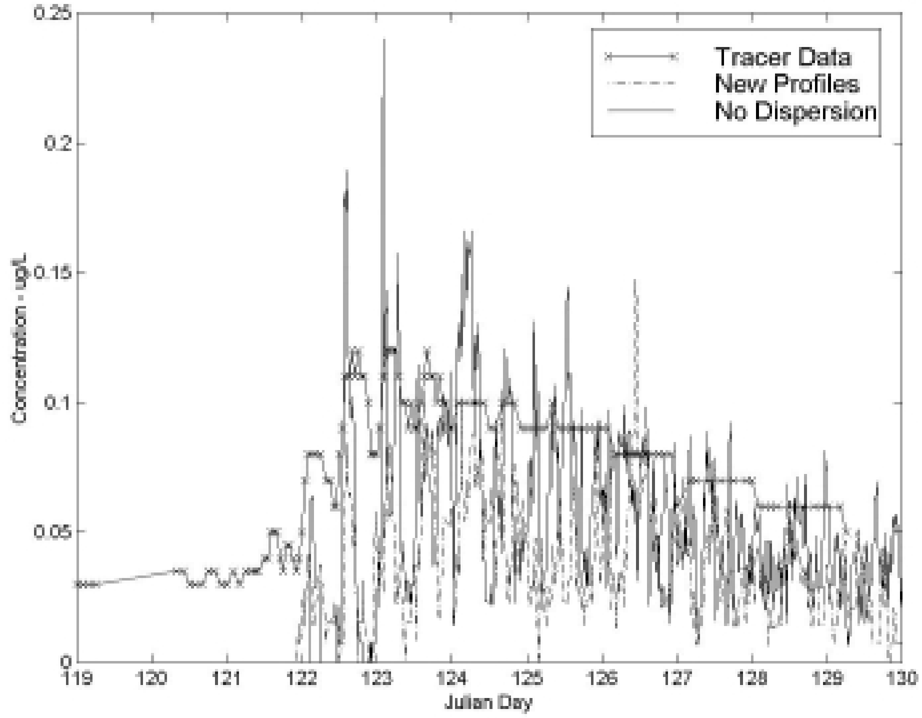

Figure II-3: PTM and Tracer, No Dispersion, Middle River bet. Col. and Turner Cut

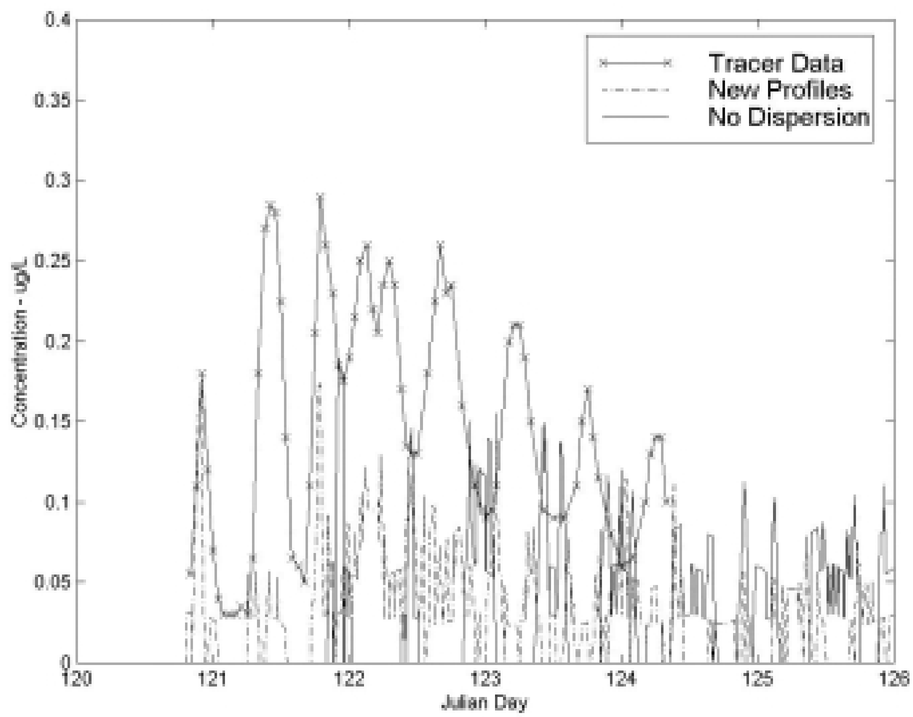

Figure II-4: PTM and Tracer, No Dispersion, Grantline Canal

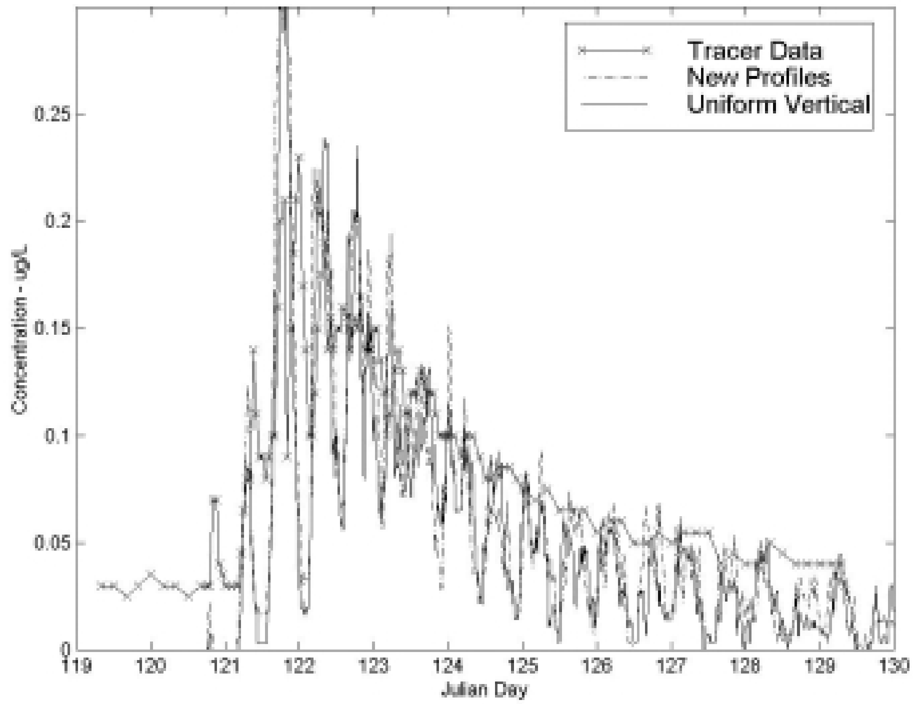

Figure II-5: PTM and Tracer, Uniform Vertical Profile, Mandeville

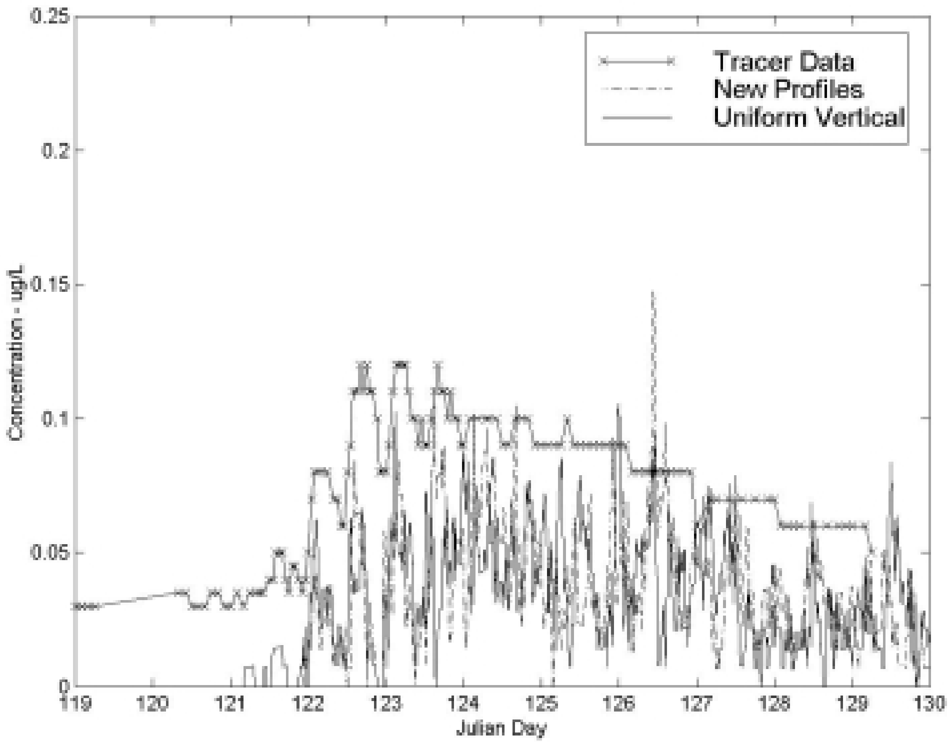

Figure II-6: PTM and Tracer, Uniform Vertical Profile, Middle River

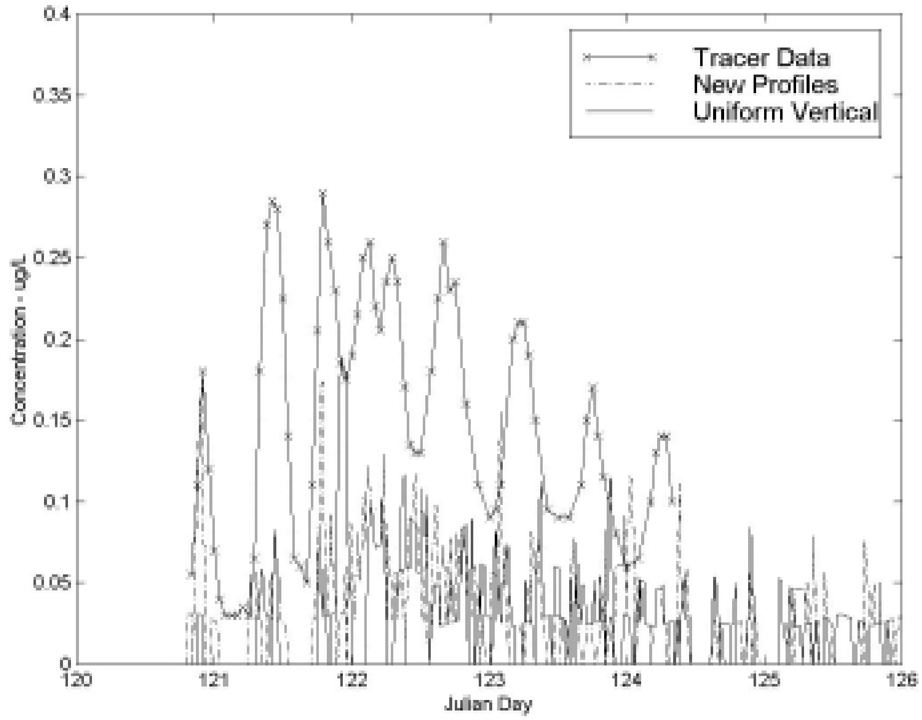

Figure II-7: PTM and Tracer, Uniform Vertical Profile, Grantline Canal

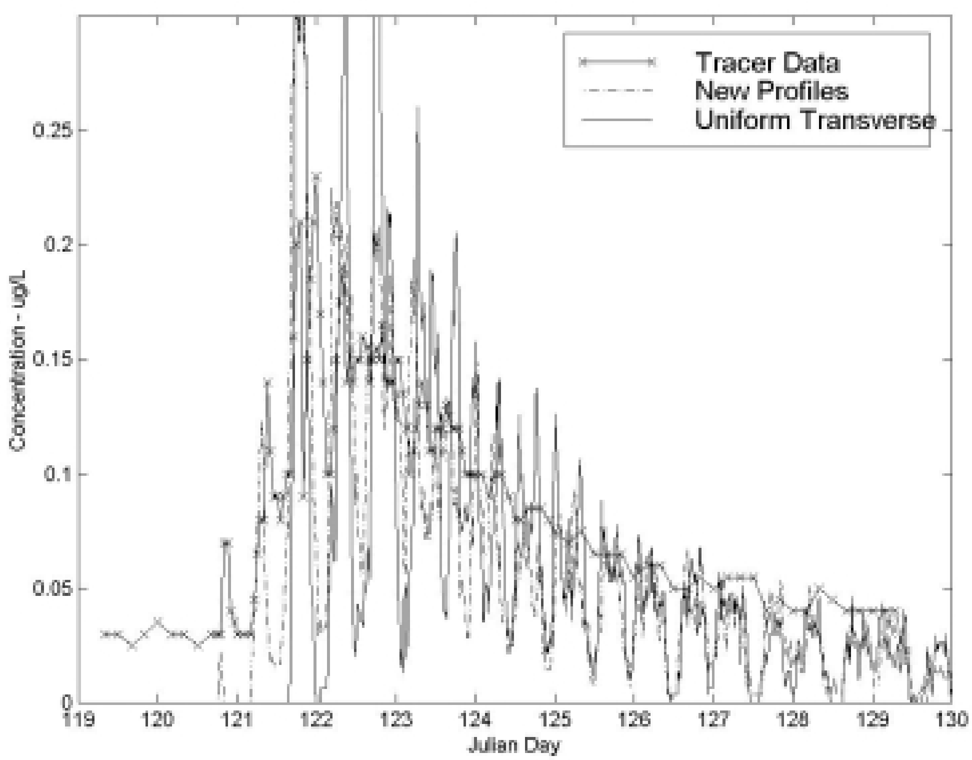

Figure II-8: PTM and Tracer, Uniform Transverse Profile, Mandeville

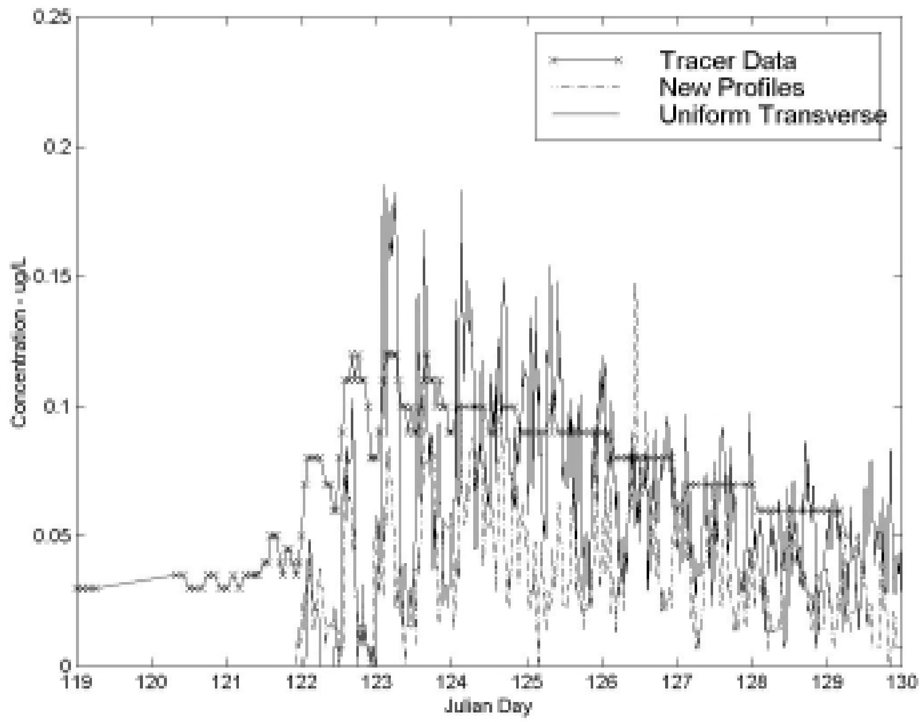

Figure II-9: PTM and Tracer, Uniform Transverse Profile, Middle River

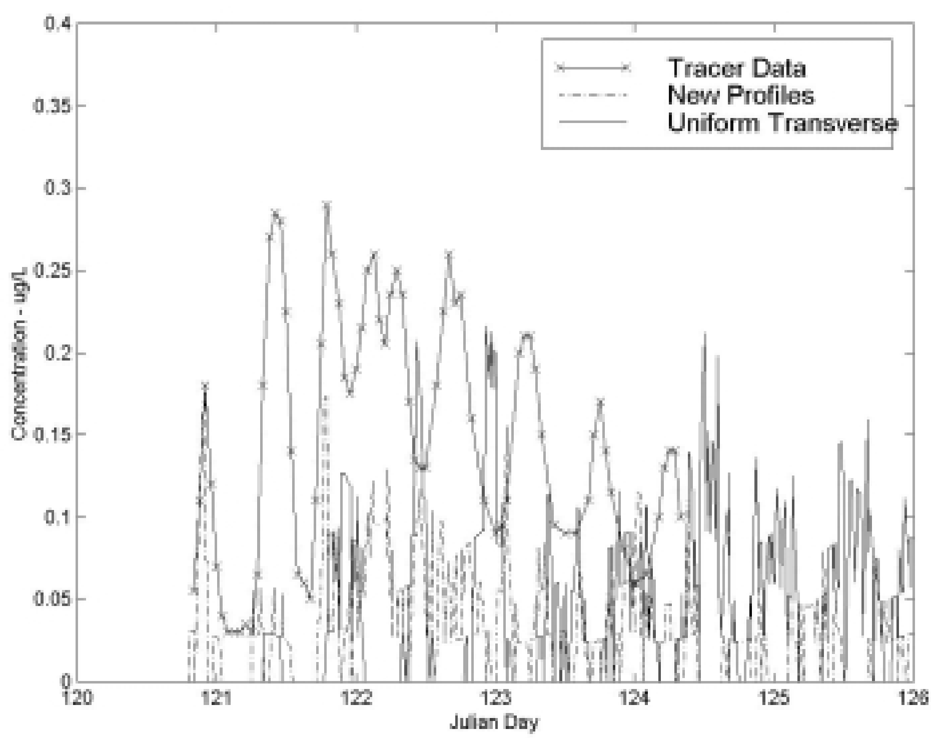

Figure II-10: PTM and Tracer, Uniform Transverse Profile, Grantline Canal